2007

Loss of Hdmx Leads to Alterations in Gene Expression and Inhibition of Cell Growth in Tumor Cells with Wild-type P53

Katherine Ann Heminger
Wright State University

LOSS OF HDMX LEADS TO ALTERATIONS IN GENE EXPRESSION AND INHIBITION OF CELL GROWTH IN TUMOR CELLS WITH WILD-TYPE p53

A dissertation submitted in partial fulfillment
of the requirements for the degree of
Doctor of Philosophy

By

KATHERINE ANN HEMINGER
B.S., The Ohio State University, 1983
M.S., Oklahoma State University, 1990

2007
Wright State University

WRIGHT STATE UNIVERSITY

SCHOOL OF GRADUATE STUDIES

March 12, 2007

I HEREBY RECOMMEND THAT THE DISSERTATION PREPARED UNDER MY SUPERVISION BY Katherine Ann Heminger ENTITLED Loss of HdmX Leads to Alterations in Gene Expression and Inhibition of Cell Growth in Tumor Cells with Wild-type p53 BE ACCEPTED IN PARTIAL FULFILLMENT OF THE REQUIREMENTS FOR THE DEGREE OF Doctor of Philosophy.

_____
Steven J. Berberich, Ph.D.
Dissertation Director

_____
Gerald M. Alter, Ph.D.
Director, Biomedical Sciences
Ph.D. Program

_____
Joseph F. Thomas, Jr., Ph.D.
Dean, School of Graduate Studies

Committee on
Final Examination

_____
Steven J. Berberich, Ph.D.

_____
Scott Baird, Ph.D.

_____
Michael Leffak, Ph.D.

_____
James McDougal, Ph.D.

_____
John J. Turchi, Ph.D.

ABSTRACT

Heminger, Katherine Ann. Ph.D., Biomedical Sciences Ph.D. Program, Wright State University, 2007. Loss of HdmX Leads to Alterations in Gene Expression and Inhibition of Cell Growth in Tumor Cells with Wild-type p53.

Mutations in the p53 tumor suppressor gene are among the most prevalent molecular abnormalities in human cancer. While half of all human tumors possess p53 mutations, inactivation of wild-type p53 can also occur through a variety of mechanisms that do not involve p53 gene mutation or deletion. This dissertation focuses on human tumor cell lines harboring wild-type p53 protein and elevated levels of HdmX and/or Hdm2, two critical negative regulators of p53 function. My hypothesis is that loss of HdmX in tumor cells with wild-type p53 and over-expressed HdmX, will activate p53 and induce p53 target genes leading to growth inhibition. To test this hypothesis, RNA interference (RNAi) was utilized to knockdown HdmX protein from HdmX over-expressing breast, colon, and bone tumor cell lines. Alterations in gene expression and effects on cell proliferation following the removal of HdmX were examined. Two RNAi approaches were assessed in this study; transient small interfering RNA (siRNA) transfection and lentivirus-delivered short-hairpin RNA (shRNA) vectors. Multiple siRNA transfections were selected as the method of choice over the shRNA vectors due to the induction of off-target genes in cells expressing the shRNA vectors. Affymetrix GeneChips and subsequent quantitative real time-PCR validations were used to uncover a subset of p53 target genes encoding proteins associated with cell cycle arrest and growth inhibition that were induced upon HdmX knockdown. In contrast, only one p53 dependent pro-apoptotic gene (i.e. Fas) was increased. The induction of these p53 target

genes following loss of HdmX was p53-dependent, as no increase in these p53 target genes were observed after HdmX knockdown in two different p53-null tumor cell lines. Cell cycle analysis and cell proliferation assays confirmed that the loss of HdmX led to a significant G1 cell cycle arrest. Similar findings were observed upon Hdm2 knockdown, and removing both HdmX and Hdm2 resulted in even greater p53 activation and a synergistic or additive induction of p53 target genes associated with cell cycle arrest. The increase in p53 transactivation following loss of HdmX was not due to p53 phosphorylation, suggesting a nongenotoxic or genotoxic stress independent p53 activation. Furthermore, the loss of HdmX did not appear to alter p53 localization or stabilization. Although the removal of over-expressed HdmX appears limited to an anti-proliferative effect in tumor cells harboring wild-type p53, loss of HdmX enhanced the cytotoxicity of several chemotherapeutic agents. Cell viability assays showed an increase in chemosensitivity in tumor cells following knockdown of HdmX and/or Hdm2. Taken together, these results suggest that removal of HdmX may be an important therapeutic target that would complement chemotherapy drugs currently used to treat tumors possessing wild-type p53

TABLE OF CONTENTS

Page

TABLE OF CONTENTS (Continued)

Page

TABLE OF CONTENTS (Continued)

Page

LIST OF FIGURES

Figure Page

LIST OF FIGURES (Continued)

Figure Page

LIST OF FIGURES (Continued)

Figure Page

LIST OF TABLES

Table Page

ACKNOWLEDGEMENTS

I would like to thank my advisor Dr. Steven J. Berberich for the opportunity to work in his lab, for the stimulating scientific discussions and for his guidance throughout my dissertation research. I would also like to thank my committee members; Drs. Baird, Leffak, McDougal, and Turchi for their time and their helpful suggestions during my committee meetings. To Madhavi Kadakia, thanks for your friendship and advice. To all the past and present members of the Berberich and Kadakia labs, thanks for your friendship and for all of your assistance over the years. You all made the lab a great place to work.

I would also like to thank my parents, Frank and Ann, for all of their support and willingness to help out in whatever way was needed. To my loving husband Bob, and my wonderful sons, Austin and Grant, thanks for all of your patience, encouragement, and support throughout my graduate school years. I couldn't have done it without you.

I would also like to thank Sigma Xi Grant-in-Aid of Research for funding and AACR for the Scholar-in-Training award.

I. INTRODUCTION

A. p53 Structure and Function

The discovery of p53 in 1979 by two independent labs (Lane and Crawford, 1979; Linzer and Levine, 1979) showed that the protein associated with the large T antigen in SV40 transformed cells. Originally, p53 was believed to be a tumor antigen, and then an oncogene since it was overexpressed in many human cancer cell lines (Crawford et al., 1981). However, by the late 1980s the paradigm shifted and p53 was later confirmed a tumor suppressor gene (Baker et al., 1990; Chen et al., 1990; Finlay et al., 1989; Mercer et al., 1990; Vogelstein et al., 1989). The p53 tumor suppressor protein consists of 393 amino acid residues which can be divided into five domains. These domains include an N-terminal transactivation domain (residues 1-43), a proline-rich region (residues 63-97), a DNA binding domain (residues 102-292), a tetramerization domain (residues 323-356) and a basic domain (residues 363-393) (Figure 1). The transactivation (TA) domain interacts with transcriptional machinery and repair factor proteins (Ko and Prives, 1996). The proline rich region binds signaling molecules which contribute to the pro-apoptotic function of p53 (Gorina and Pavletich, 1996; Harms and Chen, 2006). The central DNA binding domain of p53 is essential for its role as a sequence specific transcription factor. The p53 responsive element contains two copies or half sites of a 10 base pair consensus sequence, 5'-PuPuPuC(A/T)(T/A)GPyPyPy, which are separated by 0-13 base pairs (el-Deiry et al., 1992). In order for p53 to be transcriptionally active and bind DNA, two p53 dimers must oligomerize through their tetramerization domains to form an active p53

tetramer (McLure and Lee, 1998). A nuclear localization signal (NLS) is located at residues 305-322 and the two nuclear export signals are located at residues 11-27 and residues 340-351 (Harms and Chen, 2006). The C- terminal basic domain functions as a regulatory domain, and has multiple functions including DNA binding and nuclear import (Braithwaite et al., 2005; Liang and Clarke, 1999; Yakovleva et al., 2001).

The p53 protein is activated by a variety of genotoxic insults and cellular stresses. Once activated, p53 functions as a transcription factor to modulate the expression of a diverse array of downstream genes. These p53 target genes are involved in cell cycle arrest (i.e. p21, GADD45, BTG2), DNA repair (i.e. PCNA, p48, p53R2) and apoptosis (i.e. BAX, NOXA, PIG), and contribute to the tumor suppressor activity of p53 (Vousden and Lu, 2002). Upon DNA damage or various types of cellular stress, p53 is stabilized by post-translational modifications mainly within the N-terminal transactivation domain or the C-terminal regulatory domain. Some of these modifications are known to disrupt the interaction between p53 and its negative regulator, Hdm2 (Michael and Oren, 2003; Unger et al., 1999) or to enhance tetramerization, stability or activity of p53 (Hirao et al., 2000; Lavin and Gueven, 2006). Phosphorylations are the predominant post-translational modification of the p53 transactivation domain and are brought about by a number of protein kinases (Figure 1) (Meek, 2002). DNA damage caused by ionizing radiation induces ATM (ataxia-telangiectasia, mutated) mediated phosphorylation either directly or indirectly at serines 6, 15, 20 and 46 within the N-terminal domain of p53 (Canman et al., 1998; Saito et al., 2002). Serines 6, 15 and 20 can also be phosphorylated by other kinases, including ATR (A-T and Rad3-related), DNA-PK, and the checkpoint kinases, Chk1 and Chk2 (Appella and Anderson, 2001). Serine 46, which has been reported to be

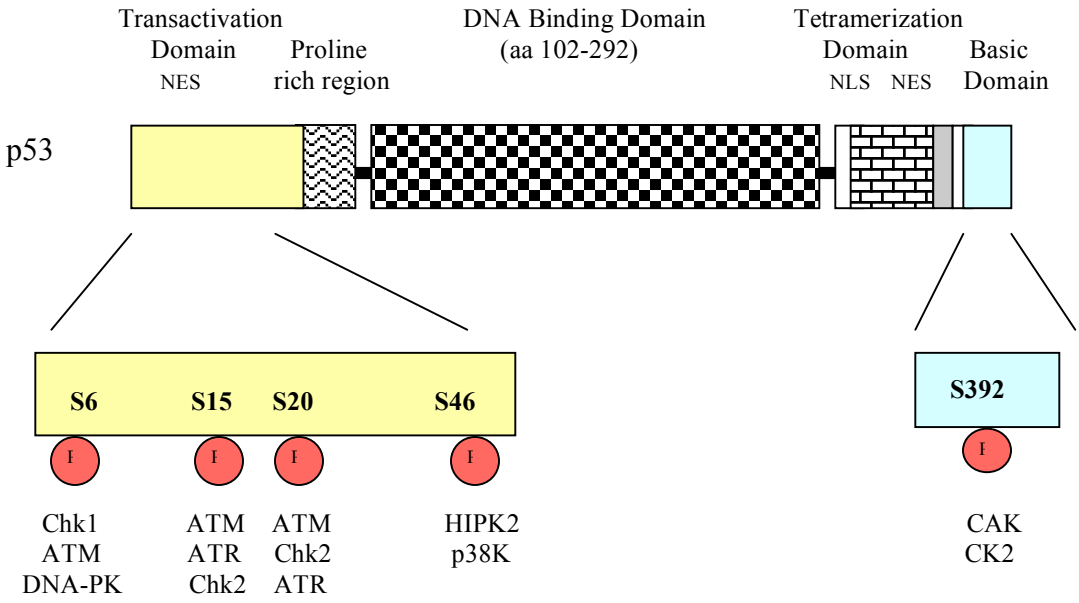

Figure 1. Schematic diagram of p53 protein and select phosphorylation sites. NLS, nuclear localization signal; NES, nuclear export signal; N-terminal Transactivation domain (yellow) and C-terminal Basic domain (blue) showing select phosphorylation sites (red circles) and the kinases responsible for phorphorylating those sites (reviewed by Lavin and Gueven, 2006).

important in regulating the ability of p53 to induce apoptosis is phosphorylated by HIPK2 (homedomain-interacting protein kinase 2) (Mayo et al., 2005; Oda et al., 2000b). In the C-terminal domain of p53, phosphorylation of serine 392 by CAK (cyclin-activating kinase) or CK2 has been reported to influence DNA binding, transcriptional activation and the growth inhibition function of p53 (Kohn, 1999; Lu et al., 1998; Prives and Hall, 1999). Additional post-translational modifications in the C-terminal tetramerization and regulatory domains include acetylation, neddylation, methylation and ubiquitination (Lavin and Gueven, 2006).

Under most non-stress conditions, p53 protein is maintained at a low basal level and p53 activity is tightly regulated by rapid p53 turnover. The N-terminal transactivation domain of p53 interacts with its negative regulators, Hdm2 and HdmX protein, which block p53 transactivation (Finch et al., 2002; Haupt et al., 1997; Kubbutat et al., 1997). The stringent regulation of p53 involves a complex network of proteins, and is critical for maintaining genomic stability and suppressing tumor formation. Hdm2 and its structural homologue, HdmX, represent two essential negative regulators of p53 (Jones et al., 1995; Montes de Oca Luna et al., 1995; Parant et al., 2001).

B. Hdm2 and HdmX Structure and Function

Hdm2 and HdmX (human homologs of the murine double minute proteins, Mdm2 and MdmX, respectively) are both p53 binding proteins that are structurally similar and share over 90% amino acid identity with their murine homologs (Shvarts et al., 1997). The Hdm2 and HdmX proteins possess the greatest similarities in the N-terminal p53 binding region, the internal zinc finger, and the C-terminal RING (really interesting new gene) finger domain (Figure 2) (Jackson et al., 2001; Shvarts et al., 1996).

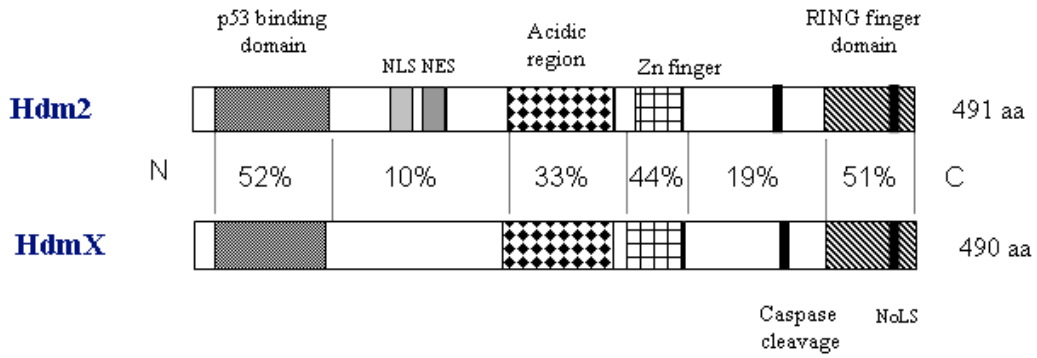

Figure 2. Schematic diagram comparing Hdm2 and HdmX protein homology. NLS, nuclear localization signal; NES, nuclear export signal; NoLS, nucleolar localization signal. The greatest amino acid similarity between Hdm2 and HdmX is found in the p53 binding domain, the Zinc (Zn) finger and the RING finger domain (adapted from Jackson and Berberich, 2001).

Both Mdm2 and MdmX act as critical negative regulators of p53 *in vivo* and the loss of either Mdm2 or MdmX leads to embryonic lethality in knockout mice if not rescued by the concurrent elimination of p53 (Finch et al., 2002; Jones et al., 1995; Montes de Oca Luna et al., 1995; Parant et al., 2001). The embryonic lethality occurs at implantation in *mdm2*-null embryos and at gastrulation for *mdmX*-null embryos, suggesting that Mdm2 and MdmX inhibit p53 function in a partially non-overlapping manner (Parant et al., 2001). Using mouse models, the loss of Mdm2 was shown to induce p53 dependent apoptosis, whereas the loss of MdmX led to a lack of cell proliferation in one model, and to cell cycle arrest and apoptosis in another (Chavez-Reyes et al., 2003; Parant et al., 2001; Xiong et al., 2006).

There are several other key differences between Hdm2 and HdmX that are critical for understanding how these two proteins regulate p53. Hdm2 directly associates with p53 resulting in inhibition of p53 transactivation (Oliner et al., 1993) and ubiquitination of p53 protein targeting it for proteosomal degradation (Haupt et al., 1997; Honda et al., 1997; Kubbutat et al., 1998; Moll and Petrenko, 2003). The evolutionarily conserved C-terminal RING finger domain of Hdm2 is critical for its E3 ubiquitin ligase activity, and it serves to target its own ubiquitination and degradation as well (Fang et al., 2000). Beside a fully functional RING finger domain, the central acidic domain of Hdm2 is essential for p53 ubiquitination as assessed through a series of Hdm2-HdmX chimeric proteins (Kawai et al., 2003b; Meulmeester et al., 2003). While HdmX shows conservation in the E3 ligase RING finger domain with Hdm2, HdmX lacks E3 ligase activity (Jackson and Berberich, 2000; Stad et al., 2001). Furthermore, Hdm2 and HdmX contain a nucleolar localization signal (NoLS) within the RING domain (Jackson et al.,

2001; Weber et al., 2000); however, HdmX does not possess nuclear localization or export signals like Hdm2 (Jackson et al., 2001; Shvarts et al., 1996). Thus Hdm2 shuttles back and forth between the nucleus and cytoplasm, while HdmX is predominantly localized in the cytoplasm (Migliorini et al., 2002; Roth et al., 1998). Hdm2 and HdmX can heterodimerize with each other through their conserved RING finger domains and this interaction stimulates the recruitment of HdmX into the nucleus (Migliorini et al., 2002; Tanimura et al., 1999). Additionally, the interaction between Hdm2 and HdmX has been shown to stabilize Hdm2 by interfering with Hdm2 auto-ubiquitination, and overexpression of HdmX stabilizes p53 by preventing Hdm2-mediated degradation of p53 while suppressing its transactivation (Jackson and Berberich, 2000; Stad et al., 2001). The regulation of p53 by Hdm2 and HdmX appears to involve cooperation between the two proteins. Both Mdm2 and MdmX were found to be essential for regulating p53 activity in a nonredundant manner, whereby, Mdm2 regulated p53 protein levels and MdmX fine-tuned p53 transcriptional activity (Francoz et al., 2006). The effect of Hdm2 and HdmX on p53 stability and activity is dependent on the relative abundance of Hdm2 and HdmX proteins. When HdmX levels are less than 2:1 with Hdm2, p53 stability is decreased, whereas overexpressed HdmX increased p53 stability by competing with Hdm2 for p53 binding (Gu et al., 2002; Mancini et al., 2004; Stad et al., 2001). However, some *in vitro* studies have suggested that HdmX acts as a stimulator of Hdm2 E3 ligase activity and facilitates ubiquitination of p53 and itself (Linares et al., 2003). Further evidence suggests that Hdm2 promotes ubiquitination and proteasomal degradation of HdmX in addition to p53 and itself (de Graaf et al., 2003; Pan and Chen, 2003).

Additionally, HdmX contains a caspase 3 cleavage site at residue 361 which is p53-dependently cleaved by caspase following DNA damage (Gentiletti et al., 2002). The larger truncated product is then degraded through the proteasomal pathway; however, HdmX degradation by Hdm2 does not depend on caspase cleavage (Kawai et al., 2003a). Taken together, the interactions between p53, Hdm2 and HdmX are critical for the stringent control of p53 activity (Marine and Jochemsen, 2004).

C. Regulation of p53

The tumor suppressor protein, p53, undergoes constant ubiquitination and proteasomal degradation in order to maintain low basal levels of p53 in non-stressed cells (Kubbutat et al., 1997). However, ubiquitination of p53 is inhibited in response to various stresses, leading to the accumulation and activation of p53, and induction of cell cycle arrest and/or apoptosis (Ashcroft and Vousden, 1999). The half-life of p53 in normal unstressed cells is approximately 30 minutes, but DNA damage increases the half-life to several hours causing accumulation of p53 (Yang et al., 2004). The stability of p53 is predominantly regulated by the action of Hdm2 which ubiquitinates p53 and promotes its degradation through nuclear and cytoplasmic proteasomes (Haupt et al., 1997; Kubbutat et al., 1998; Moll and Petrenko, 2003). Specifically, Hdm2 transfers monoubiquitin moieties onto one or more lysine residues of p53, mainly in the C-terminal region (Kubbutat et al., 1998; Rodriguez et al., 2000). Mutational analysis of six lysine residues to arginine within the C-terminal portion of p53 decreased the susceptibility of p53 to Hdm2-mediated degradation (Rodriguez et al., 2000). Additionally, the tetramerization domain of p53 is required for efficient Hdm2 binding and ubiquitination of p53 (Kubbutat et al., 1998; Maki, 1999). Recently it was shown that Hdm2 is capable

of catalyzing both mono- and polyubiquitination of p53 depending on the level of Hdm2. Low levels of Hdm2 induce monoubiquitination and nuclear export of p53, whereas p53 poly-ubiquitination and nuclear degradation is caused by high levels of Hdm2 (Brooks et al., 2004; Li et al., 2003) . Furthermore, monoubiquitination appears to be critical for p53 translocation out of the nucleus since a p53-ubiquitin fusion protein that mimics monoubiquitinated p53 was found to accumulate in the cytoplasm independently of Hdm2 (Brooks et al., 2004; Li et al., 2003). Other evidence suggests that Hdm2-mediated p53 polyubiquitination takes place in a complex with p300/CREB-binding protein (CBP) in the nucleus (Grossman et al., 2003). The intrinsic ubiquitin ligase activities of both Hdm2 and p300 are believed to be necessary for the generation of polyubiquitinated chains on p53 that target it for proteasomal degradation (Grossman et al., 2003).

In addition to Hdm2, Pirh2 (p53 induced RING-h2) has also been identified as an E3 ligase that physically interacts with p53 and promotes ubiquitination and proteasomal degradation of p53 independently of Hdm2 (Leng et al., 2003). Pirh2 contains a RING finger domain and is a p53 transcriptional target gene which participates in an auto-regulatory feedback loop that modulates p53 stability (Leng et al., 2003). Another E3 ligase, COP1 (constitutively photomorphogenic 1), is also a RING finger containing protein that causes p53 degradation through the proteasome in a ubiquitin-dependent manner, independent of Hdm2 or Pirh2 (Dornan et al., 2004). Together, Hdm2, Pirh2, and COP1 represent three ubiquitin ligases for p53 which the cell can utilize to maintain tight control of the tumor suppressor.

D. p53-Hdm2 Auto-regulatory Feedback Loop

Upon DNA damage, p53 is activated leading to the transcriptional activation of a diverse array of p53 target genes. Hdm2 is a p53 target gene which encodes a protein that directly binds p53 and inhibits its activity, thereby forming a negative auto-regulatory feedback loop (Figure 3) (Momand et al., 1992; Wu et al., 1993). The p53-Hdm2 feedback loop is further regulated by a network of other proteins which interact with p53 and/or Hdm2. One of these proteins is HdmX which directly associates with the transactivation domain of p53 and inhibits its activity (Shvarts et al., 1996). The phosphorylation of HdmX on serine 289 by casein kinase 1 alpha enhances its binding to p53 (Chen et al., 2005b) and this p53-HdmX interaction inhibits p300/CBP mediated acetylation of p53 (Sabbatini and McCormick, 2002). Similarly, Hdm2 interaction with p53 also inhibits p300-mediated acetylation of p53 (Kobet et al., 2000).

Upon DNA damage, Hdm2 mediates the ubiquitination and degradation of HdmX to facilitate p53 activation (de Graaf et al., 2003; Pan and Chen, 2003). The Hdm2-mediated ubiquitination of HdmX is dependent on functional nuclear ATM and phosphorylation on at least three sites on HdmX (Pereg et al., 2005). ATM directly targets S403, whereas Chk2 kinase is required for phosphorylation of MdmX on S342 and S367 (Chen et al., 2005a; Okamoto et al., 2005). Furthermore, phosphorylation of S367 is required for 14-3-3 binding to HdmX, which facilitates HdmX nuclear import and degradation by Hdm2 (LeBron et al., 2006). Taken together, phosphorylation of HdmX after DNA damage redirects the E3 ligase activity of Hdm2 towards HdmX instead of p53 leading to p53 activation (Chen et al., 2005a).

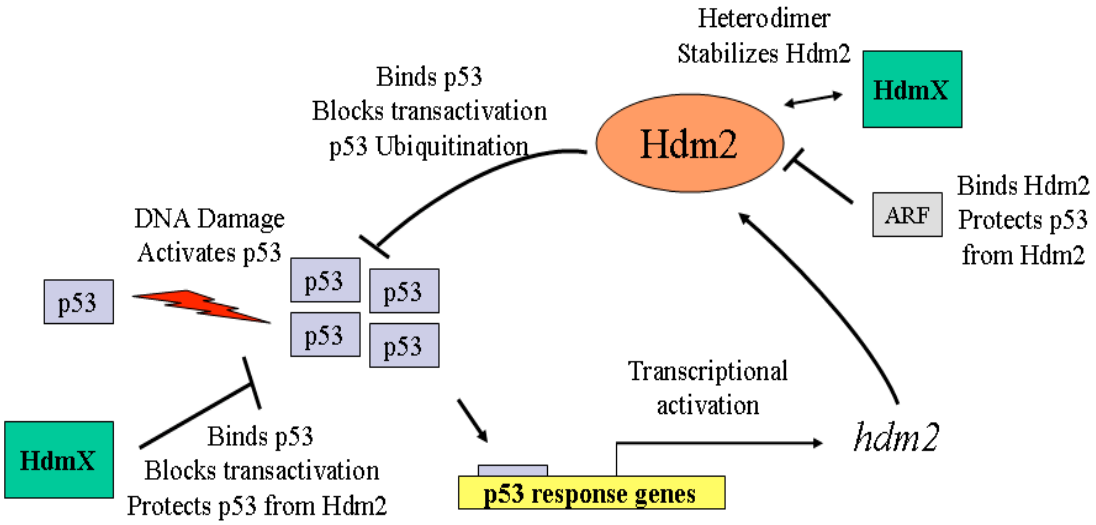

Figure 3. p53-Hdm2 negative feedback loop. Upon DNA damage, p53 is activated and p53 responsive genes are induced. Hdm2 is a p53 target gene which encodes a protein that directly binds p53 leading to inhibition of p53 transcriptional activity and Hdm2 mediated ubiquitination and proteasomal degradation; thus forming a negative feedback loop. HdmX and ARF can also impact the p53-Hdm2 feedback loop.

Post translational modifications of Hdm2 also contribute to its ability to associate with and ubiquitinate p53, HdmX or itself (Khosravi et al., 1999). In response to specific DNA damaging agents, ATM phosphorylates Hdm2 on serine 395 which appears to destabilize its interaction with p53 and inhibit the nuclear-cytoplasmic shuttling of p53 (Maya et al., 2001). Sumoylation of Hdm2 and HdmX, modification by SUMO (a small ubiquitin-like modifier), can also affect stability and protein-protein interactions, by decreasing Hdm2-mediated ubiquitination (Buschmann et al., 2001; Ghosh et al., 2005). Thus, the numerous post-translational modifications of p53, Hdm2 and HdmX add another layer of complexity to the p53-Hdm2 auto-regulatory feedback loop.

Other proteins which participate in the control of p53 activity include HAUSP (herpes virus-associated ubiquitin specific protease) which directly interacts with and deubiquitinates p53, Hdm2 and HdmX leading to stabilization of each protein (Hu et al., 2006b; Li et al., 2004; Li et al., 2002). ATM-dependent phosphorylation of Hdm2 and HdmX decreases their affinity for HAUSP resulting in the destabilization of Hdm2 and HdmX and activation of p53 (Meulmeester et al., 2005). The p14ARF (alternative reading frame protein expressed from the INK4A locus) protein also binds to Hdm2 and HdmX, sequestering these proteins within the nucleolus so that p53 can be activated (Jackson et al., 2001; Tao and Levine, 1999; Weber et al., 2000; Weber et al., 1999). The protein-protein interactions presented here are a few of the key players involved in the regulation of the p53-Hdm2 feedback loop.

E. p53 and Cancer

Mutations in the p53 tumor suppressor gene are among the most prevalent molecular abnormalities in human cancer. Half of all human tumors possess mutations in

p53 (Hollstein et al., 1996), which usually disrupts the ability of p53 to bind DNA and function as a transcription factor. The majority of tumor-derived mutations are missense mutations that can be classified as either contact site (hotspot mutations: R248 and R273) or conformational (hotspot mutations: R175, G245, R249, and R282) mutations. Mutation at a residue that is critical for p53-DNA interaction is categorized as a contact site mutation, whereas conformational mutations fail to stabilize the p53 protein necessary for proper binding to DNA (Harms and Chen, 2006). Studies conducted in mice with mutated or genetically deficient p53 were found to be extremely prone to tumor formation (Donehower et al., 1992). Furthermore, germ line mutations in p53 lead to the inherited cancer predisposing condition in humans, Li-Fraumeni Syndrome (Li et al., 1988; Malkin et al., 1990). These findings indicate the importance of p53 in suppressing tumor formation and protecting the genome.

While half of all human tumors contain mutations in the p53 gene, inactivation of wild-type p53 protein can also occur through a variety of mechanisms. The inactivation of p53 can occur by either overexpression or deregulation of proteins that are critical for controlling the p53 pathway. Overexpression of HdmX or Hdm2 can occur as a result of gene amplification, enhanced transcription, or increased translation (Oliner et al., 1992; Ramos et al., 2001; Riemenschneider et al., 1999). Furthermore, deletion or silencing of the *INK4*a locus that encodes p14ARF can lead to elevated levels of Hdm2 since ARF would not be present to inactivate Hdm2 (Lowe and Sherr, 2003). Increased Hdm2 transcription due to a single nucleotide polymorphism (SNP) in the Hdm2 promoter can also result in increased levels of Hdm2 (Bond et al., 2004). The overexpression of either HdmX or Hdm2 can inhibit the activity of p53 and directly contribute to tumor

formation. Thus it is not surprising that elevated levels of one or both of these proteins are found in many human tumors and tumor cell lines which harbor wild-type p53 (Toledo and Wahl, 2006).

F. Role of HdmX and Hdm2 in Cancer

In approximately 30% of tumor cell lines retaining wild-type p53, HdmX and/or Hdm2 were overexpressed or HdmX was expressed as a shorter protein (Ramos et al., 2001). Recent analysis of a large set of tumors showed amplified *hdmX* expression in 19% of breast carcinomas, 19% of colon cancer, 18% of lung cancer (Danovi et al., 2004) and 65% of human retinoblastomas (Laurie et al., 2006). Overall, approximately 17% of all human tumors have overexpressed HdmX (Toledo and Wahl, 2006) and the majority of these possess wild-type p53. The overexpression of MdmX in mouse embryonic fibroblasts immortalizes the cells and with an activated Ras^{V12}, HdmX transforms primary cells (Danovi et al., 2004). These results suggest that HdmX may function as an oncogene when amplified or constitutively overexpressed, leading to tumor formation. Additionally, many tumor cell lines harbor an HdmX splicing variant, HdmX-S (HdmX short form, amino acid 1-114), which appears to be very stable and capable of binding to p53 more efficiently than the full length HdmX (Rallapalli et al., 1999; Rallapalli et al., 2003). Another aberrantly spliced form of HdmX lacking the p53 binding domain, HdmX211, was isolated from a thyroid tumor cell line. HdmX211 stabilized p53 by associating with Hdm2 and inhibiting Hdm2-mediated degradation of p53 without disrupting the Hdm2-p53 interaction thereby resulting in transcriptionally inactive p53 (Giglio et al., 2005). These HdmX splice variants are very powerful inhibitors of p53 transactivation, thus a cancer therapeutic that can effectively down regulate both full

length HdmX and the aberrantly spliced forms of HdmX may represent an important molecular target.

Diverse approaches to activate the wild-type p53 in tumors with overexpressed HdmX and/or Hdm2 include the use of small molecule antagonists such as Nutlin or RITA to inhibit the Hdm2-p53 interaction (Issaeva et al., 2004; Kojima et al., 2005; Patton et al., 2006; Vassilev, 2004), the use of antisense oligonucleotides, antibodies and small interfering RNAs directed at Hdm2 or HdmX (Chene, 2003; Linares and Scheffner, 2003; Zhang et al., 2005), and the use of compounds to inhibit the E3 ligase activity of Hdm2 (Yang et al., 2005). Both the Nutlin compounds and RITA are very effective at disrupting the Hdm2-p53 interaction leading to p53 activation and toxicity in tumor cell lines and xenograft tumors in mice (Issaeva et al., 2004; Vassilev et al., 2004). The activation of p53 by Nutlin does not induce phosphorylation of p53 on any of the six major serine sites (Thompson et al., 2004), suggesting that p53 phosphorylation is not required for activation of p53, induction of p53 target genes or a biological response. Furthermore, the combination treatment of Nutlin with either etoposide or cisplatin dramatically enhanced the activity of genotoxic agents in neuroblastoma (Barbieri et al., 2006). Another recent study using Nutlin and various chemotherapy drugs reported that nongenotoxic p53 activation resulting from blocking Mdm2-p53 association led to increased chemosensitivity to DNA damaging agents but not chemotherapy agents that work by inhibiting DNA replication (Kranz and Dobbelstein, 2006). However, these small molecule antagonists are not effective at disrupting the HdmX-p53 interaction, therefore, tumors with high levels of HdmX are resistant to Nutlin leading to the continued suppression of p53 activity (Patton et al., 2006). These findings suggest that

Hdm2 and HdmX are specific independent therapeutic targets for activating wild-type p53 and anti-cancer approaches that target both Hdm2 and HdmX should be considered as a means of treatment for tumors (Patton et al., 2006; Toledo et al., 2006).

The utilization of siRNA to knockdown endogenous HdmX expression in tumor cell lines with overexpressed HdmX and wild-type p53 has gained popularity. However, the conflicting data from these studies have been difficult to reconcile. The knockdown of HdmX inU2OS cells resulted in decreased Hdm2 and increased p53 levels in one study (Gu et al., 2002), while others reported that reduction of HdmX expression in U2OS and MCF7 cells increased both Hdm2 and p53 levels (Linares et al., 2003). Still others have observed no significant effect on Hdm2 and p53 levels after partial loss of HdmX by siRNA in MCF7 cells (Danovi et al., 2004). However, the down regulation of HdmX consistently resulted in an increased expression of p53 target genes (e.g. p21) in all these studies, despite the presence or absence of alterations in p53 protein levels. Furthermore, the removal of HdmX in tumors with overexpressed HdmX sensitized these cells to p53-dependent apoptosis or cell cycle arrest in response to Nutlin treatment (Patton et al., 2006). The knockdown of Hdm2 by siRNA in a colorectal adenocarcinoma cell line inhibited cell growth and tumor formation, and enhanced the chemosensitivity to cisplatin (Yu et al., 2006). Thus, the removal of Hdm2 and/or HdmX in tumors with wild-type p53 and overexpressed Hdms by siRNA appears to be a viable option for cancer therapy.

G. RNA Interference

RNA interference (RNAi) is a naturally occurring process for sequence specific silencing of genes post transcriptionally. It is a highly conserved mechanism the cell uses to

defend the genome from viruses. RNAi was first reported in 1998 in *C. elegans* after injection with double-stranded RNA (dsRNA) (Fire et al., 1998). The dsRNA molecules are recognized by the cell and cleaved by the cytoplasmic ribonuclease Dicer, into siRNAs containing 21-23 nucleotides. The siRNA molecules are incorporated into a multiprotein RNA-induced silencing complex (RISC) which guides its cleavage of complementary mRNA (Figure 4) (Dykxhoorn et al., 2003; Meister and Tuschl, 2004; Sandy et al., 2005). Assessing the function of a gene by silencing its transcript has become a common practice. Although there are numerous methods that can successfully be employed to silence a gene, including synthetic siRNAs, expression vectors with short hairpin RNAs, viral vectors and *in vitro* transcribed siRNA (Elbashir et al., 2001a; Elbashir et al., 2001b; Katoh et al., 2003; Liu et al., 2004; Paddison et al., 2002), they do not always yield the same result. Thus, it is critical to understand that RNAi may non-specifically target unrelated genes, altering their expression and possibly leading to an unexpected or even cytotoxic phenotype (Fedorov et al., 2006; Fish and Kruithof, 2004; Jackson et al., 2003). Some of these non-specific effects can be explained by the induction of an interferon response triggered by the processing of shRNA vectors in the cell (Bridge et al., 2003; Sledz et al., 2003) or by viral infection (Stark et al., 1998). However, the activation of unexpected non-targeted genes can also occur in the absence of an interferon response (Scacheri et al., 2004) or in tumor cells that have a defective interferon response (Stojdl et al., 2000). It is speculated that partial complementary sequence matches between the siRNA and the off-target genes may account for some gene expression alterations (Lin et al., 2005), thus using the lowest effective dose of siRNA and using different siRNA target sequences for your gene of interest will decrease

the likelihood of an off-target gene being altered. Although the art of designing effective and specific siRNAs has advanced greatly over recent years (Birmingham et al., 2006; Braasch et al., 2003; Jackson et al., 2006), new concerns regarding the therapeutic potential of RNAi have arisen. These concerns include renal excretion of unmodified circulating siRNA, rapid degradation by intracellular and extracellular nucleases, and delivery of the siRNA to the target organ(s) (reviewed by Lee and Sinko, 2006). Some of these concerns have been eliminated by incorporating siRNA into particles, conjugating the siRNA to a transporter, such as cholesterol, or using the specificity of an antibody to deliver the siRNA to the target cells (Dykxhoorn and Lieberman, 2006). Modified siRNA targeting vascular endothelial growth factor (VEGF) effectively inhibited tumor growth in mice when injected locally into subcutaneous tumors (Kim et al., 2006; Takei et al., 2004).

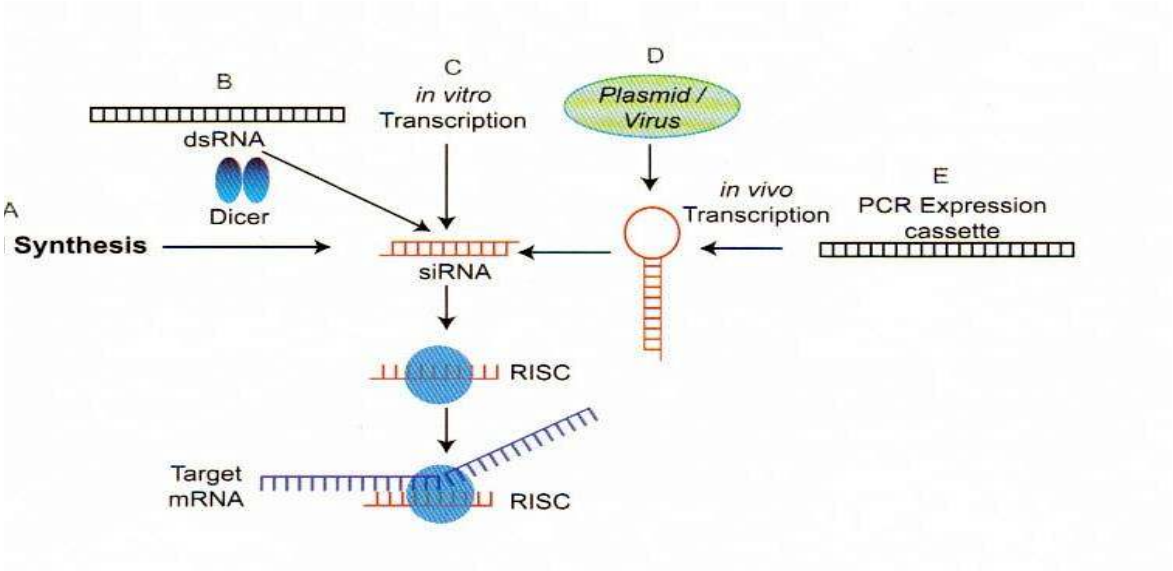

Figure 4. Mechanism of RNAi. The diagram illustrates five methods for producing siRNAs; (A) chemical synthesis, (B) digestion by Dicer, (C) in vitro transcription, (D) plasmid/viral expression vectors, and (E) PCR expression cassette. The siRNA is incorporated into RISC, and binds and cleaves the target mRNA (www.dharmacon.com).

H. Rationale for Study

The p53 tumor suppressor protein must be tightly regulated since either a gain or loss of activity can have serious physiological consequences. Hdm2 is thought to be the primary regulator of p53 and the p53-Hdm2 negative feedback loop is well established. However, the role of HdmX in the regulation of p53 and Hdm2 is still controversial and further studies are needed to specifically elucidate its function(s) in the regulation of the p53 pathway and in tumorgenesis. Since the discovery of HdmX in 1996 as a p53 binding protein with significant homology to Hdm2, research into HdmX activities has led to the conclusion that it is an essential negative regulator of p53. The importance of HdmX was demonstrated by the embryonic lethality of MdmX knockout mice, and more recently by the discovery that 17% of human tumors overexpress HdmX, with the majority harboring wild-type p53. Thus, this dissertation research takes an in depth look at the alterations in global gene expression and the biological effects of silencing HdmX and/or Hdm2 in tumor cell lines with wild-type p53. My hypothesis is that loss of HdmX in tumors with wild-type p53 and overexpressed HdmX will activate p53 and p53 target genes, leading to growth inhibition. Since HdmX binds directly to p53 and Hdm2, this study also examines how HdmX knockdown affects p53 and Hdm2 localization and stabilization. Furthermore, this study investigates how the elimination of HdmX affects the sensitivity of the tumor cells to chemotherapeutic agents. As shown with Nutlin, a small molecule that inhibits p53-Mdm2 interaction, the removal of HdmX enhances the p53-dependent cytotoxicity of Nutlin indicating that HdmX is a key therapeutic target that can complement chemotherapy drugs currently used to treat tumors with wild-type p53.

II. MATERIALS AND METHODS

A. Cell Lines, Antibodies, and Reagents

The human tumor cell lines, MCF7 (breast carcinoma), HCT116-p53+/+ and HCT116-p53-/- (colorectal carcinoma), U2OS (osteosarcoma), U87 (glioblastoma), H1299 (non-small cell lung carcinoma) and SAOS (osteosarcoma) were grown in Dulbecco's Modified Eagle's Medium (DMEM; Cellgro) supplemented with 10% bovine growth serum (BGS; Hyclone), and 10 μg/mL gentamicin unless otherwise indicated. The diploid human fibroblast cell line, IMR90 (ATCC) was grown in DMEM supplemented with 10% fetal bovine serum (FBS; Gibco), and 10 μg/mL gentamicin unless otherwise indicated. HdmX (Bethyl Laboratories, Inc.), p21, (C-19, Santa Cruz Biotechnology, Inc.), and BAX, (Ab-1, Calbiochem) polyclonal antibodies, and monoclonal p53 antibody (Ab-6, Oncogene), Hdm2 antibody (SMP-14, Santa Cruz Biotechnology, Inc.) and beta-actin antibody (Sigma, Inc.) were used as indicated. A phosphorylation-specific p53 polyclonal antibody kit (Cell Signaling Technology, Inc.) was utilized per manufacturer's protocol. Horseradish peroxidase (HRP)-conjugated anti-mouse or anti-rabbit secondary antibodies (Promega) were used with Super Signal substrate (Pierce) for chemi-luminescence detection of proteins. siGENOME duplex RNA targeting *hdmX, hdm2, p53,* and a non-targeting control siRNA (5'-UAGCGACUAAACACAUCAAUU) were obtained from Dharmacon Research, Inc. and

a 20 μM stock solution was prepared according to manufacturer's protocol. siRNA aliquots were stored at -20^{o}C and used within three freeze thaw cycles. The siRNA transfection was performed using either Oligofectamine (Invitrogen) or Lipofectamine 2000 (Invitrogen) as described below. To optimize siRNA transfection efficiency, siTOX (Dharmacon Research, Inc.) was employed. Doxorubicin hydrochloride (Tocris Bioscience) was prepared as a 5 mg/mL stock solution in water. Cytosine β-D-arabinofuranoside (Sigma, Inc.) was prepared as a 10 mM stock in DMSO and cis-diammine platinum (II) dichloride (Sigma, Inc.) was prepared as a 25 mM stock solution in Dulbecco's phosphate buffered saline (DPBS) containing Ca^{+2} and Mg^{+2}. Recombinant human Interferon-gamma (IFN-γ) was purchased from R & D Systems.

B. siRNA Transfection

Cells were either triple transfected with siRNA on three consecutive days post seeding, or reverse transfected at the time of seeding plus transfected again 24 hours later (Figure 5). Cells were seeded at 200,000 cells per well in 6-well plates (for RNA isolation), or at 700,000 cells per 6-cm dish (for protein extraction) in antibiotic free DMEM. For triple transfection, cells were plated 24 hours prior to the first siRNA transfection. Dilutions of the Oligofectamine and siRNA stock solutions were prepared as follows immediately prior to transfection (Table 1). For each well of a 6-well plate, 3 μL of Oligofectamine was diluted with 112 μL serum free media (SFM) and allowed to incubate at room temperature for 10 minutes. 5 μL of siRNA was mixed with 180 μL SFM, and then it was added to the tube containing the diluted Oligofectamine. The mixture was allowed to incubate for 20-30 minutes at room temperature. The cells were washed once in SFM, and then 700 μL SFM was added to each well of a 6-well plate.

The 300 μL of siRNA/Oligofectamine mixture was added to each well for a final concentration of 100 nM siRNA (Dharmacon Research, Inc.) per well. The volumes of Oligofectamine, siRNA, and SFM were adjusted appropriately for transfection in a 6-cm dish so that the final concentration of siRNA was 100 nM and the final volume was 1.5 mL/dish (Table 1). After a four hour incubation at 37^{o}C in a 5% CO_2 incubator, 1 mL (or an equal volume) of DMEM containing 20% BGS was added to each well without removing the transfection mixture. The siRNA transfection was repeated a second and third time at 24 and 48 hours following the first transfection, respectively.

For reverse transfection, the cells were transfected with 100 nM siRNA at the time of seeding using Lipofectamine 2000 (Invitrogen) in a small volume of antibiotic free DMEM containing 1% BGS. After a five hour incubation, the media was removed and cells were refed with DMEM containing 10% BGS. Twenty hours later, the cells were transfected a second time with siRNA in SFM using Oligofectamine as indicated above for the triple transfection. After a four hour incubation, an equal volume of DMEM containing 20% BGS was added to each well or dish without removing the transfection mixture. Total RNA was isolated 24 hours following the last siRNA transfection and protein was extracted at 48 hours following the last siRNA transfection unless otherwise indicated.

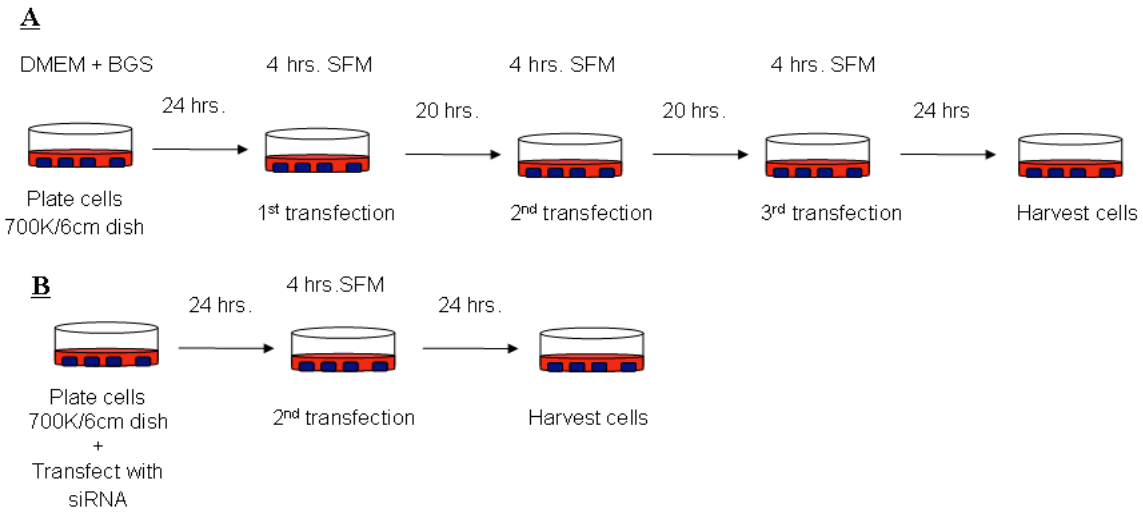

Figure 5. Timeline of siRNA transfections in human tumor cell lines.

(A) The triple transfection method involves transfecting the cells with siRNA on three consecutive days 24 hours post seeding. (B) The reverse transfection method involves seeding the cells with the siRNA:lipid mixture and then transfecting the adherent cells a second time 24 hours later.

	24-well plate	6-well plate	6-cm dish
Cell Number	100,000/well	200,000/well	700,000/dish
Volume of siRNA +SFM	2.5 µL siRNA + 182.5 µL SFM	5 µL siRNA + 180 µL SFM	7.5 µL siRNA + 177.5 µL SFM
Volume of Oligofectamine + SFM	1.5 µL lipid + 113.5 µL SFM	3 µL lipid + 112 µL SFM	4.5 µL lipid + 110.5 µL SFM
Total Volume	0.5 mL	1.0 mL	1.5 mL

Table 1. Volumes of siRNA, lipid, and serum free media (SFM) for siRNA transfections. The table lists the appropriate volumes of each component necessary to setup a 100 nM siRNA transfection in the various cell culture vessels.

C. shRNA Lentivirus Generation and Infection

Complementary DNA oligonucleotides were designed, synthesized and annealed to generate a double-stranded oligonucleotide (ds oligo). The ds oligonucleotides contain a 21 nucleotide target sequence, a four nucleotide loop sequence (GAGA), a 21 nucleotide sequence that is the reverse complement of the target sequence, and a four nucleotide 5' overhang sequence required to facilitate directional cloning (Figure 6). The double stranded oligonucleotides (5'-CACCGCAGTTAGGTGTTGGAATATTGAGA-AATATTCCAACACCTAACTGC), HdmX sequence underlined) targeting *HdmX* and *lacZ* (5'-CACCAAATCGCTGATTTGTGTAGTCGGAGACGACTACACAAATCA-GCGA) were cloned into the pENTR™/H1/TO vector (Invitrogen) using T4 DNA Ligase per manufacturer's protocol. The ligation reaction was transformed into *E coli*, kanamycin-resistant transformants were selected, and colonies were analyzed for the desired entry clone. The resulting RNAi cassette was transferred from the entry clones into either the pLenti4/BLOCK-iT™-DEST vector (Invitrogen) containing the Zeocin™ resistance gene, or the pLenti6/BLOCK-iT™-DEST vector (Invitrogen) containing the Blasticidin resistance gene via a LR clonase recombination reaction per manufacturer's protocol. The recombination reaction was transformed into *E.coli*, and ampicillin-resistant transformants were selected. The plasmid DNA was isolated using the Qiagen Maxi-prep method, quantified via absorbance spectroscopy at 260 nm, and the expression constructs were sequenced to verify that the RNAi cassette transferred properly. The pLenti/ BLOCK-iT™-shRNA expression constructs were then packaged into replication incompetent lentivirus by co-transfecting the pLenti-shRNA constructs and ViraPower™ packaging plasmids (Invitrogen) into 293FT cells per manufacturer's protocol using

Lipofectamine 2000 (Figure 7). The Lentivirus containing supernatants from the transduced 293FT cells were collected 60 hours later and the cellular debris was removed by centrifugation. The viral supernatant was aliquoted into 1 mL cryovials and stored at -80^{o}C. Viral titers were determined by preparing 10-fold dilutions of the lentiviral stocks, transducing the different dilutions of lentivirus into NIH3T3 cells, selecting for stably transduced cells using the appropriate selection agent, staining cells with 1% crystal violet and counting the number of antibiotic-resistant colonies in each dilution. Our viral titers were typically between $10^4 – 10^6$ plaque forming units (PFU) per mL.

The tumor cells were seeded at 200,000 cells per 6-cm dish 24 hours prior to infection with the shRNA containing lentivirus. The lentiviral supernatant was thawed and diluted in a small volume of antibiotic free media containing 10%BGS and 6µg/mL Polybrene®. The media was removed from the cells and 1.5 mL of diluted virus was added to the 6-cm dish to achieve a MOI (multiplicity of infection) of at least two. After incubation at 37^{o}C for 18 hours, the media containing virus was removed and replaced with fresh, complete media. The appropriate antibiotic selection was applied 24 hours later and continued for six to ten days until a control plate of non-transduced cells had all died. Blasticidin and Zeocin™ (Invitrogen) kill curves were performed to determine the lowest effective dose for selection in each of the tumor cell lines used (Table 2). Additionally, the pLenti6-GW/U6-lamin^{shRNA} control plasmid (Invitrogen) was packaged into lentivirus as previously described and used as an additional control. Antibiotic resistant cells were harvested for total RNA or protein at the time points indicated.

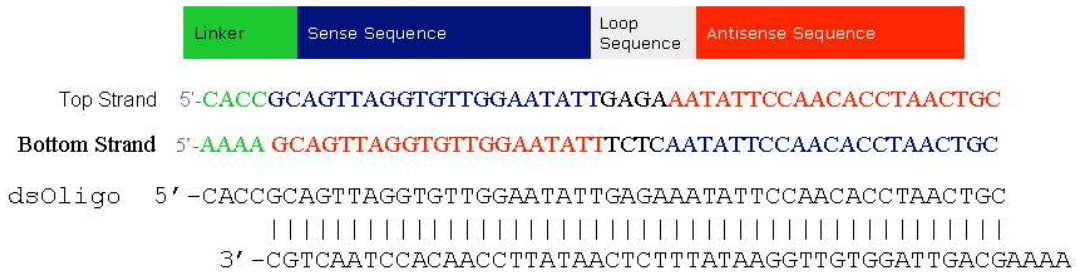

Figure 6. Design of double-stranded oligonucleotide. The ds oligos contain a 5' linker for directional cloning into the entry vector, a 21 nucleotide sense sequence, a four nucleotide loop sequence and a 21 nucleotide antisense sequence.

Cells	Zeocin™	Blasticidin
MCF7	750 μg/mL	6 μg/mL
U2OS	500 μg/mL	6 μg/mL
U87	n/a	4-6 μg/mL
HCT116-p53+/+	50 μg/mL	10 μg/mL
HCT116-p53-/-	25 μg/mL	8 μg/mL

Table 2. Dose of antibiotics used for selection. The table shows the lowest effective dose of antibiotic that was used for the selection of cells expressing the shRNA lentivirus vector.

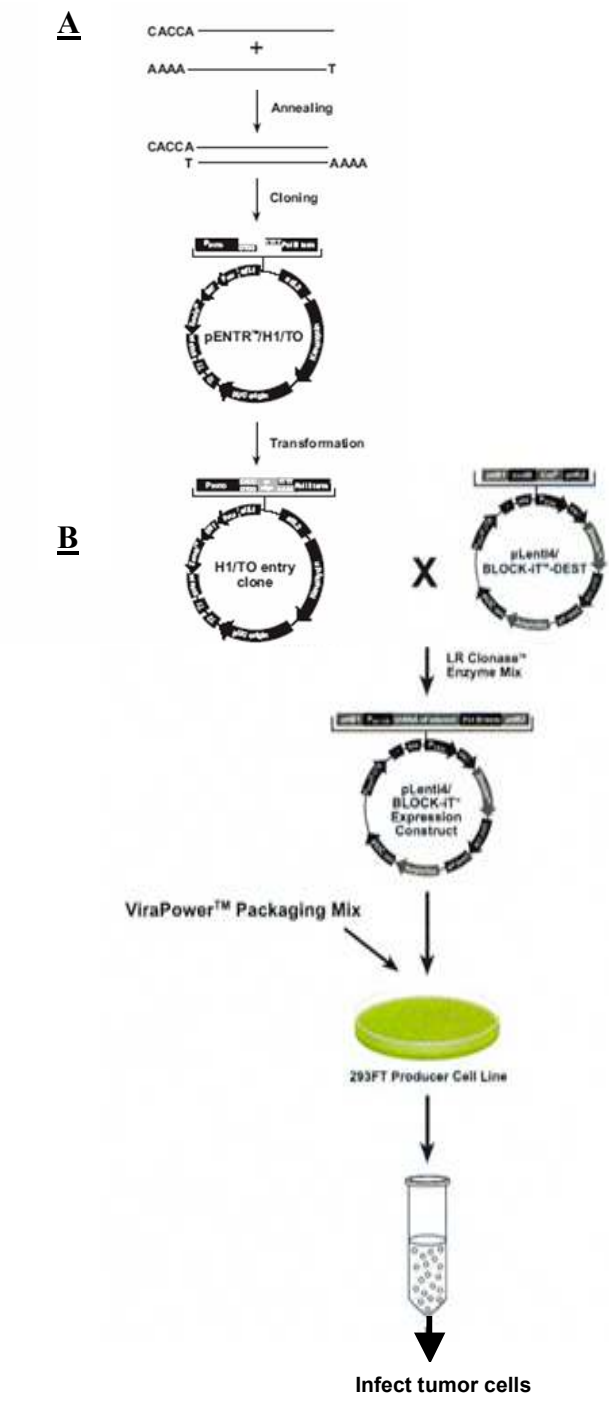

Figure 7. Preparation of shRNA expressing lentivirus. (A) Preparation of entry clone. (B) LR recombination reaction between entry construct and pLenti/BLOCK-iT™ destination construct. (adapted from www.invitrogen.com).

D. Affymetrix GeneChip Sample Preparation, Hybridization, and Scanning

MCF7 cells were seeded at 200,000 cells/well in 6-well plates 24 hours prior to siRNA triple transfection. Each treatment condition; mock, siControl, siHdmX, siHdm2, sip53 and siHdmX+sip53, was set up in triplicate and transfected as previously described. Twenty four hours following the third transfection, cells were rinsed once with DPBS and then 350 µL RLT lysis buffer (Qiagen) containing 1% β-Mercaptoethanol (β-ME) was added directly to the wells. The lysate was transferred to a sterile RNase-free 1.7 mL Eppendorf tube and total RNA was isolated using the RNeasy® Mini Kit (Qiagen) per manufacturer's protocol. The RNA was eluted from the RNeasy® spin column with 30 µL sterile RNase-free water. The RNA integrity and quantification were determined on the Agilent 2100 Bioanalyzer using the RNA6000 Nano Labchip® according to manufacturer's protocol. A small amount of the RNA was diluted 1:10 in RNase-free water prior to loading on the Nano Labchip® in order to obtain a concentration within the 25-500 ng range of the bioanalyzer.

First strand cDNA synthesis was performed with 5 µg of total RNA, 2 µL of 50 µM T7-Oligo(dT) Primer, 7 µL of First-Strand Master Mix and 1 µL of SuperScript II enzyme per the One-Cycle cDNA Synthesis Kit (Affymetrix) protocol. Eukaryotic Poly-A RNA controls (Affymetrix) were also included in the cDNA synthesis reaction as quality control markers for the length and quantity of cDNA produced. RNase H-dependent second strand cDNA synthesis was performed using 10 units of DNA ligase and 40 units of DNA Polymerase I according to the One-Cycle cDNA Synthesis Kit (Affymetrix) protocol. The double-stranded cDNA was purified using the GeneChip Sample Cleanup Module (Affymetrix) per manufacturer's protocol. Biotin-labeled

cRNA was synthesized using the GeneChip IVT Labeling Kit (Affymetrix) according to the manufacturer's protocol, utilizing T7 RNA polymerase and biotinylated nucleotides to produce labeled single stranded cRNA. The cRNA was purified using the GeneChip Sample Cleanup Module (Affymetrix) in order to remove unincorporated NTPs so that the concentration of cRNA can be accurately determined. The cRNA was eluted from the spin column in 40 μL RNase-free water, and then a small aliquot was diluted 1:10 in RNase-free water for analysis on the Agilent 2100 Bioanalyzer as previously described. Twenty micrograms of cRNA was fragmented by incubating the cRNA in Fragmentation Buffer (Affymetrix) that has been optimized to cleave full-length cRNA into 35 to 200 base fragments by metal-induced hydrolysis at 94^{o}C for 35 minutes. A small aliquot of the fragmented cRNA was analyzed on the Agilent Bioanalyzer to confirm that the cRNA was properly fragmented.

Fifteen micrograms of fragmented cRNA along with GeneChip Eukaryotic Hybridization Controls (Affymetrix) were hybridized to the GeneChip® Human Genome U133 Plus 2.0 Array (Affymetrix) containing over 47,000 transcripts and variants, representing approximately 39,000 human genes. The probe arrays were filled with 200 μL of hybridization cocktail per manufacturer's suggestion and hybridization was performed for 16 hours in an Affymetrix GeneChip Hybridization Oven 640 at 45^{o}C under constant rotation at 60 rpm. The GeneChips were subjected to multiple washing and staining cycles on the Affymetrix GeneChip Fluidics Station 450 using the EukGE-WS2v5 protocol. Immediately after staining, the GeneChips were scanned at 570 nm on an Affymetrix Scanner 3000 following protocols developed by Affymetrix for the HG-U133 Plus 2.0 Array (Figure 8). The digitized images from the scanned chips were

processed using Affymetrix GCOS software and global GeneChip scaling to a target intensity value of 150.

E. Analysis of GeneChip Data

Each siRNA transfection condition was performed in triplicate and the RNA samples were prepared individually for hybridization to three separate Affymetrix HG-U133 Plus 2.0 Arrays. All analyses of the GeneChip data were performed using Affymetrix MAS 5.0 and GeneSpring version 7.3 software. To determine which genes were altered following knockdown of HdmX, Hdm2, p53, or the combination of HdmX+p53, the following data mining approach was employed. The Affymetrix CHP files were imported into GeneSpring. In GeneSpring the chips were normalized to the fiftieth percentile and each gene normalized to its median relative expression. Next gene lists were created containing those genes which show a 2-fold increase or greater relative to siControl, or at least a 50% decrease relative to siControl. Additionally, only those genes that were identified as being present or marginal in at least two of the three replicates in the condition where expression is expected were included in the lists. Based on these criteria, 364 genes were induced and 188 genes were suppressed following knockdown of HdmX. To identify common genes between two lists (i.e. siHdmX and siHdm2), Venn diagrams were utilized in GeneSpring, and Ingenuity Pathway Analysis software was used to create pathway maps of interacting genes.

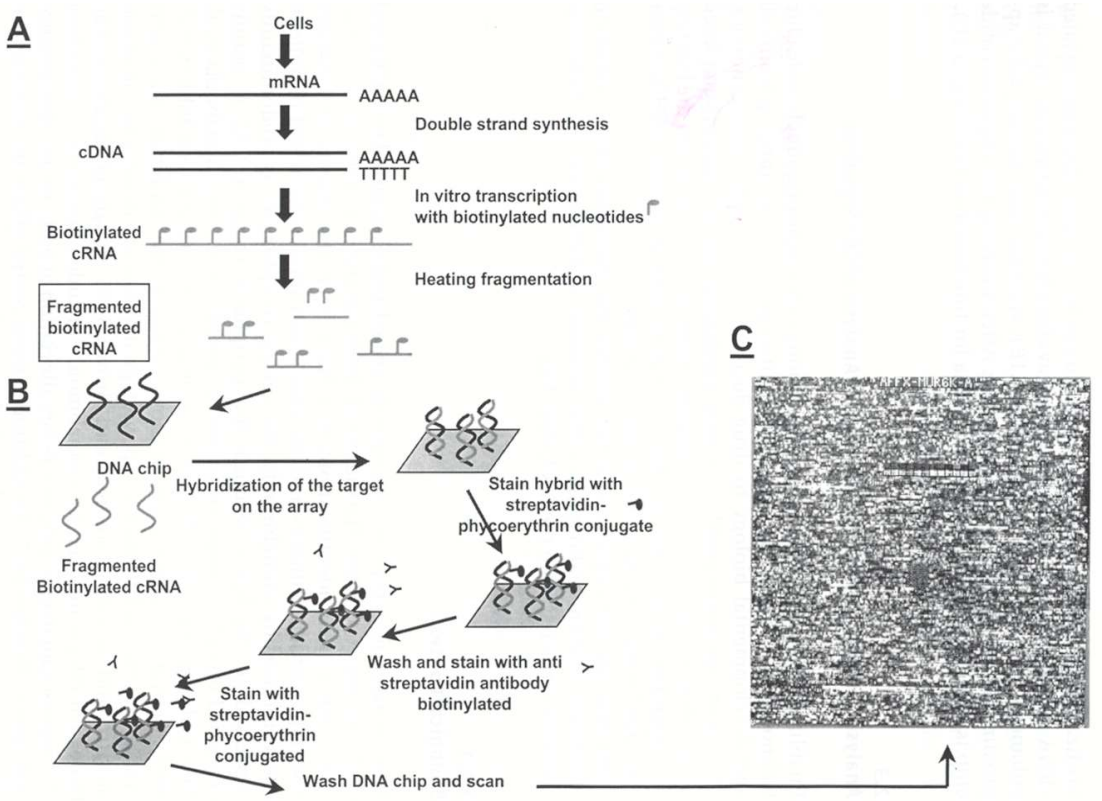

Figure 8. Affymetrix GeneChip® Protocol. (A) Preparation of fragmented, biotinylated cRNA. (B) GeneChip hybridization, staining, and washing. (C) A representative image of scanned GeneChip.

F. Quantitative RT-PCR

Cells were rinsed once in DPBS, lysed directly in the culture dish with RLT buffer as previously indicated, and total RNA was isolated using the RNeasy® Mini Kit (Qiagen) according to manufacturer's protocol. The RNA was quantified by absorbance at 260 nm (A_{260}) by diluting 2 µL of the RNA in 98 µL TE (10 mM Tris-Cl, 1 mM EDTA, pH 8.0), transferring the solution to a quartz cuvette and measuring the absorbance on a spectrophotometer relative to a TE blank. The RNA concentration was determined in µg/µL by the following equation: [RNA] = (40 µg/mL)(A_{260})(dilution factor) (1mL/1000µL) assuming that an A_{260} of 1 corresponded to 40 µg of RNA per mL. The purity of the RNA was estimated by the ratio of the absorbance at 260 nm and 280 nm (A_{260}/A_{280}), with pure RNA having a ratio of 1.8-2.1. Each RNA sample was individually reverse transcribed with random hexamers to create cDNA using the TaqMan Reverse Transcription Kit (Applied Biosystems) per manufacturer's protocol. Briefly, 1 µg of RNA was mixed with 2.5 µL of 10X TaqMan RT buffer, 5.5 µL of 25 mM $MgCl_2$, 5.0 µL of deoxyNTPs, 1.25 µL of random hexamers, 0.5 µL of RNase inhibitor, 0.625 µL of Multiscribe reverse transcriptase, and RNase-free water for a total reaction volume of 25 µL. The reverse transcription (RT) reaction was performed in a Perkin Elmer Gene Amp PCR System 2400 programmed to sequentially cycle as follows: initial 10 minute incubation at 25°C, 30 minute RT step at 48°C, 5 minute inactivation step at 95°C, and an infinite hold at 4°C. After RT reaction was complete, cDNA was diluted 1:2 by adding 25 µL sterile DNAse-free water to each sample prior to storage at -20°C.

Quantitative real-time PCR was performed in a 96-well microtiter plate format on an ABI Prism 7900HT sequence detection system. A 20 µL reaction was prepared by mixing 1µL of cDNA, 8 µL of DNAse-free water, 10 µL of 2X TaqMan Universal PCR master mix, and 1 µL of Assay-on-Demand Gene Expression product (Applied Biosystems, containing forward and reverse primers and a fluorescent Taqman probe) designed and optimized for gene of interest, to each well on the 96-well plate. The PCR conditions include a 2 minute hold at 50^{o}C, a 10 minute hold at 95^{o}C, and 40 cycles of a 15 second 95^{o}C denaturing step and a 1 minute 60^{o}C anneal and elongation step. Each cDNA sample was separately analyzed in triplicate for target gene and GAPDH, and the fold change (RQ value) relative to the control sample was calculated based on a PCR efficiency of two and normalized to GAPDH (endogenous control) RNA levels using SDS 2.0 software (ABI). Outlier cycle threshold (CT) values were eliminated and defined as being a least one full CT from the mean value of the other two replicates. The mean RQ values are plotted and the error bars represent the standard deviation of 6-9 reactions per RNAi treatment condition.

G. Western Blot Analysis

Cells were harvested following selection or at 48 hours post siRNA transfection unless otherwise indicated. The media was removed and the cells were washed once with cold DPBS. A volume of 1 mL of cold DPBS was added to each 6-cm dish, the cells were scraped from the dish, transferred to a sterile 1.7 mL Eppendorf tube and centrifuged for 5 minutes at 2000 rpm to pellet the cells. The DPBS was aspirated and the cell pellet was frozen at -80^{o}C overnight. A whole cell extract was prepared by thawing the cells on ice and resuspending the cell pellet in 150 µL cold Giordano's

buffer (Mancini et al., 2004) composed of 50 mM Tris-HCl, pH 7.4, 0.25 M NaCl, 0.1% Triton X-100, 5 mM EDTA, and 1% protease inhibitor cocktail (Sigma) by pipetting up and down to lyse the cells. The cell suspension was placed on ice for 40 minutes to allow complete protein extraction, centrifuged for 10 minutes at 10,000 rpm, and the soluble protein fraction was transferred to a separate tube. Alternatively, the cells were lysed directly in the dish by adding 250 µL of phosphatase inhibitor extraction buffer (120 mM NaCl, 50 mM Tris-HCl (pH 8.0), 5 mM EGTA, 1 mM EDTA, 5 mM NaPPi, 10 mM NaF, 30 mM p-nitrophenyl phosphate disodium salt (Pierce), 1 mM Benzamidine, 0.1% NP-40 (Ipegal Ca-630), 0.2 mM PMSF, and 1% protease inhibitor cocktail) to each dish and allowing it to sit on ice for 10 minutes. The cells were then scraped from the dish, transferred to a sterile 1.7 mL Eppendorf tube, and placed on ice for an additional 30 minutes to allow cells to lyse. The cell suspension was centrifuged for 10 minutes at 10,000 rpm and the soluble protein fraction was transferred to a separate tube. Protein concentration was determined using the Bradford method by mixing 1 µL of the whole cell extract with 799 µL sterile distilled water (SDW) and 200 µL Bradford reagent (Bio-Rad Inc.). The mixtures were transferred to a 96-well plate (200 µL/well) and absorbance at 595 nm was determined in duplicate on a spectrophotometer. A standard curve was generated using bovine serum albumin (BSA) protein ranging from 0.5 µg/µL to 10 µg/µL. The sample absorbance values were regressed against the standard curve to determine protein concentration. An amount of 200 µg of protein was mixed with an equal volume of 2X SDS loading dye (60 mM Tris, pH 7.6, 2% SDS, 10% glycerol, 5% β-ME, and 1% bromophenol blue), and boiled at 100^{o}C for 5 minutes prior to loading on a sodium dodecyl sulfate 10% polyacrylamide gel. The gel was run at 150 constant volts

for approximately 5 hours in 1X SDS running buffer (25 mM Tris pH 8.3, 250 mM glycine, 0.1% SDS). The proteins were transferred onto a polyvinylidene difluoride membrane (Millipore) in a transfer buffer (25 mM Tris, 192 mM glycine, 20% methanol, pH 8.3) using a Transblot system (Bio-Rad) overnight at 50 constant volts. The membrane was incubated in 50 mL blocking buffer (1X Tris Buffered Saline (TBS), 5% non-fat dry milk, 0.2% Tween-20) for 1 hour on a rotary platform shaker at room temperature. Immunoblotting was performed at room temperature using the appropriate primary antibodies at 1:500-1:10,000 dilution in 1X TBS containing 5% non-fat dry milk for a least 1 hour on a rocker. The blot was then washed 3 times for 15 minutes each in TTBS (1X TBS, 0.1% Tween-20) on a platform shaker. The appropriate secondary antibody, either goat anti-mouse or goat anti-rabbit HRP-conjugated (Promega), was diluted 1:5,000-1:10,000 in 1X TBS containing 5% non-fat dry milk and added to the blot for at least 1 hour on a rocker. The membrane was washed 3 times in TTBS as previously described, and then exposed to Super Signal chemiluminescent reagent (Pierce) for 3-4 minutes, and protein was visualized on a FUJI FILM LAS 3000 image reader. The antibodies were removed from the membrane by incubating the blot in Western strip buffer (25 mM glycine, 1% SDS, pH 2.0) for 30 minutes at room temperature on a platform shaker. The membrane was then immunoblotted with another primary antibody according to the method indicated above.

H. Luciferase Repoter Assay

MCF7 cells were seeded at 100,000 cells per well in a 24-well plate, and were reverse transfected with 100 nM siRNA at the time of seeding in duplicate per siRNA target. After 24 hour incubation at 37^{o}C, the cells were co-transfected with siRNA, the

p53 Luciferase reporter plasmid, pG13Luc, and the Renilla luciferase plasmid, RLuc. The pG13Luc plasmid contains 13 copies of the p53 consensus sequence, 5'-PuPuPuC(A/T)(T/A)GPyPyPy (El-Deiry et. al., 1992) in its promoter and the RLuc plasmid was used as a transfection efficiency control. The amount of luciferase protein expressed in the sample correlates with the level of p53 transcriptional activity. Twenty-four hours post co-transfection, the cells were lysed directly in the plate by adding 75 μL Passive Lysis buffer (Promega) per well and placing the plate on a rocker for 30 minutes. The lysates were transferred to a sterile 1.7 mL Eppendorf tubes and p53 transactivation was determined using the Dual-Luciferase Assay (Promega) per the manufacturer's protocol. Briefly, a 5 μL aliquot of the extract was thoroughly mixed in 50 μL LAS reagent (Promega), and place immediately in the luminometer. The value was recorded, and then 50 μL of Stop & Glo reagent (Promega) was added to the tube, mixed and placed in the luminometer to determine RLuc value. Each sample was analyzed in duplicate and the ratio of the pG13Luc value to RLuc value was determined. Cells treated with 0.5 μg/mL doxorubicin for 24 hours were used as a positive control for p53 transcriptional activity, while cells transfected with sip53 served as a negative control for the assay. Non-transfected cells were used to measure background activity. The mean pG13Luc/RLuc ratio was graphed and error bars represent the standard deviation derived from relative luciferase values from 4-6 samples per RNAi treatment condition.

I. Colony Formation Assay

Cells were reverse transfected with siRNA and 24 hours later transfected a second time with siRNA as previously described. Then 24 hours following the second transfection, the cells were trypsinized in 1 mL of 0.25% Trypsin/EDTA (Gibco) per 6-

cm dish. Once the cells detached from the dish, they were diluted in complete media, counted on a hemocytometer and reseeded at 500 cells per well in 6-well plates in antibiotic free DMEM containing 10% BGS. The cells were allowed to grow and form colonies for ten days during which time the media was changed every three days. After ten days, the colonies were fixed and stained for 20 minutes with 1% crystal violet in 70% methanol. The excess stain was removed by washing the plates with water until the water was clear. The plates were allowed to air dry, and the colonies were counted, or quantified on the FUJI FILM LAS 3000 image reader.

J. Cell Proliferation Assay

Cells were trypsinized 24 hours after the second siRNA transfection, counted on a hemocytometer, and seeded at 2,000 cells per well in quadruplicate. The seeding efficiency of the various siRNA transfected cells was determined the following day after seeding (Day 0) by removing the culture media, fixing and staining the attached cells with 1% crystal violet in 70% methanol, washing off the excess stain, extracting the bound stain with 100 µL of 10% acetic acid per well, and determining absorbance at 590 nm (A_{590}) on a spectrophotometer. The seeding efficiencies appeared to be very similar among all the transfected cells. Cell proliferation was determined on Days 2, 4, 6, and 8 relative to Day 0 by fixing and staining the cells as indicated above. The A_{590} value obtained on Day 0 was used for normalization. Growth curves were generated by plotting mean A_{590} vs. Day, and error bars represent the standard deviation of 4 samples per time point per siRNA transfection condition.

To determine cell viability post treatment with chemotherapeutic agents, cells were seeded at 20,000 cells/well in 96-well plates in triplicate. Cell viability was assessed

by using either CellQuanti-Blue™ Reagent (BioAssay Systems) according to manufacturer's protocol or by staining the cells with 1% crystal violet and quantifying the stain by reading absorbance at 590 nm as previously described. Cells were treated with various doses of the chemotherapy drug on Day 0, and incubated at 37^{o}C for 24 or 48 hours. After drug treatment, the media was removed, cells were washed once in media to remove drug, and 150 μL of fresh media containing 10% CellQuanti-Blue™ Reagent was added to each well. The plates were returned to the incubator and approximately two hours later, 100 μL of media per well was transferred to a black 96-well plate (Costar) and fluorescence intensity (FI) was determined at 530 nm excitation, 590 nm emission on a Safire^{2} Fluorescence plate reader (TECAN). The cell viability (%) was calculated by the following equation: % cell viability = 100 x (FI_{cmpd}/FI_{con}) where FI_{cmpd} is the FI in the presence of drug and FI_{con} is the average FI in the absence of the drug. The average % cell viability is plotted for each dose and error bars represent the standard deviation of 3 samples.

K. Flow Cytometry

Cells were trypsinized in 1 mL of 0.25%Trypsin/EDTA per 6-cm dish 18-24 hours after the last siRNA transfection. Trypsinized cells were collected in a 15 mL sterile centrifuge tube, centrifuged at 1200 rpm for 5 minutes to pellet the cells and then the cells were washed once in 5 mL DPBS. The cells were pelleted by centrifugation as above, the DPBS was decanted and the cells were resuspended in the small volume remaining by flicking the tube. While vortexing, 2 mL of 70% ethanol was added to each tube in a drop-wise manner, and the tubes were stored at -20^{o}C until ready to do flow analysis. The tubes were centrifuged at 1200 rpm for 5 minutes to pellet the cells, the

cells were washed once in DPBS, centrifuged again, and the cells were suspended in the remaining liquid. The cells were treated with 500 µL of RNAse A (1 mg/mL) in DPBS for 20 minutes at 37°C, and then stained with 50 µg/mL propidium iodide (Sigma, Inc.) and placed on ice for 30 minutes. The cell suspensions were transferred to flow tubes and covered with foil to protect from light. Cell cycle distribution was determined by flow cytometry (channel FL2) on a FACSCAN (Becton Dickinson). The experiment was repeated three times and the percentage of cells in G1, S, and G2/M phases were obtained using ModFit LT 3.0 software (Verity Software House, Inc.). The ratio of G1 to S phase cells is indicated in the bar graph.

L. Nuclear and Cytoplasmic Protein Extraction

MCF7 cells were triple transfected and 24 hours following the last siRNA transfection, the cells were refed with fresh media containing 20 µM MG132 for 4 hours to inhibit proteosomal degradation of HdmX, Hdm2 and p53 protein. After 4 hours, the cells were washed once with DPBS, scraped from the dish, and transferred to a sterile tube for centrifugation. The cell pellet was resuspended in 200 µL cold CER I reagent (Pierce) by vigorously vortexing, and then the cells were placed on ice for 10 minutes. Next, 15 µL CER II reagent (Pierce) was added to each tube and the cytoplasmic extract fraction was prepared. The remaining cell pellet was resuspended in 90 µL cold NER reagent (Pierce) and the nuclear extract fraction was isolated per manufacturer's protocol. Protein concentration was determined by Bradford method and extracts were stored at -80°C. 150 µg of protein was loaded per lane on a SDS 10% polyacrylamide gel and Western blot analysis was performed as previously described.

III. RESULTS

A. Selection of *hdmX* target sequence and siRNA transfection optimization.

To examine the effects of HdmX knockdown on tumor cells with wild-type p53 and over-expressed HdmX, several human tumor cell lines were utilized. The baseline levels of *hdmX*, *hdm2*, and *p53* gene expression were determined for each cell line by quantitative real time-PCR (RT-PCR) (Figure 9). Likewise, HdmX protein expression level relative to normal melanocytes were previously reported (Ramos et al., 2001) for some of the cell lines and determined by Western blot relative to MCF7 and H1299 cells for the others. Table 3 summarizes the relative endogenous HdmX expression level and the p53 status of all the cell lines utilized in this study.

Initial experiments were conducted using a pool of four siRNAs obtained from Dharmacon (SMARTpool™) which target the *hdmX* transcript, but have different target sequences. The pooled siRNAs successfully decreased *hdmX* gene expression by approximately 50% relative to a pool of non-targeting siRNAs (siCon) in MCF7 cells 24 hours following a single siRNA transfection using Oligofectamine (Figure 10A). Although the knockdown of HdmX was modest, the p53 target gene, p21, was induced both transcriptionally and at the protein level (Figure 10B). The increase in p21 was also observed in U2OS cells following loss of HdmX despite no significant effect on Hdm2 or p53 levels (data not shown). These results correlate with previous reports that showed

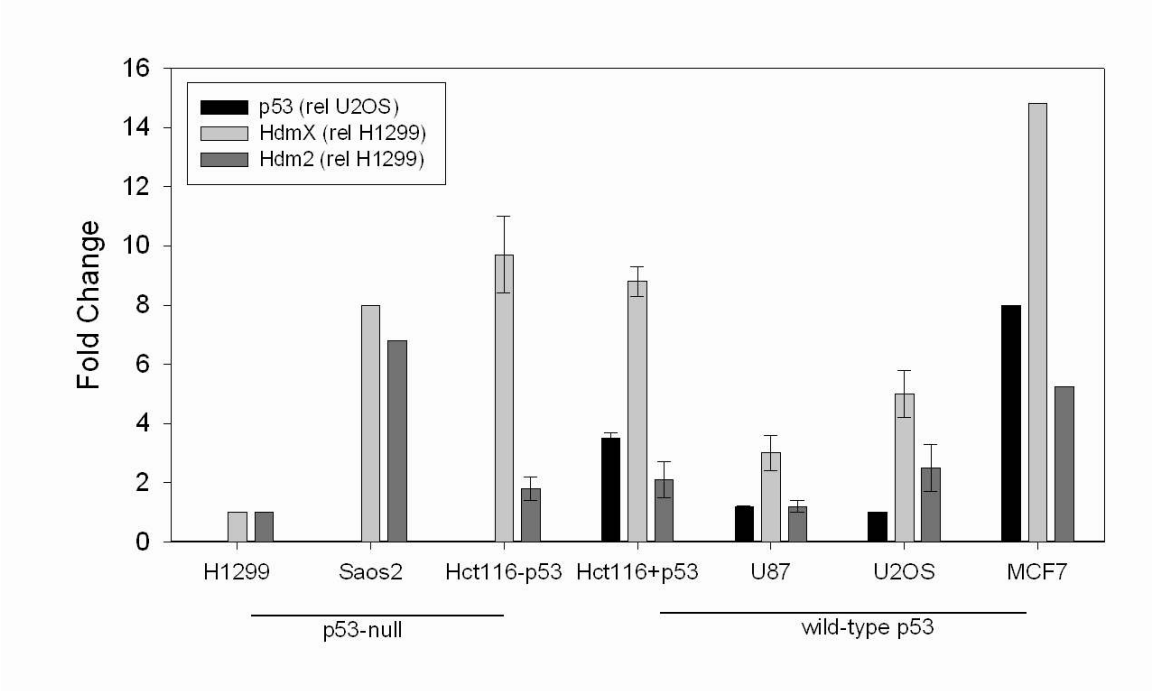

Figure 9. RT-PCR analysis of *hdmX*, *hdm2*, and *p53* gene expression in various tumor cell lines. The endogenous levels *of hdmX* and *hdm2* were determined relative to the levels in H1299 cells. The endogenous levels of *p53* were determined relative to the levels in U2OS cells since the H1299 cells are p53 null. All samples were normalized to GAPDH (internal control).

Cell line	p53 status	HdmX level
MCF7	wild-type	high
U2OS	wild-type	high
HCT116-p53+/+	wild-type	high
HCT116-p53-/-	null	high
U87	wild-type	normal
H1299	null	low
Saos-2	null	low
IMR90	wild-type	normal

Table 3. HdmX level and p53 status of various cell lines. HdmX protein levels were determined via Western blot relative to normal non-tumor cells, whereby high indicating at least a 2 fold increase and low representing half the level of HdmX (Ramos et al., 2001). B-Actin was used as a loading control.

Figure 10. Loss of HdmX induces p21 expression. (A) RT-PCR analysis of *hdmX*, *p21*, and *hdm2* gene expression in MCF7 cells 24 hours post siRNA transfection. The fold change relative to siCon transfected cells is shown. (B) Western blot analysis (Top panel) and quantification (Bottom panel) of p21 protein levels in MCF7 cells 48 hours following siRNA transfection. Loss of HdmX leads to a 2.5 fold increase in p21 protein expression. Actin was used as a loading control.

A

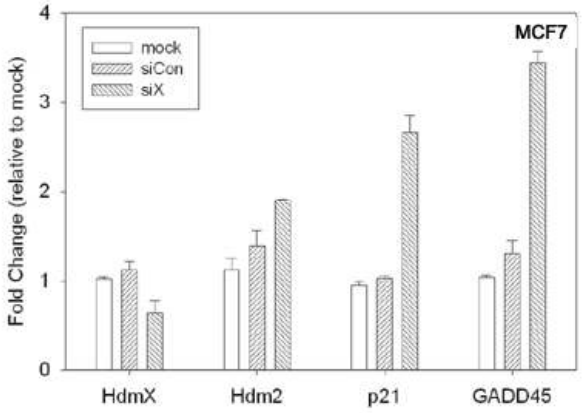
MCF7
mock
siCon
siX
Fold Change (relative to mock)
0
1
2
3
4
HdmX
Hdm2
p21
GADD45

B

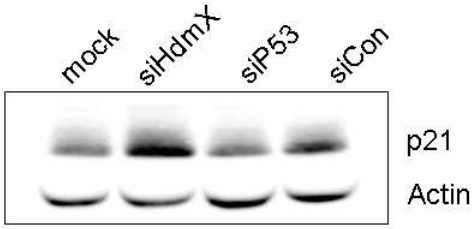
mock
siHdmX
siP53
siCon
p21
Actin

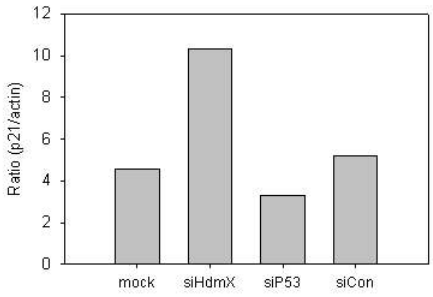
Ratio (p21/actin)
0
2
4
6
8
10
12
mock
siHdmX
siP53
siCon

partial HdmX knockdown induced p21 without a detectable increase in Hdm2 or p53 (Danovi et al., 2004).

To identify the most effective target sequence for silencing *hdmX*, each siRNA was individually transfected into U87 cells. The location of the four different target sequences on the hdmX gene is illustrated in Figure 11A. Twenty four hours following transfection, total RNA was isolated and *hdmX* and *p21* gene expression was determined by TaqMan-based RT-PCR. Two of the siRNA target sequences (#1 and #4) decreased hdmX transcript by 44% and 46%, respectively, while the other two siRNAs were less effective (Figure 11B). The induction of p21 generally correlated well with the level of HdmX knockdown. Thus, siRNA sequence #1 (siHdmX1) and sequence #4 (siHdmX4) targeting hdmX were used throughout this study. Similar experiments were performed to identify the most effective target sequences for knockdown of hdm2 in MCF7 cells. The siRNA sequence #6 (siHdm2(6)) was the best followed by sequence #9 (siHdm2(9)).

To properly assess the effect of HdmX knockdown on p53 activity in tumor cells with wild-type p53 by RNAi, it was necessary to improve upon the ~45% reduction seen with the single siRNAs following a single transfection. In order to optimize the siRNA transfection efficiency, a cytotoxic RNA-based reagent for optimizing siRNA delivery into cultured cells (siTOX; Dharmacon), was employed. MCF7 cells were transfected once with either 50 nM or 100 nM siTOX or siCon using Lipofectamine 2000 or Oligofectamine, and 72 hours later cell viability was determined by CellQuanti-Blue™ reagent (Figure 12). There was 38-47% cell viability detected in the siTOX transfected cells compared to mock transfected (lipid only) control cells, suggesting that

A

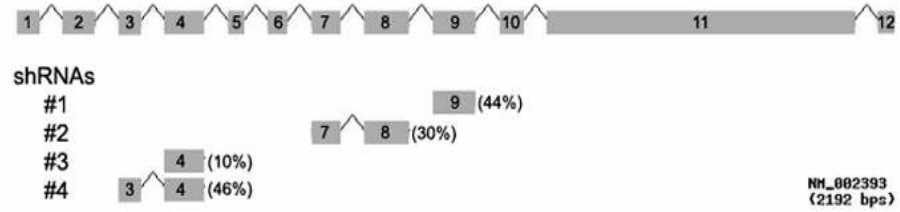

B

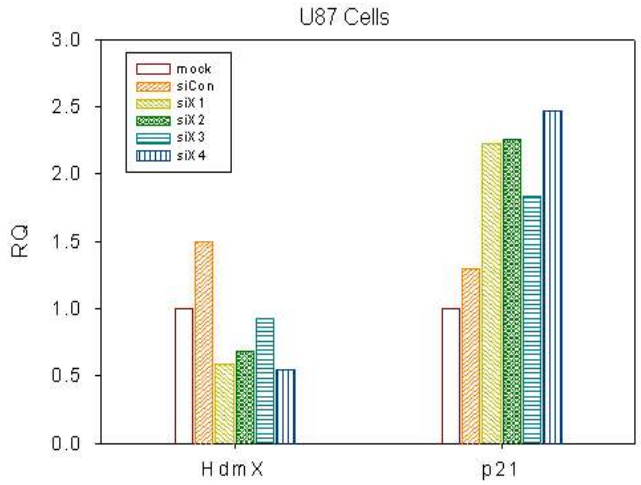

Figure 11. **Selection of target sequence for silencing HdmX expression.**

(A) Schematic representation of the HdmX gene showing exons 1-12 and the location of the four siRNA target sequences examined (shRNAs #1-4). The numbers in the parentheses are the percent knockdown in U87 cells relative to mock (lipid only) transfected control (B) RT-PCR analysis of *hdmX* and *p21* gene expression in U87 cells 24 hours following a single siRNA transfection. Relative quantity (RQ) represents the fold change relative to mock.

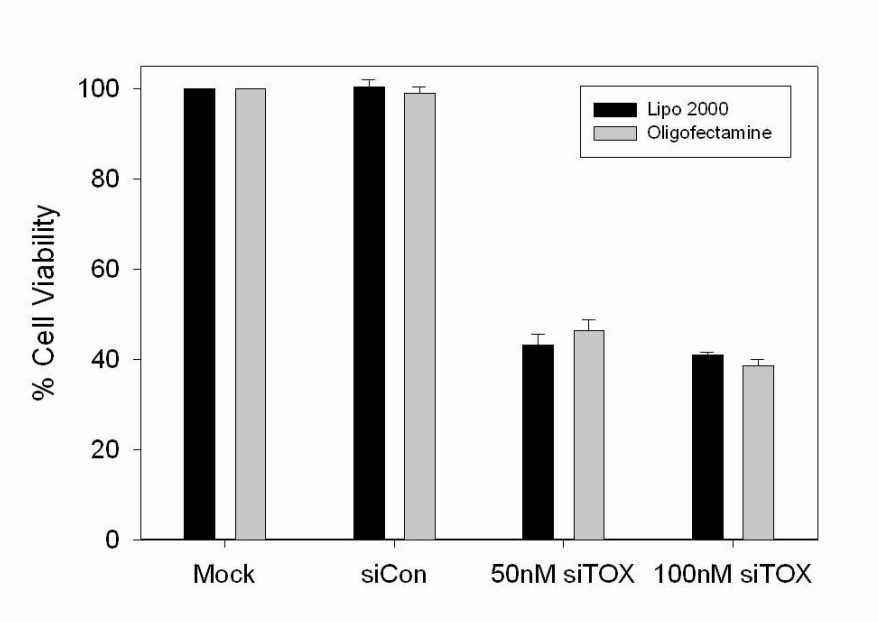

Figure 12. MCF7 cell viability 72 hours post siTOX transfection.

The % cell viability relative to mock transfected cells was determined by CellQuanti-Blue™ reagent. A single siTOX transfection resulted in about 40% cell viability whether Lipofectamine 2000 and Oligofectamine was used.

approximately 55-60% of the cells were transfected with the siRNA. This result correlated well with the ~ 50% knockdown of hdmX observed following a single siHdmX transfection. The cells transfected with siCon retained 100% cell viability relative to mock indicating that siRNA transfection does not lead to cytotoxicity. There was no significant difference in transfection efficiency observed between Lipofectamine 2000 and Oligofectamine, or 50 nM and 100 nM siTOX.

Multiple siRNA transfections were utilized to increase the siRNA delivery into the cells. Increasing the concentration of siRNA molecules per transfection was not a feasible option due to increases in off-target effects when greater than 100 nM of siRNA was used. MCF7 cells were transfected with 100 nM siTOX on three consecutive days and cell viability was assessed at 48 and 72 hours later. By 48 hours, cell viability had decrease to 40% and by 72 hours, less than 10% of the cells were remaining on the plate, indicating that ~90% of the cells had been transfected with siTOX. The siCon triple transfected cells retained 93-98% cell viability relative to non-transfected control cells. Triple transfection with siHdmX effectively decreased *hdmX* gene expression by 85-90% in MCF7 cells (Figure 13A) and HdmX protein was almost completely eliminated as determined by Western blot (Figure 13B). The loss of HdmX led to an increase in both *p21* and *hdm2* gene expression, but not *p53* gene expression. Using the reverse transfection method (see Materials & Methods) was equally as effective as triple transfection at decreasing hdmX levels in MCF7 cells, so it was also used throughout this study. However, the reverse transfection method was recommended for the MCF7 cells only (Invitrogen technical bulletin), so triple transfection was used for the other cell lines. Although the transfection efficiency is very good using the triple transfection and reverse

A

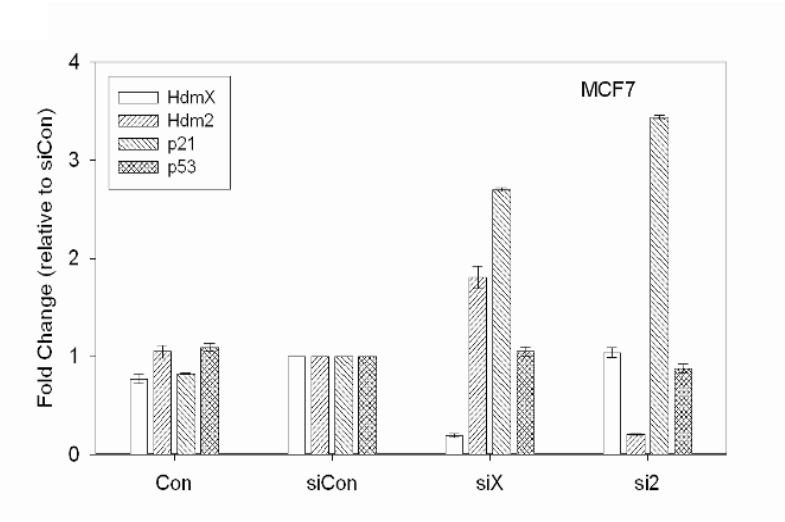

B

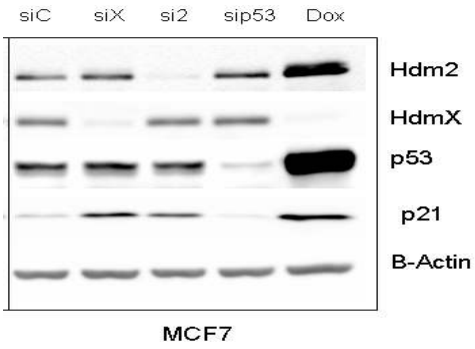

Figure 13. HdmX and Hdm2 knockdown following triple siRNA transfections. (A) RT-PCR analysis of *hdmX, hdm2, p21*, and *p53* in MCF7 cells 24 hours after the third siRNA transfection. (B) Western blot analysis showing loss of HdmX and Hdm2 protein by siHdmX and siHdm2 transfections, respectively. Cells treated with 0.5 μg/mL doxorubicin for 24 hours served as a positive control of p53 activation.

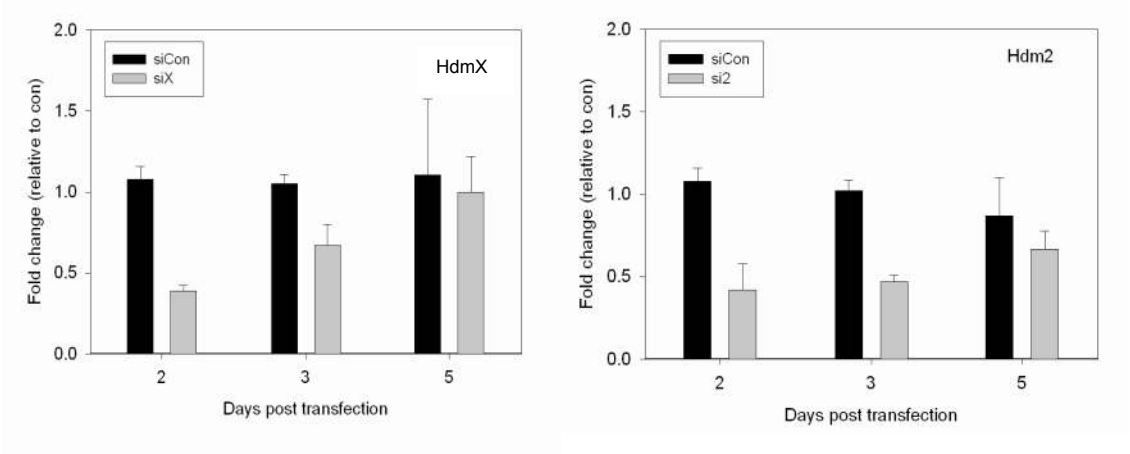

Figure 14. Duration of HdmX and Hdm2 knockdown following triple transfection in MCF7 cells. RT-PCR analysis of *hdmX* and *hdm2* gene expression shows that *hdmX* is reduced for three days post transfection (left panel) and *hdm2* is decreased for up to five days post transfection (right panel).

transfection methods, the knockdown was only a transient effect. After triple transfection, *hdmX* gene expression was reduced for three days and *hdm2* expression was reduced for five days (Figure 14) following siHdmX and siHdm2, respectively, in MCF7 cells. In order to achieve a stable long term knockdown, the siHdmX1 sequence was cloned into a lentivirus vector expressing a short-hairpin RNA that targets *hdmX* (shHdmX), and stable cell lines were established.

B. Non-specific induction of p53 target genes by Lentivirus-delivered shRNA.

U2OS and MCF7 cell lines stably expressing shHdmX or the control short-hairpin RNAs targeting Lamin (shLamin) or LacZ (shLac) were established. The Lentivirus delivered shHdmX was effective at reducing *hdmX* transcript in U2OS cells (Figure 15 A), but not as effective in MCF7 cells (Figure 15B), although HdmX protein levels were reduced by at least 50% in MCF7 cells stably expressing shHdmX (Figure 15C). The control cells expressing shLamin and shLac had no effect on HdmX expression as expected. To determine if silencing HdmX in tumor cells which retain wild-type p53 will activate p53 and induce p53 target genes (i.e. *p21*, *hdm2 and gadd45*), quantitative RT-PCR was performed on total RNA isolated from the stable cells. Unexpectedly the stably infected shLamin and shLacZ control cells also expressed increased levels of several p53 target genes in both U2OS and MCF7 cells (Figure 15), suggesting that lentiviral shRNA vectors may cause non-specific effects on untargeted gene expression. To examine the possibility that these alterations in gene expression resulted from the viral infection rather than the presence or processing of the shRNA vectors in the cell, U2OS cells were infected with a tetracycline repressor (TR) expressing lentivirus. The induction of *p21* and *hdm2* was not observed after TR-lentiviral infection, suggesting that the increase in

Figure 15. Non-specific induction of p53 target genes by Lentivirus-delivered shRNA vectors. (A) RT-PCR analysis of *hdmX*, *hdm2*, *p21*, and *p53* gene expression in U2OS cells stably infected with the indicated shRNA lentivirus. (B) RT-PCR analysis of *hdmX*, *hdm2*, *p21,* and *gadd45* gene expression in MCF7 cells stably infected with the indicated shRNA lentivirus. (C) Western blot of HdmX, p21, and β-actin in MCF7 cells either uninfected, infected with shHdmX lentivirus (shX) or infected with shLacZ lentivirus. HdmX was reduced by shX, but p21 was induced by both shX and shLacZ.

A

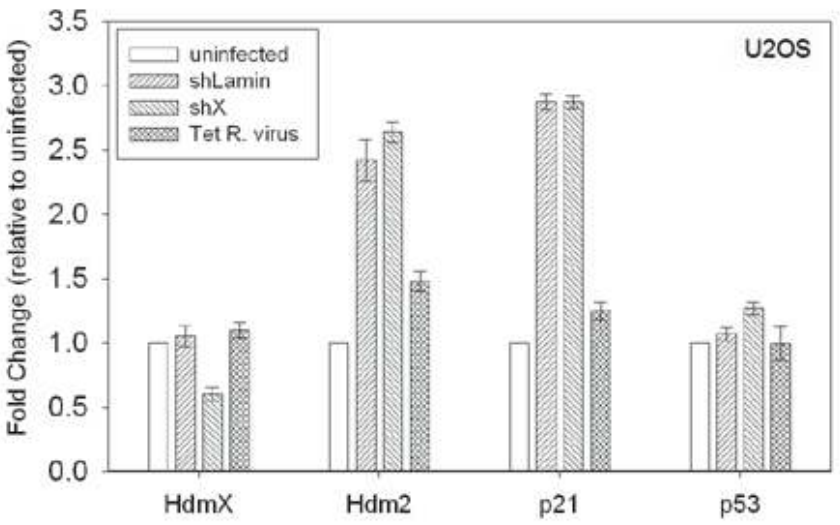
U2OS
uninfected
shLamin
shX
Tet R. virus
Fold Change (relative to uninfected)
3.5
3.0
2.5
2.0
1.5
1.0
0.5
0.0
HdmX
Hdm2
p21
p53

B

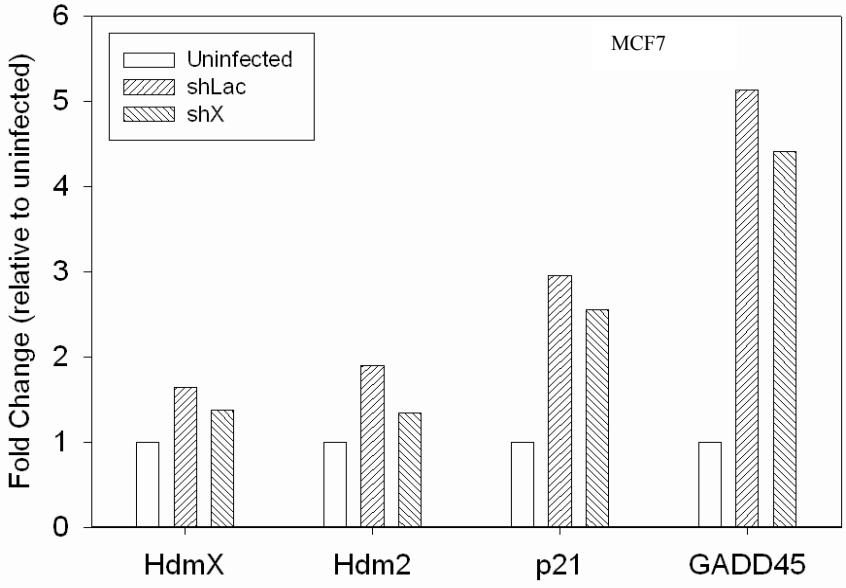
MCF7
Uninfected
shLac
shX
Fold Change (relative to uninfected)
6
5
4
3
2
1
0
HdmX
Hdm2
p21
GADD45

C

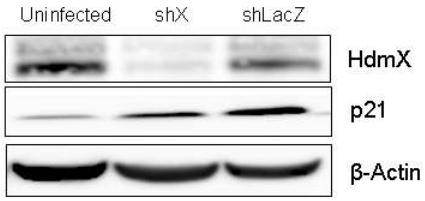
Uninfected
shX
shLacZ
HdmX
p21
β-Actin

p53 target gene expression is specific to virus containing shRNA vectors rather than to a general antiviral response by the cells. The p53 transcript level was not altered by expression of shRNA vectors or viral infection as expected (Figures 15A & 15B). Lastly, p21 protein levels where increased in all shRNA expressing cells relative to uninfected, which correlates with the increased p21 gene expression that was observed (Figure 15C).

C. Induction of p21 is both p53-dependent and independent.

To determine if the non-specific untargeted induction of p21 mRNA by lentiviral-delivered shRNA vectors is p53 dependent, HCT116-p53+/+ and HCT116-p53-/- cells were infected with lentiviral shRNA vectors targeting *hdmX* or *LacZ*. The cells were put under selection for ten days and stable cells were harvested for protein. Western blot analysis demonstrated an increase in both p53 and p21 protein levels in HCT116-p53+/+ cells following lentiviral infection (Figure 16A). This induction of p53 and p21 was not specific to the cells with knocked down HdmX, but rather observed with both lentivirus containing shRNAs. The HCT116 cells devoid of p53 (HCT116-p53-/-) also showed an increase in p21 protein, but to a lesser degree than the HCT116 cells containing wild-type p53, indicating both a p53-dependent and independent induction of p21 by shRNA containing lentivirus (Figure 16A). The induction of p21 protein in HCT116-p53-/- cells is the result of an increase in *p21* transcripts, as the experiment was repeated and RNA levels were quantified by RT-PCR. Again, increases in p21 mRNA levels were detected in both p53-null and p53 wild-type cell lines expressing shRNAs (Figure 16B). To confirm that the p53-independent induction of p21 is not specific to the HCT116-p53-/- cells, the same experiment was performed in p53-null Saos-2 cells.

Figure 16. Induction of p21 in HCT116 cells stably expressing shRNA vectors. (A) Western blots of HdmX, Hdm2, p53 and p21 proteins in HCT116 cells either uninfected (Con) or infected and selected for stable expression of the indicated shRNA vector. HdmX protein levels were reduced in both HCT116-p53+/+ and HCT116-p53-/- cells stably infected with lentiviral-delivered shX, but not in shLacZ stable cells as expected. Unexpectedly, p53 and p21 expression were increased in both shX and shLacZ HCT116-p53+/+ cells. Additionally, p21 and Hdm2 protein levels were also induced in a p53-independent manner in HCT116-p53-/- cells stably infected with either shX or shLacZ lentivirus. (B) RT-PCR analysis of *hdmX* and *p21* gene expression from HCT116 cells either uninfected (con) or infected with shX or shLacZ. Fold change was normalized to HCT116-p53-/- Con cells.

A

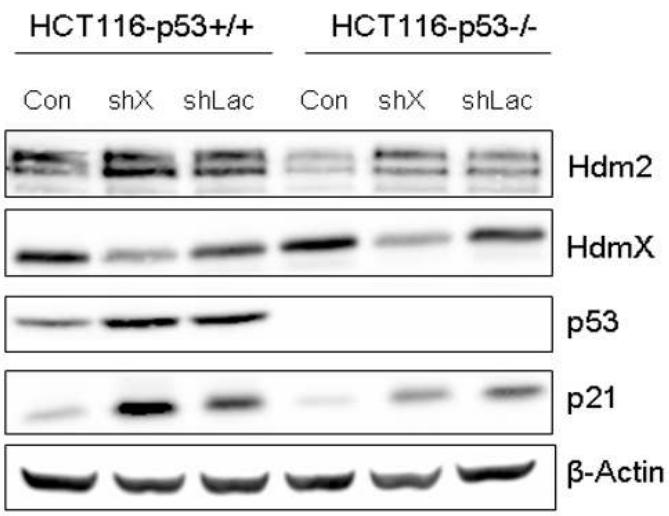
HCT116-p53+/+
HCT116-p53-/-
Con
shX
shLac
Con
shX
shLac
Hdm2
HdmX
p53
p21
β-Actin

B

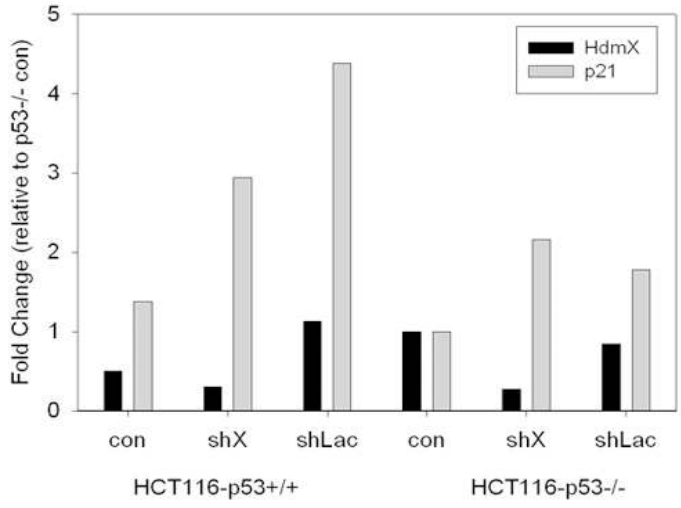
Fold Change (relative to p53-/- con)
5
4
3
2
1
0
HdmX
p21
con
shX
shLac
con
shX
shLac
HCT116-p53+/+
HCT116-p53-/-

Figure 17. Induction of p21 in p53-null Saos-2 cells expressing shRNA vectors. (A) RT-PCR analysis of *hdmX* and *p21* gene expression in Saos-2 cells stably infected with shHdmX (shX) or shLacZ (shLac) expressing lentivirus. Fold change is relative to expression in uninfected cells. Results show an induction of *p21* in both shRNA expressing cells and knockdown of *hdmX* mRNA only in the shX expressing cells. (B) Western blot showing induction of p21 protein in both shRNA-expressing stable cell lines. Since the levels of HdmX protein are low in Saos-2 cells, it is difficult to detect the knock-down of HdmX protein by Western blot.

A

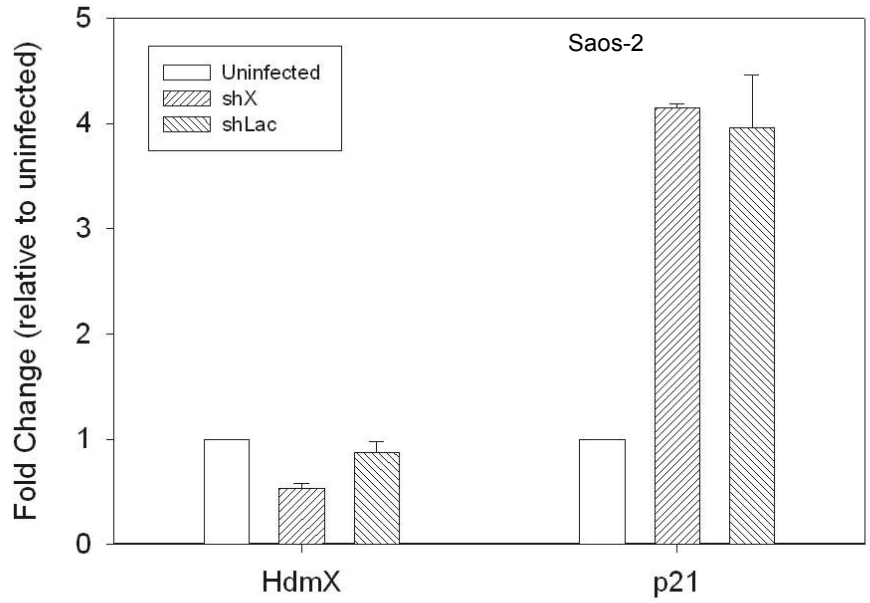
Saos-2
Uninfected
shX
shLac
Fold Change (relative to uninfected)
0
1
2
3
4
5
HdmX
p21

B

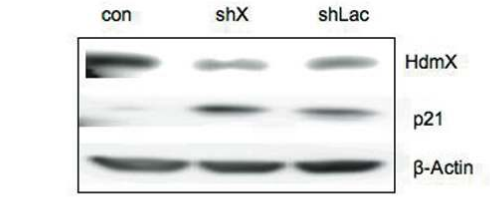
con
shX
shLac
HdmX
p21
β-Actin

Indeed, the non-specific induction of p21 gene and protein expression was observed in Saos-2 cells as well post shHdmX and shlacZ lentiviral infections relative to uninfected cells (Figure 17). Overall, these results suggest that the off-target effect seen with the shRNA vectors is predominantly p53-independent. Conversely, transient transfection with siCon did not induce the off-target expression of p21 as seen with the shRNA vectors (Figure 9). The induction of p53 target genes suggests that p53 is being activated by shRNA in a non-specific untargeted manner in tumor cells harboring wild-type p53. To examine the transcriptional activity of p53, cells were co-transfected with a p53 luciferase reporter plasmid (pG13Luc) containing thirteen p53 consensus binding sites in its promoter, and with a transfection control plasmid (RLuc). HCT116-p53+/+ cells stably infected with lentiviral-delivered shRNA targeting *hdmX* and *LacZ* had increased levels of activated p53 relative to uninfected cells (Figure 18) The HCT116-p53-/- cells stably expressing shHdmX and shLacZ were co-transfected with pG13Luc and RLuc, and used as a negative control. Thus, it appears that the presence and/or processing of the lentiviral delivered shRNA vectors are causing a non-specific cellular stress leading to a modest increase in p53 transactivation and an induction of untargeted p53 response genes.

D. Investigation of shRNA lentivirus mediated interferon response.

Some shRNA vectors have been reported to activate a non-specific antiviral response against dsRNA molecules in cells (Bridge et al., 2003). To investigate whether or not the lentiviral shRNA vectors are triggering an interferon response (IFN) in the MCF7, HCT116, and U2OS cells, the expression of *OAS1* (2'5'-oligoadenylate synthetase) a classic IFN target gene that is induced by >50-fold upon activation of the IFN response

(Bridge et al., 2003) was measured. Quantitative RT-PCR analysis of *OAS1* expression in shHdmX and shLacZ lentiviral infected MCF7 cells showed a 29 and 16 fold induction, respectively, relative to uninfected control (con) cells (Figure 19A), suggesting a possible activation of the interferon response. However, no effect on *OAS1* gene expression was observed in the HCT116-p53-/- cells following infection of lentiviral-delivered shRNA vectors, and HCT116-p53+/+ cells had a less than 4-fold induction (Figure 19B). Furthermore, stably infected U2OS cells showed little or no induction of *OAS1* gene expression (Figure 19C), suggesting that p21 induction is not the result of a classic anti-viral interferon response. Similar results were observed with *IFIT1* (interferon-induced protein with tetratri-copeptide repeats 1) expression, another interferon response gene, in HCT116 cells (Figure 20A) and MCF7 cells (Figure 20B). Since p21 was induced in a non-specific untargeted manner in all of the shRNA expressing stable cell lines tested, these results indicate that an interferon response is not necessary to elicit induction of p21 by lentivirus delivered shRNA.

To examine if IFN can trigger an increase in p21 gene expression in tumor cells, MCF7 and HCT116 cells were treated with 50 ng/mL IFN-γ for 24 hours. Quantitative RT-PCR analysis clearly demonstrated that IFN treatment does not induce p21 in MCF7 or HCT116 cells, while significantly inducing the IFN target gene, *OAS1* by >18 fold in MCF7 cells, 80-fold in HCT116-p53+/+ cells and 45-fold in HCT116-p53/- cells (Figures 20A & 20C). Finally, western blots of MCF7 cells treated with IFN or infected with lentiviral delivered shRNA-vectors confirm that p21 protein induction occurs upon shRNA expression but not with interferon treatment (Figure 20B).

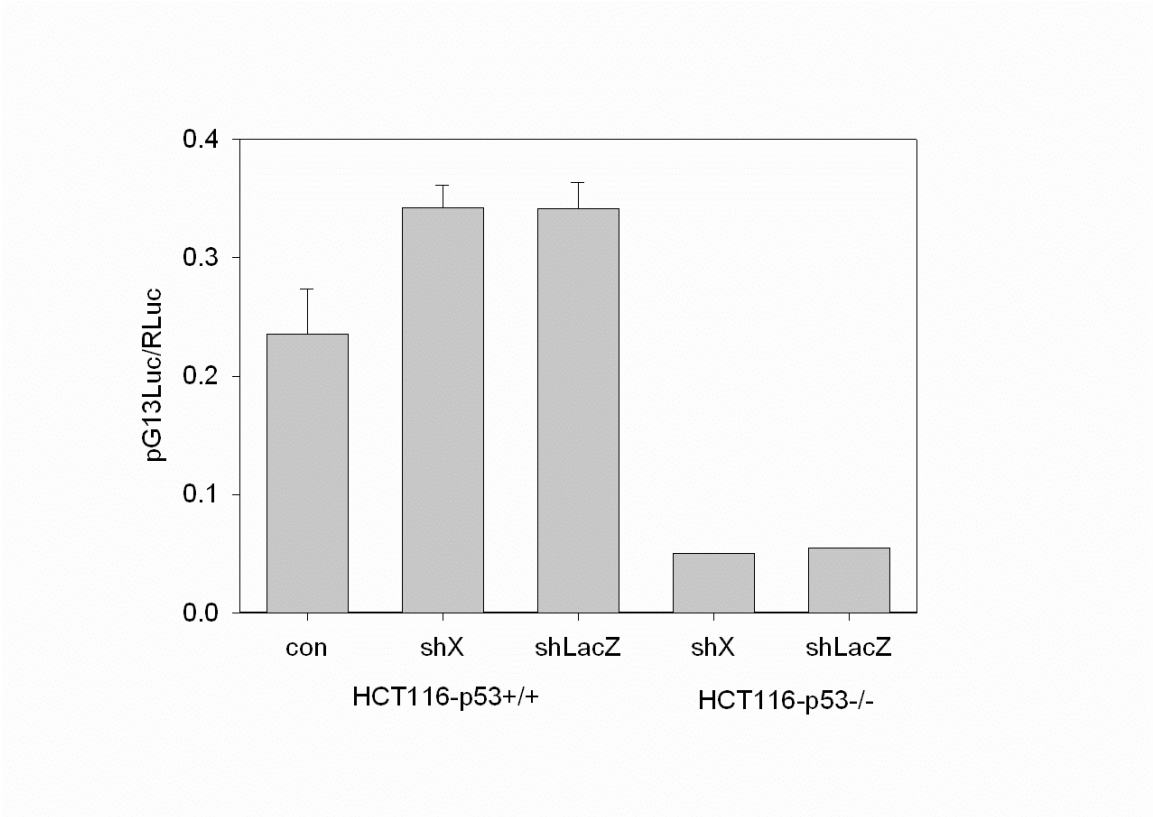

Figure 18. Lentivirus-delivered shRNAs activate p53 in HCT116-p53+/+.

A p53 luciferase reporter plasmid (pG13Luc) was employed to measure p53 transcriptional activity and a renilla luciferase plasmid (RLuc) was used to normalize transfection efficiency. Both shHdmX and shLacZ lentiviral infected HCT116-p53+/+ cells showed increased p53 transactivation relative to uninfected cells (Con). HCT116-p53-/- cells showed background levels only. Bars represent the mean pG13Luc/RLuc ratio and error bars represent standard deviation of four samples.

Figure 19. RT-PCR analysis of *OAS1* and *p21* gene expression. (A) *OAS1* gene expression is highly induced in MCF7 cells stably expressing shRNA relative to uninfected cells (con). (B) *OAS1* mRNA levels were not altered in HCT116-p53-/- cells, while HCT116-p53+/+ cells infected with lentivirus containing shRNAs showed <4 fold increase. (C) *OAS1* levels were not changed in U2OS cells, however, *p21* gene expression was consistently increased by 2-3 fold in all cell lines infected with shRNA expressing lentivirus.

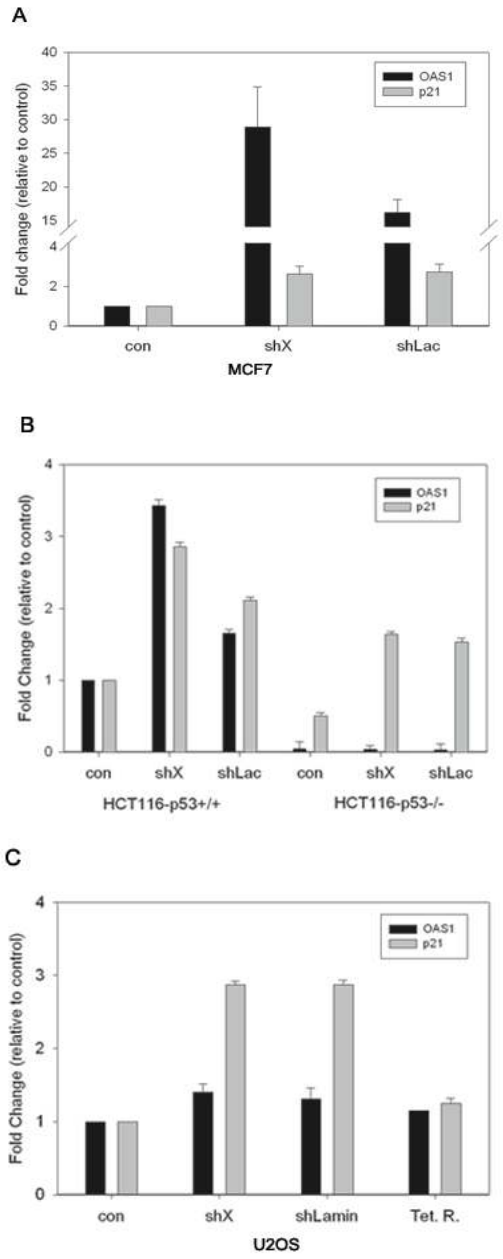
A
Fold change (relative to control)
OAS1
p21
con
shX
shLac
MCF7
B
Fold Change (relative to control)
OAS1
p21
con
shX
shLac
con
shX
shLac
HCT116-p53+/+
HCT116-p53-/-
C
Fold Change (relative to control)
OAS1
p21
con
shX
shLamin
Tet. R.
U2OS

Figure 20. RT-PCR analysis of *IFIT1* gene expression. (A) *IFIT1* gene expression in HCT116 cells stably expressing shHdmX or shLacZ. IFIT1 transcripts were induced in HCT116-p53+/+ cells, but not p53 null HCT116 cells (B) *IFIT1* gene expression in MCF7 cells either uninfected (con), stably infected with shX or shLacZ lentivirus, or treated with 50 ng/mL Recombinant human Interferon-gamma (IFN). *IFIT1* expression is induced by both lentiviral-delivered shRNA vectors and by IFN treatment.

A

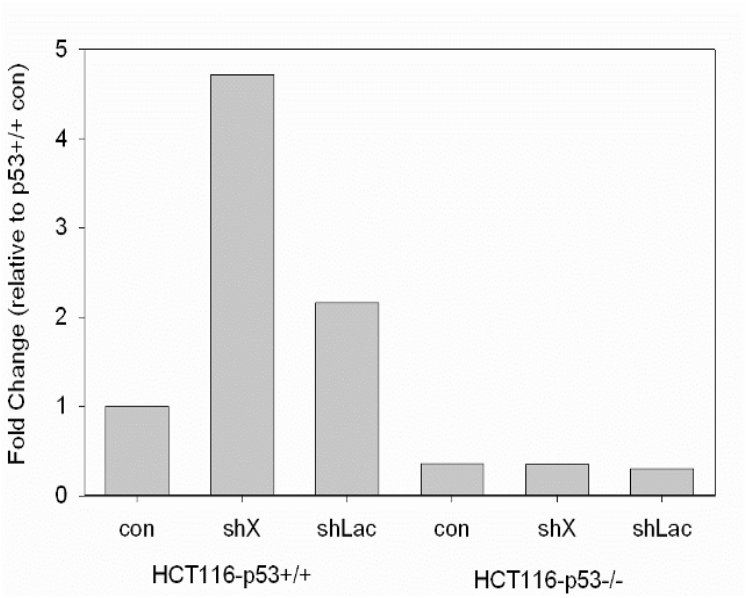
Fold Change (relative to p53+/+ con)
5
4
3
2
1
0
con
shX
shLac
con
shX
shLac
HCT116-p53+/+
HCT116-p53-/-

B

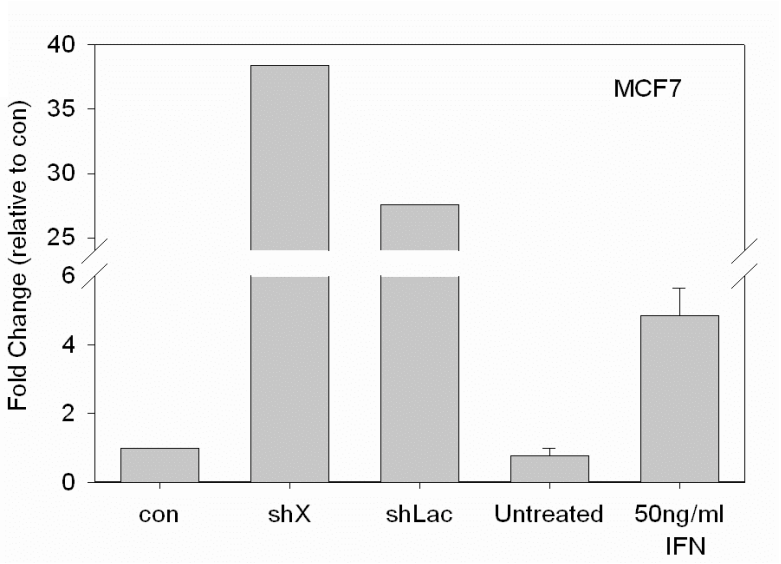
Fold Change (relative to con)
40
35
30
25
6
4
2
0
MCF7
con
shX
shLac
Untreated
50ng/ml IFN

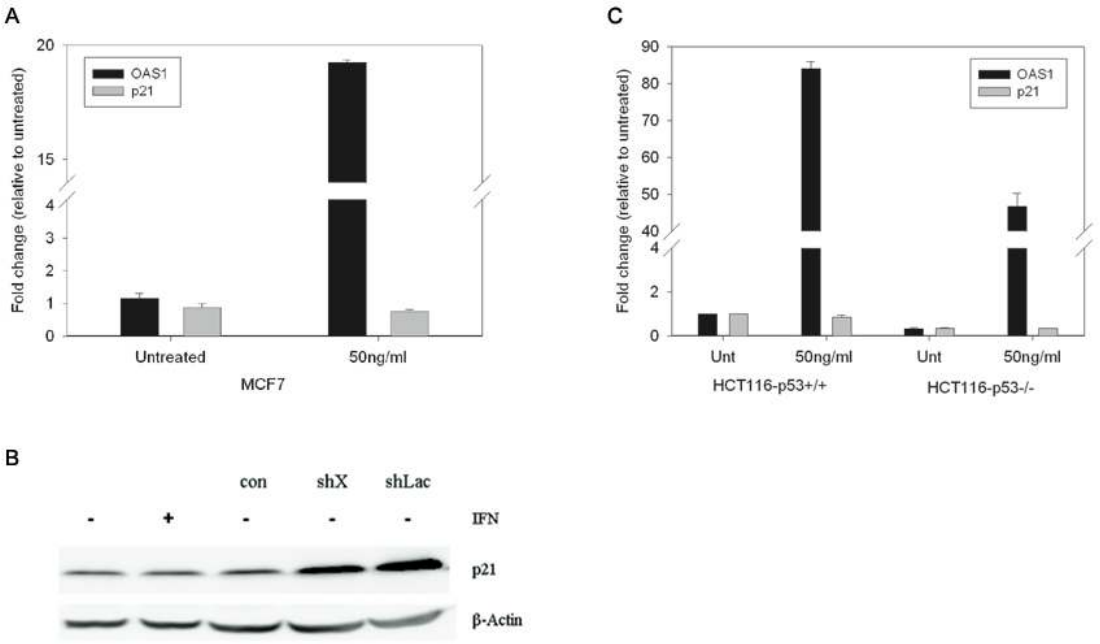

Figure 21. p21 is not induced by IFN in MCF7 cells or HCT116 cells.

(A) RT-PCR results from MCF7 cells treated with 50 ng/mL IFN for 24 hours. While *OAS1* gene expression increased 18-fold, no change in *p21* gene expression relative to untreated, was observed. (B) Western blot analysis of p21 protein levels in MCF7 cells treated with interferon-gamma (IFN+) or infected with lentivirus expressing shHdmX or shLacZ showed p21 protein was induced in the shRNA-expressing MCF7 cells only. Beta-actin was used as a loading control. (C) RT-PCR results from HCT116 cells treated with 50 ng/mL IFN for 24 hours. *OAS1* gene expression was significantly induced in both wild-type p53 and p53 null HCT116 cells, while *p21* gene expression was not altered.

Since lentiviral delivered shRNA has the advantage of stable long term silencing over transient siRNA transfections, viral shRNA delivery systems have gained wide use in creating stable knockdown cell lines. To investigate the role of HdmX deregulation of p53 function in tumor cells, we designed lentiviral-delivered shRNA vectors which were effective in knocking down HdmX expression and inducing p53 target genes. However, it was quickly determined that expression of control shRNAs (shLamin, shLacZ) also triggered activation of *p21* and *gadd45*. The non-specific induction of these p53 target genes was not sequence-dependent since every shRNA control used elicited a similar response, nor was it due to the drug selection since elevated p21 levels were observed even after removal of selection. Additionally, since Lentivirus expressing the Tetracycline repressor did not induce *p21* transcripts, the possibility that the off-target p21 induction was due to a general anti-viral response by the cells was excluded. Since p21 expression was also increased in p53 null cell lines expressing shRNA, it implied that this effect was both p53-dependent and independent. For these reasons, the lentivirus shRNA system could not be used in our studies to identify alterations in gene expression in tumor cells following the loss of HdmX.

E. Alterations in gene expression following the loss of HdmX

MCF7 cells which possess wild-type p53 and elevated levels of both HdmX and Hdm2 were used to elucidate alterations in gene expression following the loss of HdmX or Hdm2. Triple siRNA transfections were performed to knockdown approximately 90% of the HdmX or Hdm2 in the cells and an Affymetrix GeneChip® experiment was conducted. Each experimental siRNA was transfected into three separate wells and 24 hours after the last transfection, total RNA was isolated individually from each well for

hybridization onto three separate GeneChips. The expression levels of select genes were monitored to confirm that the GeneChip experiment had run as expected and that the knockdown was detected (Figure 22). The levels of knockdown of HdmX, Hdm2, and/or p53 detected by the GeneChips are illustrated in Figure 22.

GeneSpring software was employed to generate lists of genes that were induced by at least two fold following knockdown of HdmX or Hdm2 relative to siControl. Additionally, lists of genes that were suppressed by a least 50% after loss of HdmX or Hdm2 relative to siControl were created using GeneSpring. The total number of genes altered in MCF7 cells after triple transfection with the indicated siRNAs are summarized in Table 3. As shown in the table, two different target sequences were used to knockdown HdmX (#1 and #4) and two target sequences were used for Hdm2 knockdown (#6 and #9). Using GeneSpring, we identified the number of genes that are common to both lists (i.e. siHdmX1 + siHdmX4). Focusing only on those genes that were present in the combined list decreased the probability that the gene alterations represented off-target effects from the siRNA for either hdmX or hdm2. The knockdown of HdmX or Hdm2 in MCF7 cells led to the induction of several p53 regulated genes (Table 4). Interestingly, the majority of these genes encoded proteins involved with p53-mediated cell cycle arrest with only one pro-apoptotic gene showing a significant increase (Fas, Table 4). Several of the other p53 target genes induced, whose functions are not as well known, appear to play a role in growth inhibition, cell adhesion, and differentiation. While the loss of either HdmX or Hdm2 did not appear to activate p53 pro-apoptotic genes, the removal of p53 from MCF7 cells by siRNA targeting p53

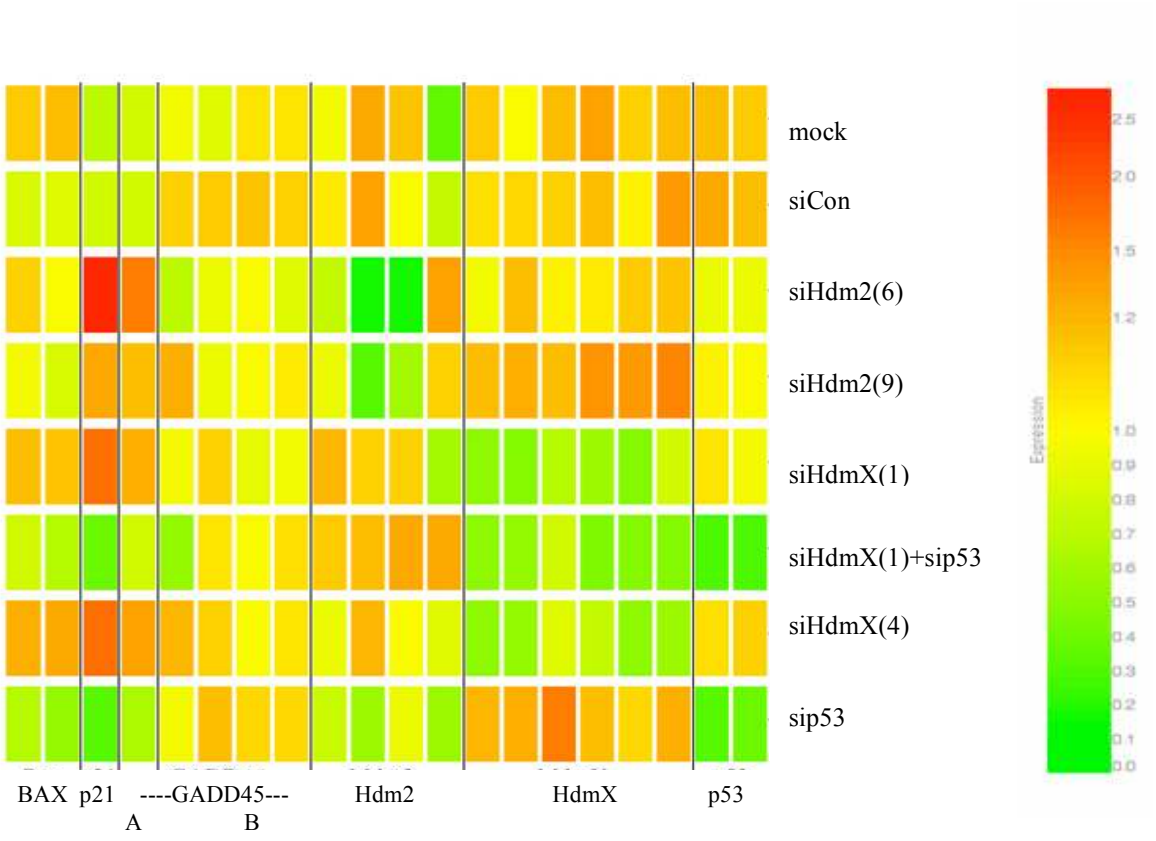

Figure 22. Expression levels of select genes following siRNA transfection. The color scheme represents the average signal for the three replicates per condition. Red represents genes which are induced, while green represents genes which are suppressed and yellow are genes which are not altered 24 hours following triple siRNA transfection in MCF7 cells.

Treatment	Induced	Suppressed
Mock	0	149
siHdmX1	364	188
siHdmX4	332	162
siHdmX1+siHdmX4	95	32
siP53	195	222
siX1+siP53	258	211
siHdm2(6)	389	307
siHdm2(9)	245	163

Table 4. Number of genes altered relative to siControl. Number of genes induced and suppressed by the indicated siRNA transfections in MCF7 cells. siHdmX+siHdmX4 shows the number of common genes between the siHdmX1 list and the siHdmX4 list.

Cell Cycle	Apoptosis	DNA Repair	Growth Inhibition/ Unknown	Other/ Unknown
p21	Fas	p48	ACTA2	Hdm2
GADD 45	BAX	p53R2	WIG1	RAI
BTG2	IGF-BP3	PCNA		
Cyclin G	NOXA			
14-3-3σ	PIGs			
Reprimo	PUMA			
B99	p53AIP			
	PERP			

Table 5. Functional groups of selected p53 target genes. The genes in red indicate genes that were induced by loss of HdmX or Hdm2, and the genes in green represent genes suppressed by loss of p53 in MCF7 cells. (Functional groupings adapted from Levine and Feng, 2006; Jackson and Pereira-Smith, 2006)

did lead to significant decreases in Fas, and two other pro-apoptotic genes, NOXA and IGF-BP3. Taken together, our targeted analysis of known p53 regulated genes suggested that the loss of either HdmX or Hdm2 led to a preferential induction of p53 regulated genes involved in the inhibition of cell proliferation.

F. Validation of GeneChip data and induction of p53 target genes

In order to confirm the GeneChip results, quantitative RT-PCR using Taqman primers targeting five known p53 target genes was performed. ACTA2, BTG2 and p21 are all p53 target genes that have been associated with growth inhibition (Boiko et al., 2006; Comer et al., 1998) and cell cycle arrest (el-Deiry et al., 1993), while Hdm2 is a negative regulator of p53 (Marine et al., 2006) and Noxa is a pro-apoptotic factor (Oda et al., 2000a). All of these genes were induced following loss of hdmX and hdm2 in the GeneChip experiment with the exception of NOXA. MCF7 cells were either mock-transfected (Con), transfected with siRNA that does not target any human gene (siCon) or transfected with siRNA targeting HdmX or Hdm2 either alone or in combination. The loss of HdmX or Hdm2 led to a significant increase in p21 gene expression relative to siCon and the combination of HdmX and Hdm2 knockdown resulted in a greater, synergistic increase in p21 (Figure 23A). The loss of HdmX also led to an increase in *hdm2* transcripts, which would be predicted if the removal of HdmX led to an increase in p53 transactivation. BTG2 and ACTA2 gene expression relative to control cells were induced following knockdown of HdmX and/or Hdm2, while no significant change in gene expression was observed with Noxa (Figure 23B). Finally, when both HdmX and Hdm2 were eliminated, the transcript levels of BTG2 and ACTA2 increased additively. These results validate our GeneChip data that p53 target genes were induced upon HdmX

and Hdm2 knockdown, and that cell cycle arrest and growth inhibition genes appeared most sensitive to the loss of HdmX and/or Hdm2 in MCF7 cells.

To confirm that these increases in p53 target gene expression was the result of p53 transactivation, p21 transcript levels were determined by RT-PCR in two different p53 null cell lines. HCT116 cells with wild-type p53 (HCT116-p53+/+) and HCT116 cells lacking p53 (HCT116-p53-/-) were transfected with either siCon, siHdmX, siHdm2, or the combination of siRNAs targeting HdmX and Hdm2. p21 gene expression was induced in the HCT116-p53+/+ cells after loss of HdmX or Hdm2 (Figure 24A), but not in the HCT116-p53-/- cells relative to control cells (Figure 24B). Furthermore, in the p53 null H1299 cells, neither p21 nor BTG2 expression were significantly altered following knockdown of HdmX or Hdm2 (Figure 25). Taken together, these results confirm that the loss of HdmX and Hdm2 leads to an increase in p53-dependent activation of cell cycle arrest genes.

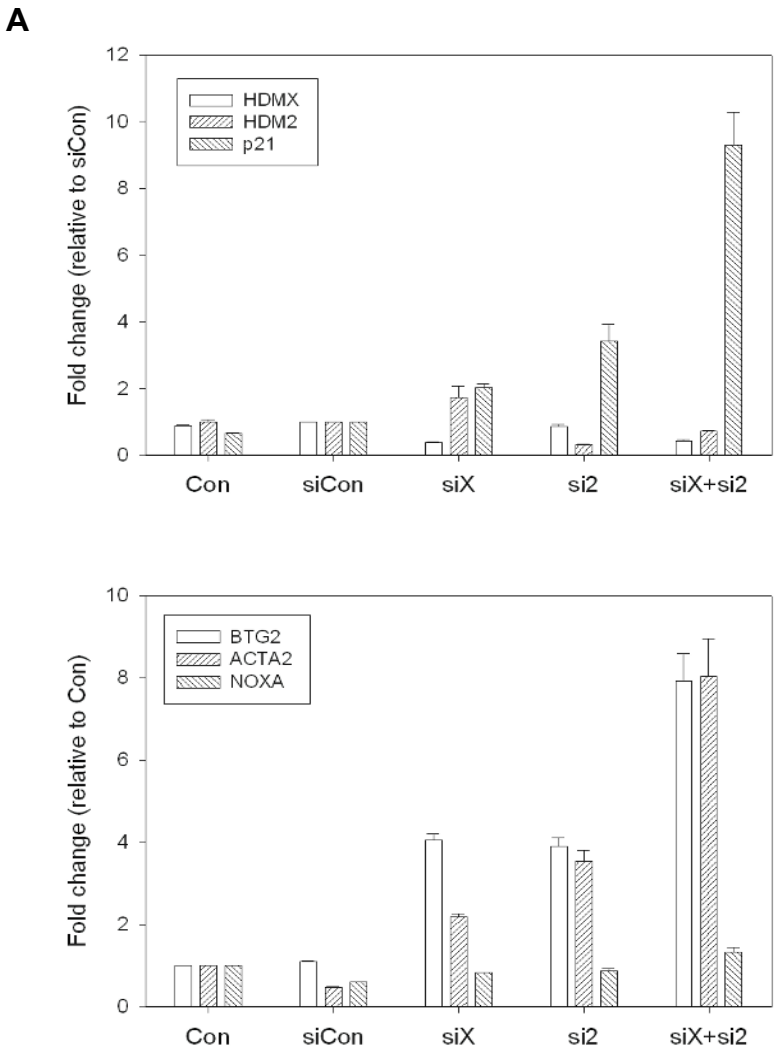

Figure 23. **RT-PCR validation of siRNA knockdown in MCF7 cells.**

(A) The *hdmX*, *hdm2*, and *p21* mRNA expression relative to siCon (non-targeting siRNA) is shown. The *p21* transcript is induced following loss of HdmX or Hdm2, and synergistically induced following loss of both HdmX and Hdm2. (B) *BTG2*, *ACTA2*, and *NOXA* mRNA expression relative to untransfected control (Con). The p53 target genes, BTG2 and ACTA2, are induced by loss of HdmX and/or Hdm2, while the expression of the pro-apoptotic gene, NOXA, is not altered.

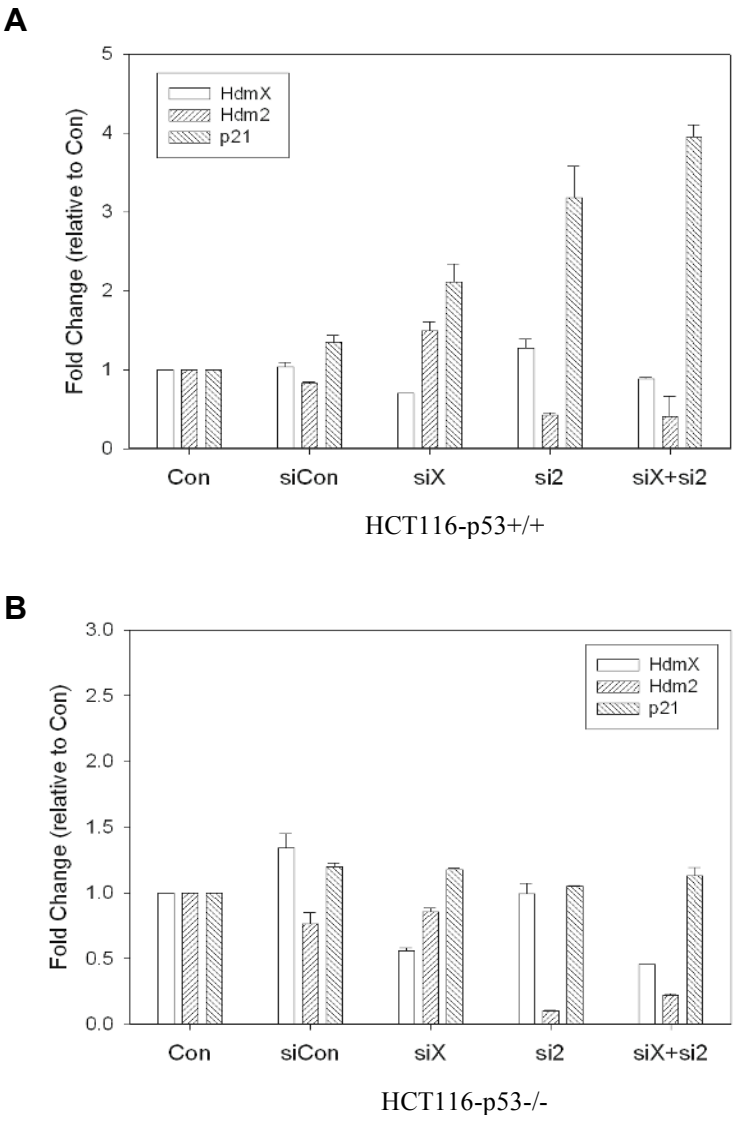

Figure 24. Loss of HdmX and Hdm2 induce *p21* in a p53-dependent manner. Knockdown of HdmX, Hdm2 or the combination of Hdms in HCT116-p53+/+ cells (A) or HCT116-p53-/- cells (B). *p21* transcript levels are significantly induced in HCT116 cells harboring wild-type p53 following knockdown of HdmX and/or Hdm2, but are not induced in p53-null HCT116 cells.

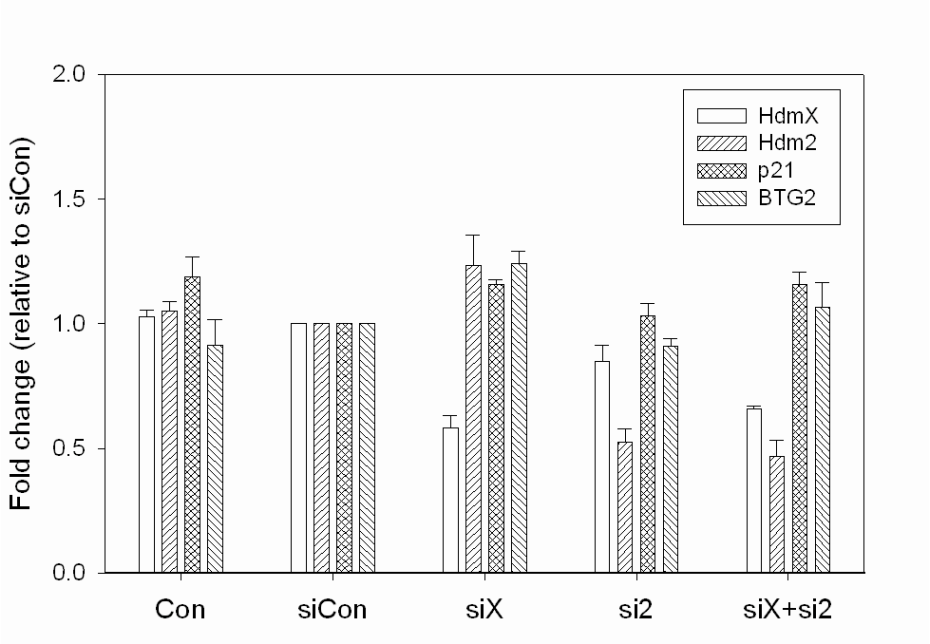

Figure 25. **Loss of HdmX does not induce p21 or BTG2 in p53-null H1299 cells**. RT-PCR analysis of *hdmX*, *hdm2*, *p21*, and *btg2* gene expression in H1299 cells 24 hours post siRNA infection. The p53 target genes; *hdm2*, *p21*, and *btg2* were not induced following partial knockdown of HdmX and/or Hdm2.

G. Loss of HdmX increases p53 transactivation

To examine how the knockdown of HdmX, Hdm2 or p53 in MCF7 cells affected p53 transcriptional activity, a p53 luciferase reporter gene possessing 13 copies of the p53 consensus DNA binding site (pG13-Luc) was employed. As a positive control, MCF7 cells were transfected with the p53-reporter and then the cells were treated with 0.5 μg/mL doxorubicin (Dox) to trigger DNA damage and induce p53 transactivation (Kurz et al, 2004). As expected, the loss of HdmX or Hdm2 led to an increase in p53 transactivation which was completely eliminated by the knockdown of p53 (Figure 26, top panel). Interestingly, loss of HdmX resulted in greater p53 activation than the loss of Hdm2 and the combined knockdown was similar to that seen with siHdmX alone. The level of p53 transactivation following doxorubicin treatment was significantly greater than that seen when HdmX and/or Hdm2 were eliminated (Figure 26, top panel). Western blot analysis of HdmX, Hdm2, p53, p21, and β-actin was performed to confirm knockdown of the indicated proteins and to evaluate protein levels following gene silencing. The p21 protein levels were increased after loss of HdmX and/or Hdm2, and after doxorubicin treatment as expected (Figure 26, bottom panel). However, p53 protein levels were not significantly altered by HdmX and/or Hdm2 knockdown, while p53 stability was greatly increased following DNA damage triggered by doxorubicin. Since the transfection of siRNAs targeting HdmX or Hdm2 increased p53 transactivation and induced p53 response genes, but appeared to have little effect on p53 stability, we investigated the phosphorylation of p53 following loss of HdmX and/or Hdm2.

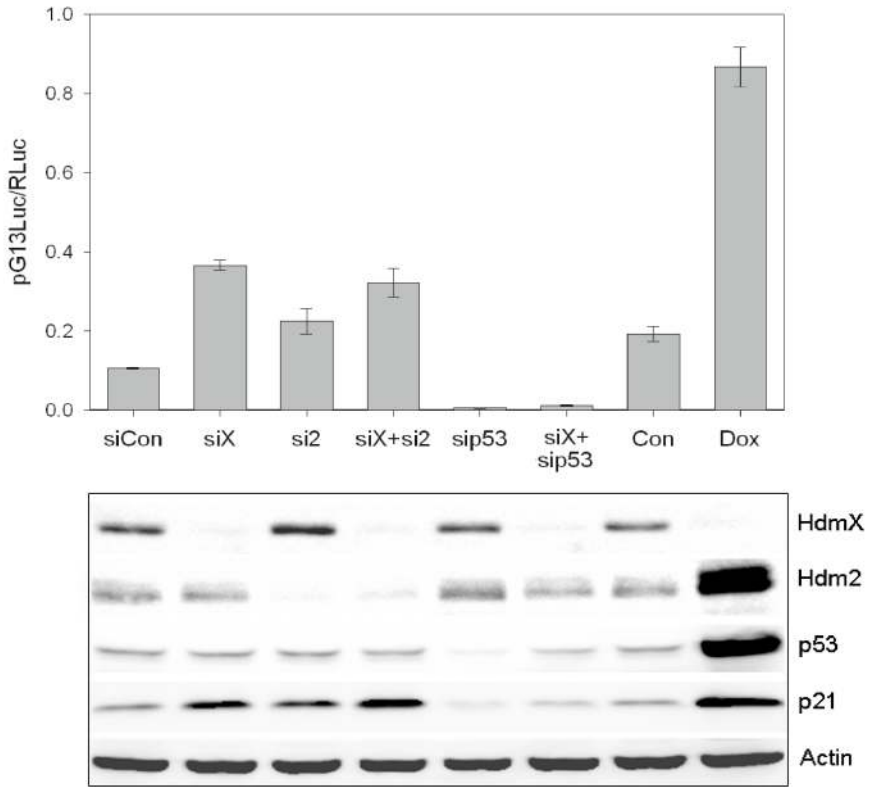

Figure 26. p53 transactivation is increased in MCF7 cells following loss of HdmX or Hdm2. MCF7 cells were transiently co-transfected with a p53 reporter (pG13Luc) and a CMV-driven renilla luciferase (RLuc) expression vector with the second siRNA transfection or with 0.5 μg/mL doxorubicin for 24 hours. Top panel: Dual luciferase activity reported as the ratio of pG13Luc/RLuc. The transcriptional activity of p53 is increased following Dox treatment and knockdown of Hdms, and eliminated in cells transfected with siRNA targeting p53. Bottom panel: Western blot analysis of indicated proteins from the various siRNA or Dox treated cells. p21 protein levels are increased following knockdown of HdmX and/or Hdm2 and with dox treatment as expected.

H. Loss of HdmX does not trigger p53 phosphorylation.

Post-translational modifications of p53 are induced by genotoxic stress in order to facilitate p53 stabilization and activation (Unger et al., 1999). One such modification is phosphorylation, which occurs at multiple sites including serines 6, 9, 15, 20, 37, 46, and 392. The phosphorylation of p53 at serines 6, 15, 20, 46, and 392 was assessed in MCF7 cells following knockdown of HdmX and/or Hdm2 by Western blot using phosphor-specific p53 antibodies (Cell Signaling Technology, Inc.). Cells treated with 0.5 μg/mL doxorubicin showed a significant induction of p53 and p53 phosphorylation at serines 15, 20, 46, and 392. A slight increase in p53 protein level was observed when both HdmX and Hdm2 were eliminated, but no significant p53 phosphorylation was detected using phospho-specific antibodies targeting serines 6, 15, 20, 46 or 392 (Figure 27). Based on these results, we conclude that the loss of HdmX and Hdm2 does not trigger a cellular stress that leads to any significant phosphorylation of p53.

I. Inhibition of cell growth after HdmX knockdown.

Since the loss of HdmX or Hdm2 appeared to preferentially activate p53 target genes encoding proteins associated with cell cycle arrest and growth inhibition, we examined how cell proliferation was impacted by HdmX knockdown. MCF7 cells were plated at low density in 6-well plates following siRNA transfection, and cells were allowed to grow for an additional ten days. Colony formation was assessed after fixing and staining the cells. Transfection with siCon or siRNA targeting p53 (sip53) showed only minimal changes in colony formation relative to non-transfected control cells (Con), while knockdown of either HdmX or Hdm2 alone or in combination led to significantly fewer colonies (Figure 28).

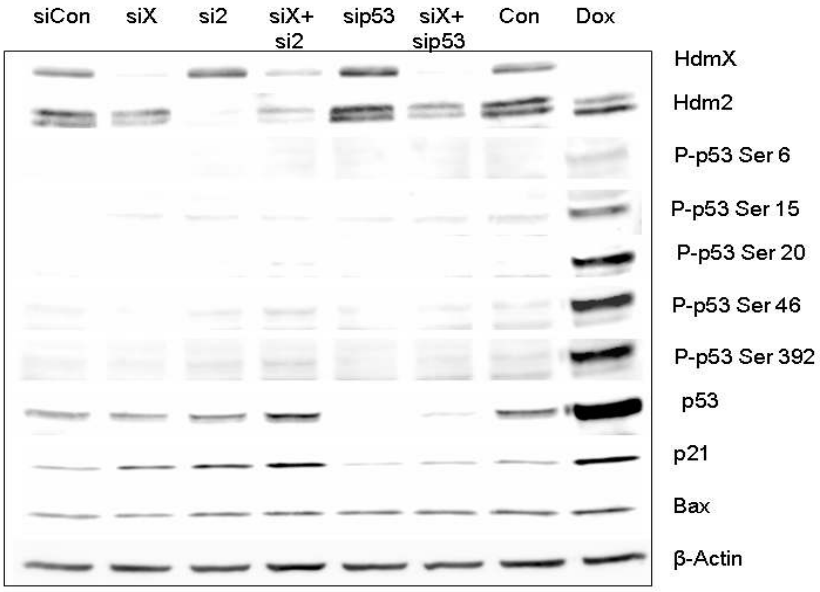

Figure 27. Neither HdmX nor Hdm2 knockdown triggers p53-phosphorylation. Whole cell extracts from MCF7 cells were prepared 48 hours after siRNA transfection. Cells treated with 0.5 μg/mL Doxorubicin were used as a positive control. Western blot analysis was performed with phospho-specific antibodies for p53. Dox treatment triggered phosphorylation on serine 15, 20, 46, and 392, while the knockdown of HdmX or Hdm2 did not result in any detectable p53 phosphorylation.

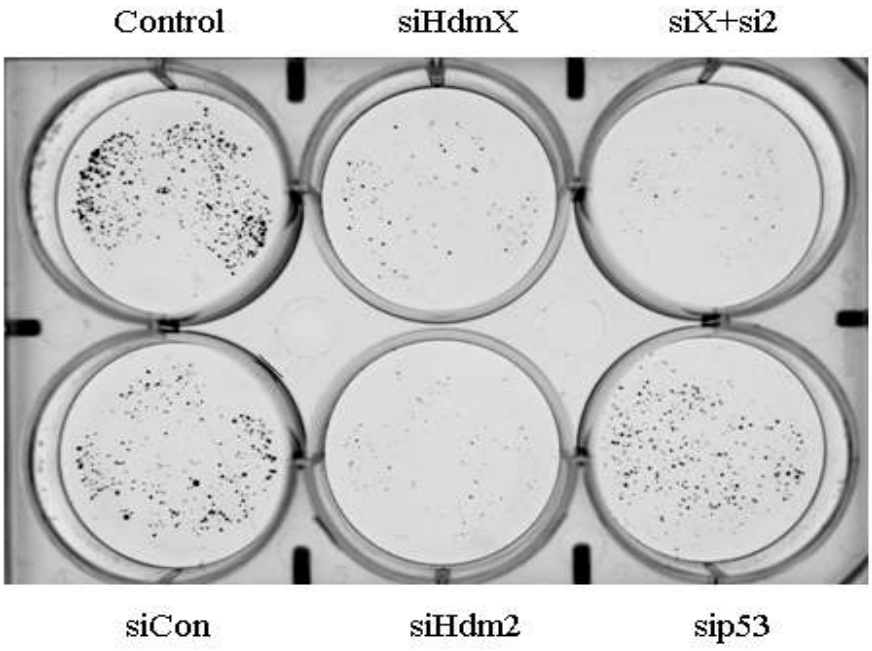

Figure 28. Loss of HdmX and/or Hdm2 inhibits MCF7 colony formation. Following siRNA transfections, MCF7 cells were seeded at 500 cells/well in 6-well plates. The cells were allowed to grow for ten days then the colonies were stained with crystal violet. Significantly fewer colonies were present following knockdown of HdmX (siHdmX) or Hdm2 (siHdm2), with the fewest number of colonies present after removal of both Hdms (siX+si2). The cells transfected with sip53 or a non-targeting control (siCon) showed minimal effects on colony formation relative to non-transfected control (Con).

Knockdown of both HdmX and Hdm2 led to the fewest colonies and the greatest growth inhibition, which correlates well with the synergistic induction of the anti-proliferative genes, p21, BTG2, and ACTA2.

In addition to colony formation, cell growth was assessed following loss of HdmX and/or Hdm2 in MCF7 cells. Following triple siRNA transfection, MCF7 cells were trypsinized and reseeded in quadruplicate at 2,000 cells/well in 96-well plates. The cells were allowed to grow for 48 hours and the percent cell growth relative to untransfected control was determined by staining the cells, solubilizing the stain and reading absorbance at 590 nm. Transfection with siCon or sip53 had minimal effects on cell growth, while siHdmX or siHdm2 alone inhibited growth by 30%, and the combination of HdmX and Hdm2 knockdown led to a 50% reduction in cell growth compared to an untransfected control (Figure 29). Growth curves were also generated over an eight day period following siRNA transfection. Cells were seeded at 2,000 cells/well in quadruplicate in 96-well plates 24 hours post siRNA transfection, and then 2, 4, 6, and 8 days later the cells were stained, the stain was extracted, and the absorbance was determined by spectro-photometer reading at 590 nm. The experiment was repeated three separate times and each time cell growth was significantly inhibited by the loss of HdmX and/or Hdm2, especially prior to day 6 (Figure 30). Once the transient knockdown of HdmX and/or Hdm2 ended, the cells began to proliferate at a rate similar to untransfected control cells. The siCon led to a slight delay in cell proliferation relative to untransfected cells, while cells transfected with sip53 had a more significant, and unexpected growth inhibition.

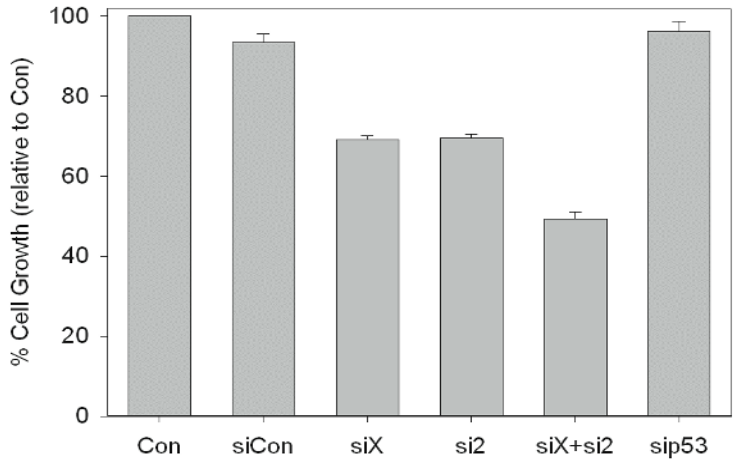

Figure 29. Loss of HdmX and Hdm2 inhibits cell proliferation. Following transfections with the indicated siRNAs, MCF7 cells were seeded at 2,000 cells/well in quadruplicate in 96-well plates. The percent cell growth relative to untransfected control (Con) was determined by staining the cells and then quantifying the stain by reading absorbance at 590 nm.

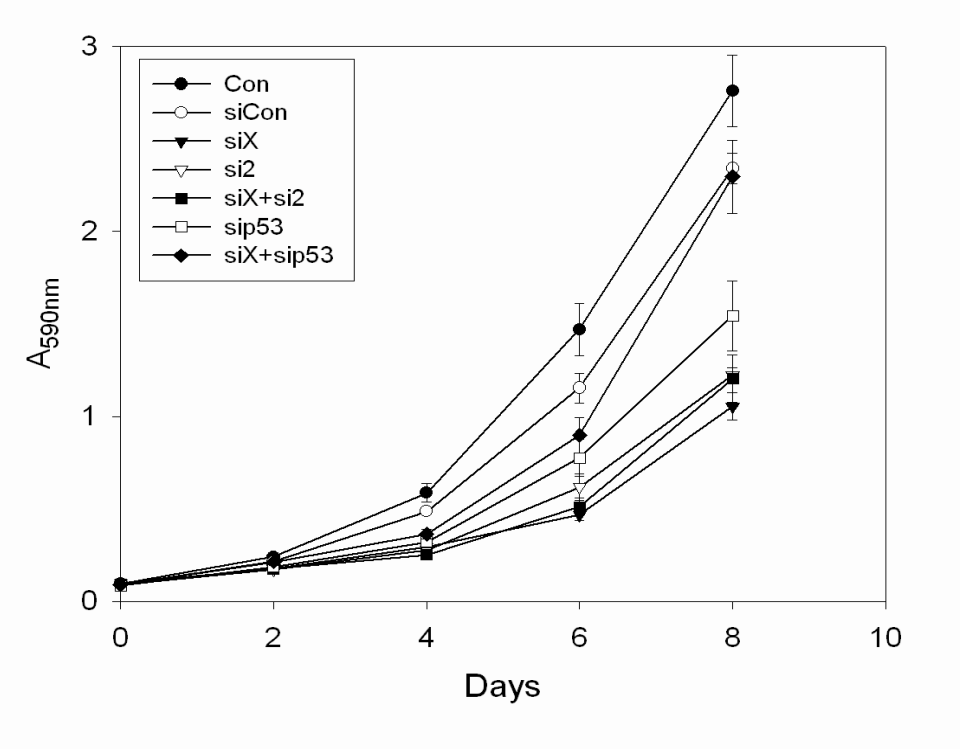

Figure 30. MCF7 cell proliferation is inhibited by knockdown of HdmX and Hdm2. Following siRNA transfections, MCF7 cells were seeded at 2,000 cells/well in 96-well plates and allowed to grow for 2, 4, 6, and 8 days. The absorbance at 590 nm (A_{590nm}) was determined by staining the cells with crystal violet and then quantifying the stain on a spectrophotometer after extraction with 10% acetic acid. The absorbance is proportional to cell number.

To assess how the decrease in cell proliferation induced by loss of HdmX and Hdm2 affected cell cycle progression, the same experiments were repeated in MCF7 cells and DNA content was analyzed by flow cytometry. The loss of either HdmX or Hdm2 led to an increase in G1 cells and a decrease in S phase cells (Figure 31A). MCF7 cells transfected with siCon or sip53 maintained a cell cycle distribution similar to that of non-transfected cells (Con). The changes in cell cycle were quantified by plotting the G1/S ratio for the various siRNA transfections. Both siHdmX and siHdm2 transfection resulted in an approximately four fold increase in the G1/S ratio when compared to non-transfected cells (Con) or cells transfected with siCon or sip53 (Figure 31B). A similar G1 cell cycle arrest was also observed in U2OS cells following HdmX knockdown by a single siRNA transfection (Figure 32A). The difference in cell cycle distribution was plotted as a ratio of the percentage of G1 cells to S phase cells. As seen with MCF7 cells, loss of HdmX led to a significant increase in the G1/S ratio compared to mock transfected and siCon transfected cells (Figure 32B).

J. Enhanced chemosensitivity after loss of HdmX

Since the knockdown of HdmX and Hdm2 appears to result in an anti-proliferative effect rather than cell death, I examined whether the loss of HdmX or Hdm2 might sensitize the cells to chemotherapeutic agents. MCF7 cells were transfected with the indicated siRNA, and 24 hours post transfection RT-PCR was performed to confirm that the siRNA led to alterations in gene expression (Figure 33A). The cells were trypsinized, counted and seeded at 20,000 cells/well in 96-well plates. Twenty-four hours later (Day 0), cell viability was assessed to determine seeding efficiency and the cells were treated with varying doses of doxorubicin (Dox) for 48 hours.

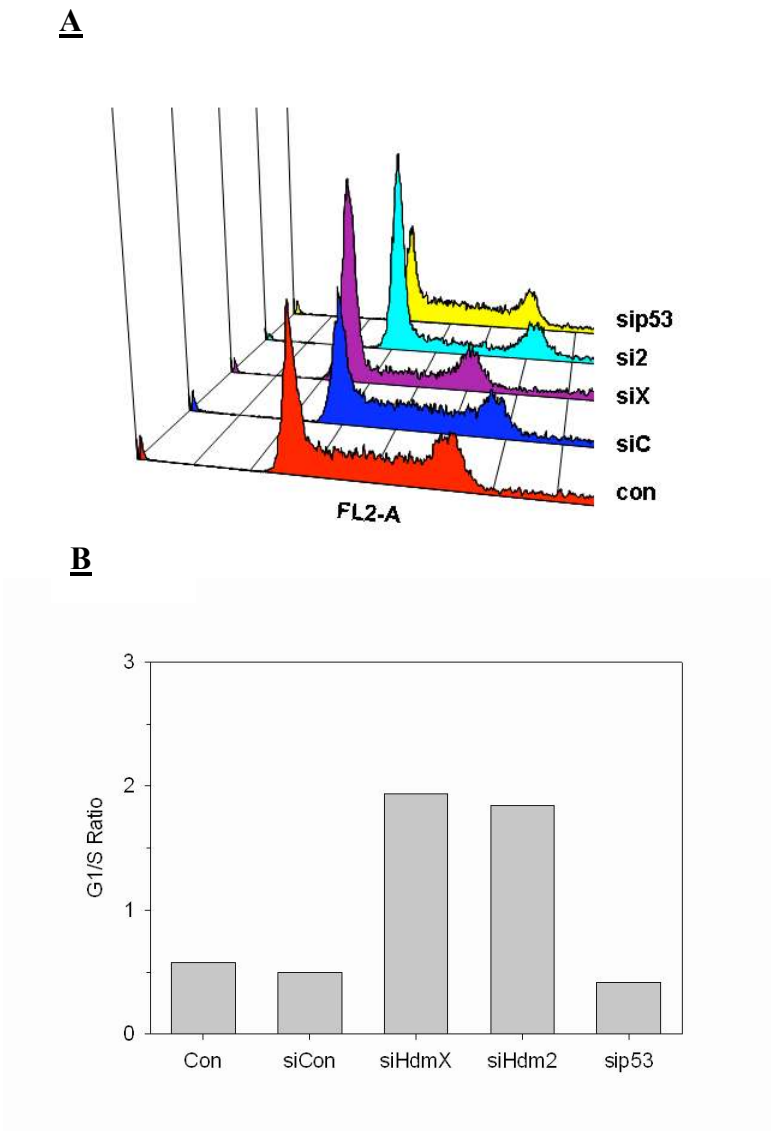

Figure 31. HdmX knockdown triggers G1 cell cycle arrest in MCF7 cells. MCF7 cells were stained with propidium iodide four hours after the second siRNA transfection and cell cycle distribution was determined by flow cytometry. (A) Histograms illustrating the cell cycle profiles after transfection with the indicated siRNAs. (B) Ratio of the percentage of G1/S phase cells. An increase in G1 and a decrease in S phase cells were observed following loss of HdmX or Hdm2 indicating a G1 cell cycle arrest.

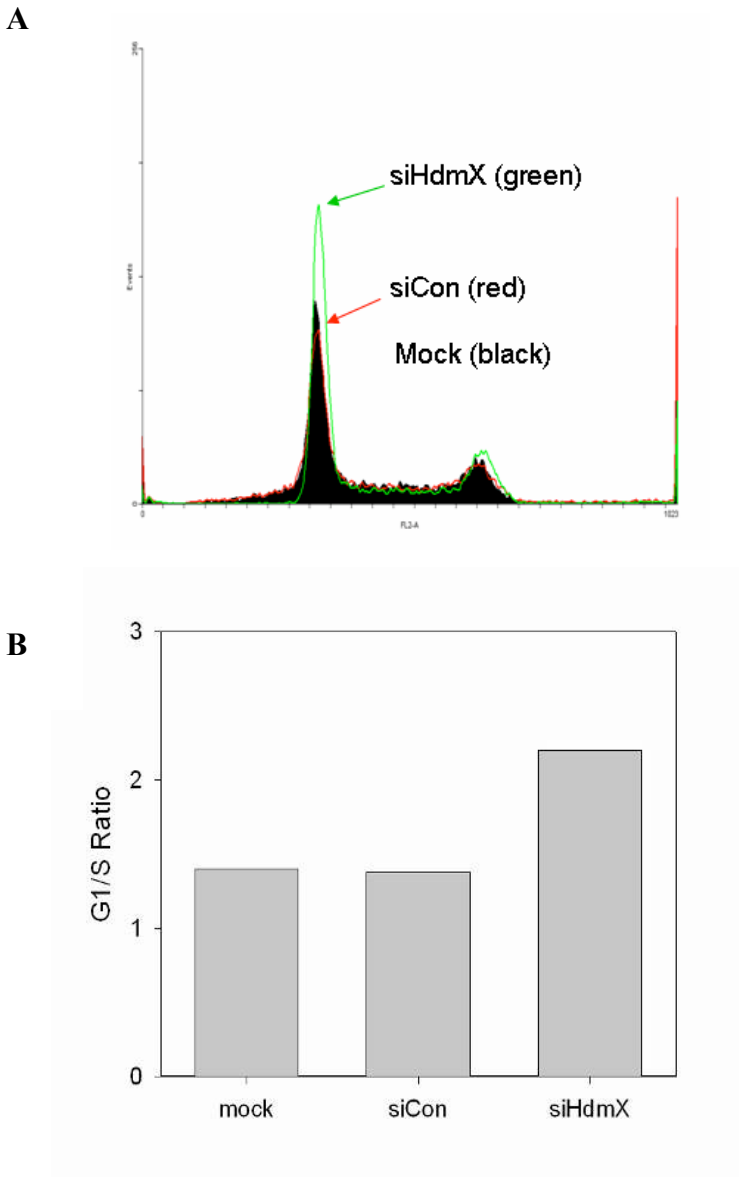

Figure 32. Loss of HdmX triggers G1 cell cycle arrest in U2OS cells. U2OS cells were stained with propidium iodide 24 hours after siRNA transfection and DNA content was analyzed by flow cytometry. (A) Histogram overlay comparing cell cycle profiles from mock, siCon, and siHdmX transfected cells. (B) Ratio of G1/S phase cells. Loss of HdmX resulted in an increase in G1 and a decrease in S phase cells.

Figure 33. Knockdown of HdmX enhances doxorubicin-induced cytotoxicity. (A) RT-PCR analysis of *hdmX*, *hdm2*, *p21* and *p53* gene expression in the indicated siRNA transfected MCF7 cells. The *hdmX*, *hdm2*, and *p53* transcripts were effectively knocked down by siRNA prior to drug treatment. (B) Percent cell viability relative to untransfected untreated control cells. MCF7 cells were treated with doxorubicin (0.25-1.0 μg/mL) for 48 hours and cell viability was determined by absorbance at 590 nm. The loss of HdmX and/or Hdm2 showed an enhanced cytotoxicity relative to control cells.

A

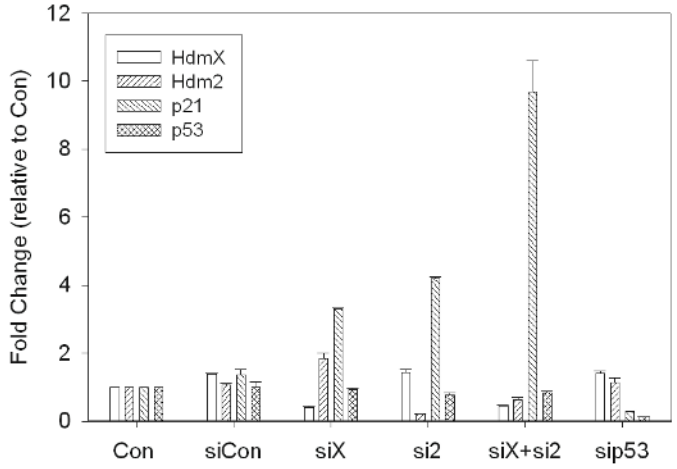
HdmX
Hdm2
p21
p53
Fold Change (relative to Con)
12
10
8
6
4
2
0
Con
siCon
siX
si2
siX+si2
sip53

B

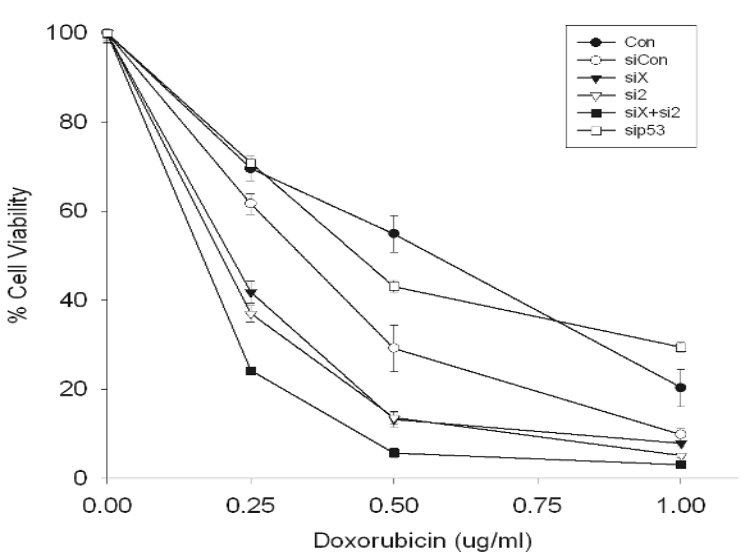
Con
siCon
siX
si2
siX+si2
sip53
% Cell Viability
100
80
60
40
20
0
0.00
0.25
0.50
0.75
1.00
Doxorubicin (ug/ml)

Cell viability was determined by staining the cells, reading absorbance at 590 nm and normalizing to Day 0. Knockdown of HdmX and/or Hdm2 increased the cytotoxicity of doxorubicin, a topoisomerase II inhibitor, suggesting that the removal of p53 negative regulators enhances the chemosensitivity of MCF7 cells to DNA damaging agents (Figure 33B).

MCF7 cells were also treated with varying doses of AraC or cisplatin following HdmX and/or Hdm2 siRNA transfection, and cell viability was assessed by the fluorescent redox reagent, CellQuanti™-Blue. Western blot analysis of HdmX, Hdm2, p53, and p21 was used to confirm successful knockdown by the indicated siRNA, and activation of p21 (Figure 34A). Transfection with siRNAs targeting HdmX or Hdm2 increased the cytotoxicity of AraC, a DNA replication inhibitor (Figure 34B), similar to doxorubicin. The removal of HdmX and Hdm2 enhanced the cytotoxicity of cisplatin, a chemotherapy drug that cross links DNA to form adducts, however at doses of 20 μM or greater this effect was seen in all siRNA transfected cells including siCon compared to untransfected control cells (Figure 34C). As predicted by the alterations gene expression, colony formation assays, and cell proliferation assays, the knockdown of both HdmX and Hdm2 created the most cytotoxicity when combined with any of the agents tested.

K. Investigation of HdmX knockdown on Hdm2 and p53 localization and stabilization.

Since HdmX can interact with both Hdm2 and p53, I examined how the removal of HdmX would affect Hdm2 and p53 localization and stability. HdmX is predominantly a cytoplasmic protein, where as Hdm2 is known to shuttle between the nucleus and the cytoplasm. To assess Hdm2 and p53 localization in MCF7 cells following the loss of

Figure 34. Knockdown of HdmX enhances Ara-C induced cytotoxicity.

(A) Western blot analysis of Hdm2, HdmX, p53 and p21 proteins in MCF7 cells following the indicated siRNA transfections confirms knockdown. (B&C) Percent cell viability relative to untransfected untreated control cells. MCF7 cells were treated with AraC (0.1-0.5 μM) for 48 hours (B) or with cisplatin (5-20 μM) for 24 hours (C) and viability was determined by CellQuanti-Blue reagent. The loss of HdmX and/or Hdm2 showed an enhanced cytotoxity relative to control cells.

A

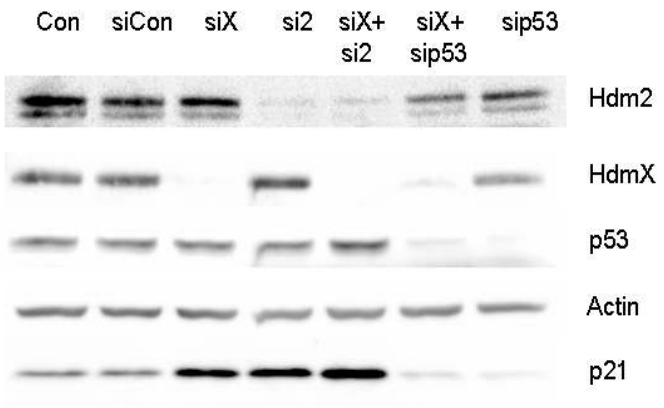
Con
siCon
siX
si2
siX+ si2
siX+ sip53
sip53
Hdm2
HdmX
p53
Actin
p21

B

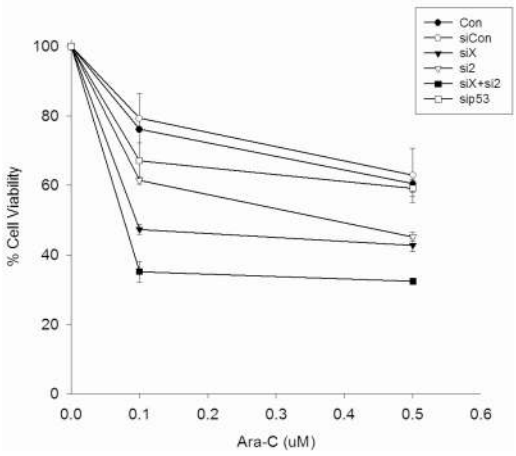
Con
siCon
siX
si2
siX+si2
sip53
% Cell Viability
Ara-C (uM)

C

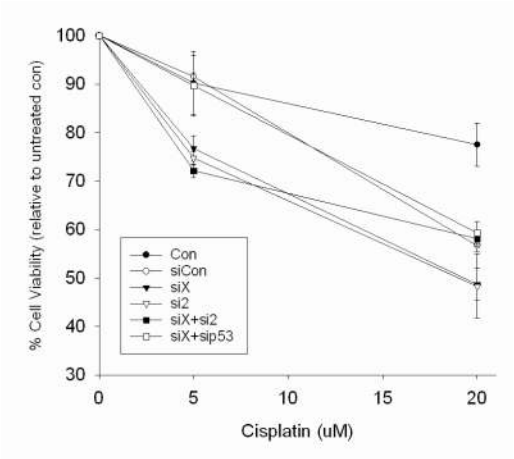
% Cell Viability (relative to untreated con)
Con
siCon
siX
si2
siX+si2
siX+sip53
Cisplatin (uM)

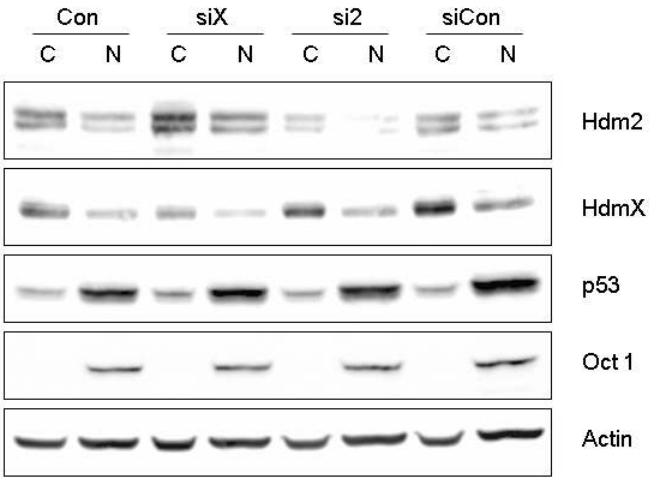

Figure 35. Loss of HdmX or Hdm2 does not alter p53 localization. Nuclear and cytoplasmic extracts were prepared from MCF7 cells following HdmX or Hdm2 knockdown. The localization of p53, HdmX, or Hdm2 was not altered by treatment with the indicated siRNA. The nuclear protein, Oct-1, was used to monitor the purity of the protein extracts.

HdmX, nuclear and cytoplasmic extracts were prepared and the proteins were resolved on a SDS 10% polyacrylamide gel. Western blot analysis of HdmX, Hdm2, p53, Oct-1, and β-actin revealed no significant changes in p53 or Hdm2 localization following HdmX knockdown (Figure 35). The p53 protein is predominantly nuclear and its localization is not changed by either removal of HdmX or Hdm2.

To assess Hdm2 and p53 localization in MCF7 cells following the loss of HdmX, nuclear and cytoplasmic extracts were prepared and the proteins were resolved on a SDS 10% polyacrylamide gel. Western blot analysis of HdmX, Hdm2, p53, Oct-1, and β-actin revealed no significant changes in p53 or Hdm2 localization following HdmX knockdown (Figure 35). The p53 protein is predominantly nuclear and its localization is not changed by either removal of HdmX or Hdm2. HdmX was predominantly cytoplasmic as expected, and loss of Hdm2 did not appear to impact its localization. Similarly, Hdm2 cellular distribution was not altered by the removal of HdmX, although the total level of Hdm2 was increased following loss of HdmX likely resulting from increased p53 transactivation since a proteasome inhibitor was present. These observations were confirmed by measuring the density of each band on the Western blot and determining the ratio of nuclear to cytoplasmic protein expression level. The ratios were very similar among all the siRNA transfected cells. Oct-1, which is only found in the nucleus, was used to monitor the purity of the nuclear and cytoplasmic protein extraction. As expected, Oct-1 was only detected in the nuclear fraction (Figure 35). Beta-actin was included as a loading control since it is found in both the nuclear and cytoplasmic fractions.

To examine Hdm2 and p53 stability following HdmX knockdown, MCF7 cells were triple transfected with siRNA and 24 hours later the cells were treated with 20 μM MG132 for four hours. The MG132 is a proteasome inhibitor which prevents proteasomal degradation of p53, HdmX, and Hdm2. Since the loss of HdmX increased *hdm2* gene expression (Figures 23 and 33A), but an increase in Hdm2 protein by Western blot was not detectable without a proteasome inhibitor, I investigated whether or not Hdm2 stability was altered by the removal of HdmX. In the presence of MG132, an increase in Hdm2 protein expression was detectable following the loss of HdmX; suggesting that the increase in Hdm2 transcripts did led to increased protein levels (Figure 36). Additional experiments were performed to assess if p53, Hdm2, or HdmX half-life was altered after siRNA transfection in MCF7 cells. The cells were treated with 50 μg/mL cycloheximide (Sigma, Inc), a protein synthesis inhibitor, 24 hours after the third siRNA transfection and protein was extracted 0, 1, 2, and 4 hours later. The loss of Hdm2 stabilized p53 slightly as expected, whereas the loss of HdmX had little effect on p53 stability (Figure 37A & B). However, the removal of HdmX, a binding partner of Hdm2, appears to decrease Hdm2 stability possibly by leaving Hdm2 more vulnerable to auto-ubiquitination and proteasomal degradation (Figure 37A & C). Likewise, removal of Hdm2 appears to decrease HdmX stability relative to siCon transfected MCF7 cells (Figure 37A). This is an unexpected result since upon DNA damage Hdm2 promotes the ubiquitination and proteasomal degradation of HdmX, thus the removal of Hdm2 would be expected to stabilize HdmX. The experiment was repeated and similar results were observed following knockdown of HdmX and Hdm2 relative to untransfected control (Con) cells (Western blot not shown).

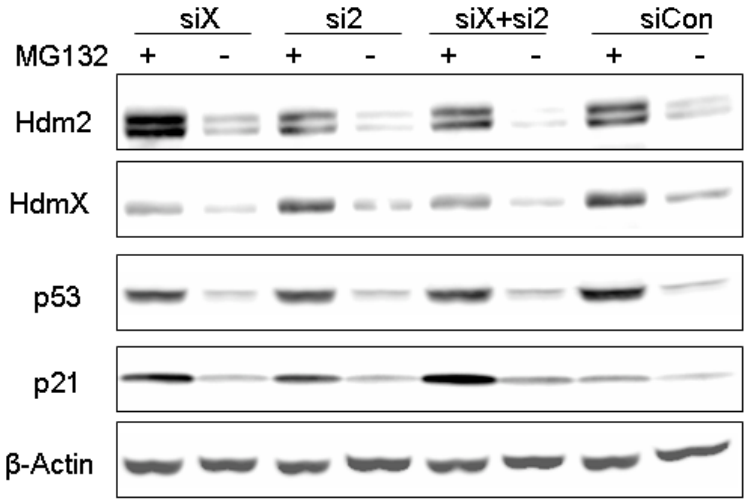

Figure 36. HdmX knockdown increases Hdm2 expression. MCF7 cells were treated with 20 μM MG132 for 4 hours, one day after the final siRNA transfection, and Hdm2, HdmX, p53, p21, and β-actin were analyzed by Western blot. p21 expression was induced by loss of HdmX and/or Hdm2, as expected.

The stability of Hdm2 and p53 over time post cycloheximide in the untransfected control cells was quantified by measuring the density of the bands normalized to β-actin (Figures 37B and 37C).

Finally, the effect of HdmX or Hdm2 knockdown on normal non-tumor IMR90 cells was investigated. IMR90 cells were triple transfected and total RNA was isolated 24 hours after the third transfection and protein was extracted 48 hours following the third siRNA transfection. RT-PCR analysis showed a 1.5 fold increase and a 2.5 fold increase in p21 gene expression following loss of HdmX or loss of Hdm2, respectively (Figure 38A). These levels of p21 induction are slightly less in IMR90 cells than those seen in MCF7 cells following triple siRNA transfection (compare Figure 13A to 38A). Western blot analysis of p21 protein expression correlated with the p21 transcript levels (Figure 38B). Interestingly, a slight increase in p53 protein was detectable following loss of HdmX and a greater increase in p53 levels were observed following removal of Hdm2. This result differs from that seen in MCF7 cells, where a slight increase in p53 protein expression was detected only when both HdmX and Hdm2 were removed. Hdm2 protein levels are low in IMR90 cells and were below the detectable limits of the antibody/Western blot protocol used. Both siHdmX and sip53 successfully eliminated HdmX and p53 protein respectively (Figure 38). Beta-actin was used as a loading control.

Figure 37. Loss of Hdm2 stabilizes p53, while loss of HdmX destabilizes Hdm2. MCF7 cells were treated with 50 μg/mL cycloheximide (CHX) for 0, 1, 2, and 4 hours following HdmX or Hdm2 knockdown. (A) Western blot of HdmX, Hdm2, p21 and p53 protein expression. (B) Percentage of p53 protein remaining over time post CHX treatment relative to time 0. (C) Percentage of Hdm2 protein remaining over time post CHX treatment relative to time 0. Protein levels were quantitated by measuring the density of each band relative to β-actin (loading control). The half-life of p53 was slightly increased by loss of Hdm2. Removal of HdmX appears to decrease Hdm2 stability relative to untransfected control (Con) or siCon transfected cells.

A

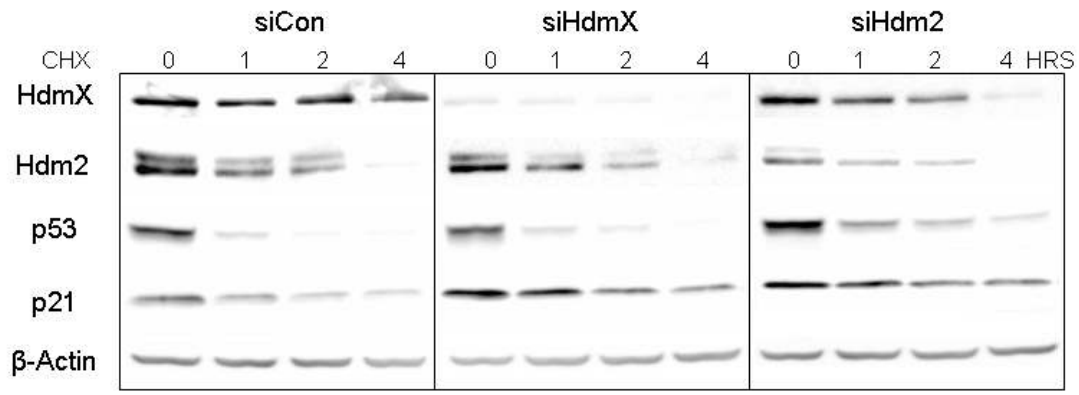
siCon
siHdmX
siHdm2
CHX
0 1 2 4 0 1 2 4 0 1 2 4 HRS
HdmX
Hdm2
p53
p21
β-Actin

B

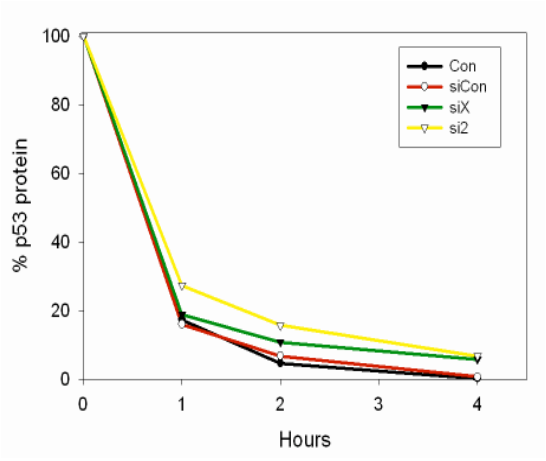
% p53 protein
Hours
Con
siCon
siX
si2

C

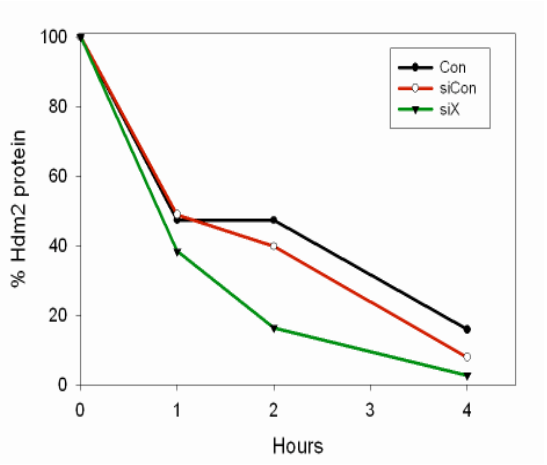
% Hdm2 protein
Hours
Con
siCon
siX

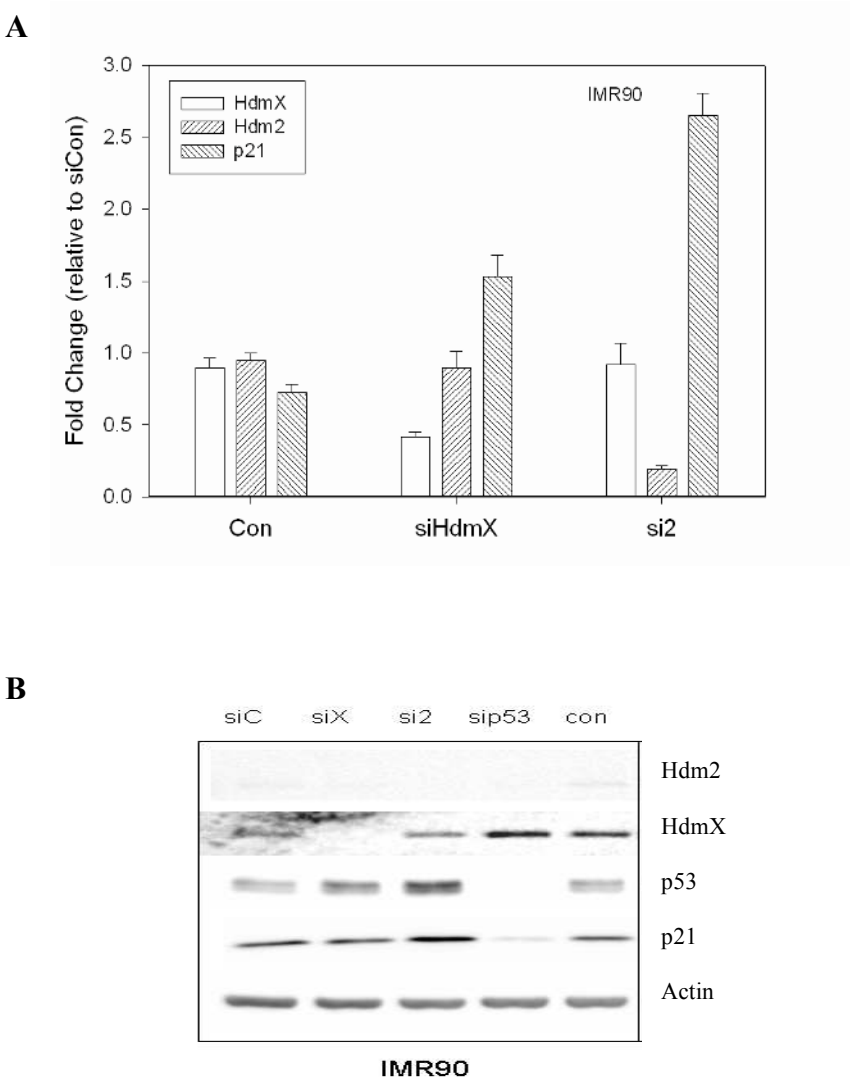

Figure 38. HdmX knockdown in non-tumor IMR90 cells. (A) RT-PCR analysis of *hdmX, hdm2*, and *p21* gene expression following triple transfection with the indicated siRNA. (B) Western blot of Hdm2, HdmX, p53, p21, and actin. Hdm2 levels are low in IMR90 cells, thus were not detectable. p53 is increased following loss of Hdm2, but only slightly increased by loss of HdmX relative to siCon or untransfected control (con).

IV. DISCUSSION

A. HdmX knockdown by RNAi

Two RNAi approaches were assessed in this study to knockdown HdmX; transient transfection of siRNA and stable transduction of shRNA using a lentivirus-delivered shRNA vector. Since lentiviral delivered shRNA has the advantage of stable long term silencing over transient siRNA transfections, viral shRNA delivery has gained wide use in creating stable knock-down cell lines. The viral shRNA delivery system is particularly useful for cells which are difficult to transfect. To investigate the role of HdmX deregulation of p53 function in tumors with wild-type p53 and overexpressed HdmX, shRNA vectors were designed containing the same target sequence as the siRNA used to silence HdmX. Both transient siRNA transfection and shRNA vectors were effective at decreasing HdmX transcript and protein levels, and at inducing p53 target genes (Figures 10, 13, 15). Multiple siRNA transfections using Oligofectamine were especially effective at knocking down HdmX expression with greater than 90% of the cells taking up the siRNA as determined by siTOX transfection experiments (data not shown). However, the knockdown of HdmX and Hdm2 by siRNA transfection only lasted for three and five days, respectively (Figure 14). The knockdown of HdmX in cells stably expressing shRNA targeting HdmX remained down regulated for up to 30 days, but it too eventually returned to levels of uninfected cells. The loss of knockdown

over time in stable cell lines has been reported previously and is hypothesized to occur because high expression levels of shRNAs are cytotoxic to cells (Fish and Kruithof, 2004). Neither the siRNA control nor the shRNA control vectors affected HdmX expression relative to mock transfected or uninfected cells, respectively. Surprisingly, the expression of control shRNA vectors (shLamin, shLacZ, or sh scrambled sequence) triggered activation of the p53 target genes, *p21* and *gadd45,* in several tumor cell lines (Figure 15 and data not shown). Since all three control shRNA vectors tested induced non-targeted genes suggests that this is a sequence-independent effect. Transfection of siRNA control (siCon) which does not target any known genes, did not alter the p53 target genes examined (Figure 13). Previous reports have shown that the viral DNA integration process and survival of transduced cells requires ATR kinase activity which leads to a DNA damage response (Daniel et al., 2003). Thus the non-specific induction of p21 with lentiviral-delivered shRNA vectors could have been the result of the viral DNA integration process. However, since infection with lentivirus expressing the Tetracycline repressor gene (Figure 15A) did not induce *p21* transcripts, the possibility that the off-target p21 induction was due to a general anti-viral response by the cells was excluded. To determine if the non-targeted induction of p21 by the lentivirus-delivered shRNA control vectors is p53-dependent, two p53-null tumor cell lines were infected with lentivirus containing shRNA. In the HCT116 cells containing wild-type p53 and in the HCT116 cells devoid of p53, p21 protein and transcript levels were increased in both the shHdmX and shLacZ expressing cells relative to uninfected (Figure 16). The induction of p21 was greater in the HCT116-p53+/+ cells compared to the HCT116-p53-/- cells as expected since the lentivirus-delivered shRNA vectors increased p53 protein

levels (Figure 16A) and p53 transactivation (Figure 18). Likewise, p53-null Saos-2 cells stably infected with lentivirus containing shHdmX and shLacZ also expressed elevated levels of p21; implying that the induction of p21 by the shRNA vectors was predominantly p53-independent (Figure 17).

In an effort to uncover the mechanism by which shRNA vectors were triggering the non-specific induction of p21, the gene expression of *OAS1* and *IFIT1*, two interferon response genes, was determined following RNAi (Bridge et al., 2003). While the three cell lines tested showed variable levels of *OAS1* activation after lentiviral shRNA infection, they all consistently expressed 2-4 fold increases in *p21* mRNA (Figure 18). These results suggest that the level of interferon activation does not correlate with the off-target *p21* induction being triggered by the lentiviral delivered shRNA vectors. Given that interferon has been reported to activate p21 in MCF7 cells (Gooch et al., 2000), the cells were treated with interferon-gamma (IFN) and OAS1 and p21 mRNA levels were measured by real-time PCR. Surprisingly, IFN treatment did not induce p21 gene expression in either MCF7 cells or HCT116 cells (Figure 21). However, given that induction of *OAS1* and *IFIT1* was detected upon IFN treatment in both MCF7 and HCT116 cells, indicates that both of these cell lines possess an interferon response mechanism (Figure 20 and 21). Taken together, these findings suggest that an interferon response to the lentivirus delivered shRNAs does not account for all the non-specific induction of p53 target genes in the tumor cell lines examined.

Although the non-targeted induction of p53 target genes like *p21* and *gadd45* did not result in a level of protein induction sufficient to trigger a significant cell cycle arrest (data not shown), these results still raise concern regarding the use of lentiviral-delivered

shRNAs to study gene function in tumor cells. Clearly the presence and/or processing of the lentiviral-delivered shRNA vectors appeared to cause a non-specific cellular stress that is altering the expression of untargeted genes. Given these results, transient siRNA transfection was selected as the method of choice for the GeneChip experiment over the shRNA vectors due to the induction of off-target genes in cells expressing shRNA vectors. Others have also raised concerns with constitutive shRNA expression using lentiviral shRNA vectors employing polIII promoters (Liu et al., 2004; Makinen et al., 2006). The utilization of a tetracycline inducible lentiviral shRNA system (Szulc et al., 2006; Wiznerowicz et al., 2006; Wiznerowicz and Trono, 2003) was also assessed as a way to minimize the non-specific effects on untargeted genes such as *p21*. However, there were many issues with this system as well. I am currently investigating other vector systems to deliver shRNA that are not lentiviral based to determine if this non-specific gene induction is specific to lentiviral vectors or any shRNA vector. Although the exact mechanism of the cellular stress caused by the lentiviral-delivered shRNAs that trigger p53 activation and induction of p53 target genes remains unclear, this study demonstrates that neither an interferon response nor a sequence specific effect is the cause of these alterations in gene expression.

B. Alterations in Gene Expression following loss of HdmX

While half of all human tumors possess p53 mutations, inactivation of wild-type p53 can also occur through a variety of mechanisms that do not involve p53 gene mutation or deletion. Diverse approaches have been proposed to reactivate wild-type p53 protein in those tumors which do not harbor p53 mutations. Recent studied have uncovered that the activation of p53 is blocked in human tumors harboring elevated

levels of HdmX (Danovi et al., 2004; Laurie et al., 2006), suggesting that HdmX:p53 interaction is a relevant and novel target for therapeutic approaches. For these reasons, an Affymetrix GeneChip experiment was performed to determine how loss of HdmX or Hdm2 affects global gene expression in MCF7 cells. MCF7 cells were chosen because they possess wild-type p53 and elevated levels of HdmX and Hdm2 (Ramos et al., 2001). The overexpression of HdmX and/or Hdm2 is one mechanism to inactivate wild-type p53 and the inactivation of the p53 signaling pathway is essential for tumor formation (Danovi et al., 2004; Laurie et al., 2006; Toledo and Wahl, 2006). Lists of genes that were induced by at least two fold or suppressed by at least 50% following knockdown of HdmX or Hdm2 were created using GeneSpring software (Table 4). The datasets were initially screened for known p53 target genes since my hypothesis is that loss of HdmX will activate p53 and induce p53 target genes. As expected, a subset of p53 target genes was induced, however this set of genes only accounted for 10-15% of the total genes on the lists. It is difficult to estimate how many genes out of the total number of known p53 target genes this subset represents, since there is not an all inclusive list of p53 target genes available (Levine et al., 2006; Qian et al., 2002). Interestingly, the subset of p53 target genes that were induced upon HdmX or Hdm2 knockdown predominantly encoded proteins associated with cell cycle arrest and growth inhibition (Table 5). Included on this list are a couple of less well known p53 target genes reported to inhibit cell growth, *ACTA2* (smooth muscle actin alpha 2) (Comer et al., 1998) and *wig-1* (Hellborg et al., 2001). In contrast, only one p53 dependent pro-apoptotic gene (i.e. Fas) was increased. This result was surprising, and implies that the knockdown of HdmX or Hdm2 may not be a viable antitumor therapeutic approach since it only induced one apoptotic p53 gene.

A comparison of the genes induced following loss of HdmX to the genes induced following loss of Hdm2 in the MCF7 cells found 144 genes common to both lists. Thus, there were similar patterns of p53 target gene activation in the MCF7 cells lacking either HdmX or Hdm2 indicating that loss of either negative regulator would lead to the same outcome, predominantly cell cycle arrest. The concurrent knockdown of HdmX and Hdm2 led to either synergistic or additive activation of several p53 target genes as determined by RT-PCR (Figure 23). Furthermore, the induction of these target genes are p53-dependent, as no induction of these p53 target genes where observed after HdmX or Hdm2 knockdown in several p53-null tumor cell lines (Figures 24B and 25). These findings in MCF7 breast cancer cells are in contrast to recent mouse model studies whereby removal of p53 from adult tissues lacking either Mdm2 or MdmX, led to distinct and synergistic effects between the two proteins depending on the tissue examined (Boesten et al., 2006; Francoz et al., 2006; Maetens et al., 2006; Marine et al., 2006; Xiong et al., 2006). The removal of HdmX was anti-proliferative in some tissues, while loss of Hdm2 caused apoptosis. Additionally, the removal of both caused extensive cell damage and synergistic expression of several p53 target genes. Other studies to elucidate the mechanisms by which Mdm2 and MdmX regulate p53 imply that MdmX regulates p53 transactivation, while Mdm2 controls p53 stability but does not control transcriptional activity per se (Toledo et al., 2006). Here I observe that in MCF7 tumor cells, knockdown of HdmX or Hdm2 appear to have similar, but synergistic effects on p53 activity and gene expression. To examine how loss of HdmX and/or Hdm2 effects p53 transactivation, a p53 luciferase reporter was tranfected into MCF7 cells lacking HdmX and/or Hdm2. Interestingly, loss of HdmX resulted in greater p53 transcriptional

activity than loss of Hdm2, and the combined knockdown was similar to loss of HdmX alone (Figure 26). These results support the hypothesis that the primary function of HdmX is to regulate p53 transactivation, while Hdm2 is not as effective at regulating p53 transcriptional activity. Additionally, since Hdm2 can ubiquitinate HdmX and mediate HdmX degradation (de Graaf et al, 2003; Pan and Chen, 2003; Marine and Jochemsen, 2004), the loss of Hdm2 may lead to more HdmX available to bind p53. Thus, the balance between HdmX and Hdm2 levels appears to be critical for the regulation of p53, which is in agreement with the mutual dependency model (Gu et al., 2002).

The elimination of p53 via siRNA in MCF7 cells led to significant decreases in the expression of p53 target genes associated with both cell cycle arrest and apoptosis (Table 5). Therefore, the lack of pro-apoptotic genes induced following the loss of HdmX or Hdm2 is not due to the inability of these genes to be regulated by p53. In fact, several p53 regulated pro-apoptotic genes were activated when MCF7 cells were treated with the DNA damaging agent, doxorubicin (Figure 27 and data not shown). It is clear from the GeneChip experiment that HdmX or Hdm2 knockdown in MCF7 cells results in p53 transactivation of a subset of target genes that are predominantly involved in cell cycle arrest and growth inhibition.

How activated p53 selectively turns on one subset of genes or another subset of genes is still unclear. The two most studied biological outcomes of p53 activation are cell cycle arrest and apoptosis. The induction of cell cycle arrest occurs as a result of p53 transcriptional activation of the *CDKN1A* gene that encodes p21, a cyclin-dependent kinase (CDK) inhibitor (Prives and Hall, 1999). The p21 protein prevents cell cycle progression and causes a G1 cell cycle arrest by associating with and inhibiting cyclin-

CDK complexes (el-Diery et al, 1993; Harper et al, 1993). The induction of apoptosis by p53 is less understood, however it has been suggested that the *BCL-2* family is important, especially the transactivation of *NOXA* and *PUMA* (Nakano and Vousden, 2001; Oren, 2003; Shibue et al., 2006; Yu et al., 2001). In this study, *CDKN1A* was induced by loss of HdmX and Hdm2, but neither *NOXA* nor *PUMA* were altered. The activation of p21 following HdmX knockdown correlates with previous reports (Gu et al, 2002; Linares et al, 2003; Danovi et al, 2004), however the induction of a subset of other p53 target genes involved in growth inhibition uncovered in this study is a novel finding. In addition to GeneSpring, Ingenuity Pathway Analysis (IPA) software was used to identify unique genes and pathways that may be regulated by HdmX. The lists of genes induced and suppressed following the loss of HdmX in MCF7 cells were uploaded into the IPA software. Several different networks or pathway maps were created from the gene lists, which enabled me to identify unique interactions between genes or the proteins that they encode which may not be obvious. The pathway map associated with p21 (Figure 39) contained the greatest number of gene expression alterations, thus emphasizing that the induction of p21 is a key outcome of HdmX or Hdm2 knockdown in MCF7 cells. It would be interesting to knockdown p21 in combination with siHdmX or siHdm2 to evaluate the biological effect and role of p21.

To understand how the loss of HdmX or Hdm2 in MCF7 cells could lead to p53 transactivation and the induction of a specific subset of p53 target genes, p53 phosphorylation was assessed using phospho-specific antibodies. Post-translational modifications of p53 are induced by various genotoxic stresses leading to p53 stabilization and increasing transactivation (Unger et al, 1999; Lavin and Gueven, 2006).

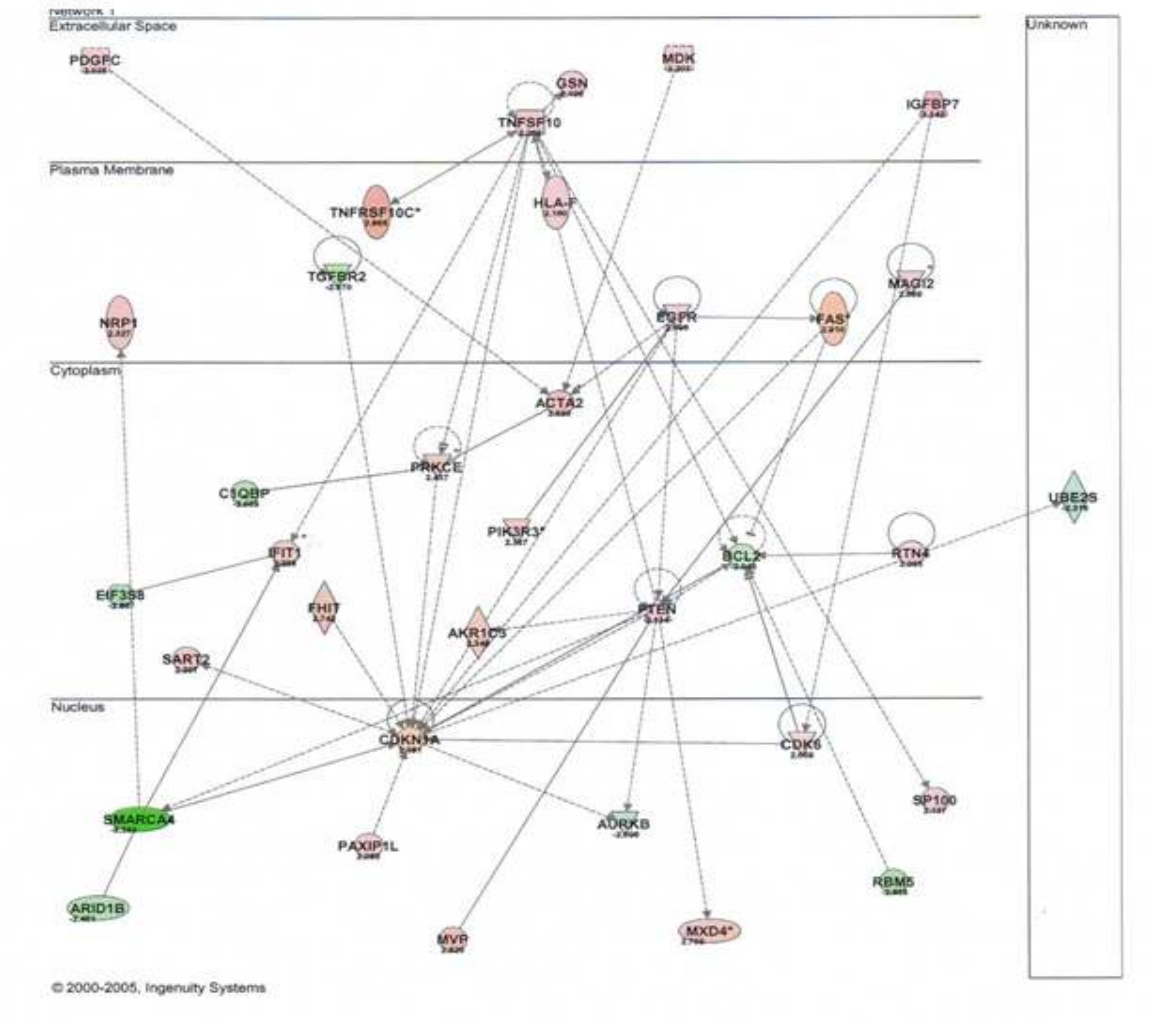

Figure 39. Ingenuity Pathway Analysis of genes altered by HdmX knockdown in MCF7 cells. The network shows cellular localization of the gene products induced (red) and suppressed (green).

While a slight increase in p53 protein level was observed when both HdmX and Hdm2 were eliminated concurrently in MCF7 cells, no significant p53 phosphorylation was detected on serines 6, 15, 20, 46, or 392 (Figure 27). Since the siRNA knockdown of HdmX or Hdm2 did not trigger p53 phosphorylation or a significant induction of p53 protein suggests that the knockdown of HdmX or Hdm2 did not elicit a genotoxic stress. These results suggest that the increase in p53 transactivation and induction of p53 target genes is the result of nongenotoxic activation of p53. The successful activation of p53 in a nongenotoxic fashion was demonstrated with the small molecule Nutlin, which inhibits the p53:Mdm2 interaction, thus leading to activation of p53 (Vassilev, 2004). Other nongenotoxic stresses that have been shown to induce a p53 response include premature senescence, hypoxia, osmotic shock, and microtubule disruption (Lavin and Gueven, 2006).

C. Biological effects of HdmX knockdown.

After examining the list of p53 target genes induced following the loss of HdmX or Hdm2, and how the increase in p53 transactivation was not due to p53 phosphorylation, the biological effects of HdmX and Hdm2 knockdown was assessed in MCF7 cells. As expected, a significant decrease in colony formation was observed upon the loss of either HdmX or Hdm2 with the greatest decrease occurring when both HdmX and Hdm2 were removed (Figure 28). Similarly, in a less stringent cell proliferation assay, knockdown of HdmX or Hdm2 led to a 30% reduction in cell growth, whereas the concurrent knockdown of HdmX and Hdm2 led to 50% reduction in growth after 48 hours (Figure 29). These results are consistent with the synergistic induction of the anti-proliferative genes, p21, BTG2, and ACTA2 observed following loss of both HdmX and

Hdm2 (Figure 23). MCF7 growth curves also showed that cell proliferation was inhibited by the elimination of HdmX and/or Hdm2 (Figure 30), particularly when HdmX and Hdm2 levels were coordinately down regulated by the transient siRNA. Since one function of Hdm2 is to regulate p53 stability through ubiquitin-mediated proteasome degradation, knockdown of Hdm2 was expected to increase p53 protein levels in addition to increase p53 transactivation. However, no dramatic change in p53 protein levels following Hdm2 knockdown were observed by Western blot analysis (Figures 13, 26 and 27). This is most likely not the result of MCF7 cells being unable to degrade p53, as the overexpression of Hdm2 in these cells can lead to p53 degradation (S. Berberich, personal communication). To determine if Hdm2 is capable of E3 ligase activity in MCF7 cells, p53 ubiquitination could be monitored under the various siRNA conditions. Since HdmX levels are elevated in MCF7 cells, it may be preventing Hdm2 from binding p53 efficiently, thus the removal of Hdm2 would have little effect on p53 stability. Another possible explanation for the lack of p53 stability following loss of Hdm2 is that other E3 ligases such as Pirh2 and COP1 are preventing an increase in p53 protein levels. Taken together, these results suggest that the overexpression of HdmX and Hdm2 in MCF7 cells appears to inactivate p53 primarily through inhibition of transcription.

To assess how the decrease in cell growth and the activation of cell cycle arrest genes affect cell cycle progression, DNA content was analyzed by flow cytometry. As expected, the loss of either HdmX or Hdm2 led to a significant increase in G1 cells and a subsequent decrease in S phase cells in both MCF7 and U2OS cells (Figures 31 and 32). Since p21 inhibits cyclin-CDK complexes (Xiong et al, 1993) and BTG2 down regulates the cyclins (Boiko et al, 2006) an arrest in cell cycle progression was anticipated. Thus,

the gene expression profiles, colony formation, growth curves and cell cycle profiles are all consistent with the removal of HdmX or Hdm2 leading to a cell cycle arrest that is dependent on wild-type p53. Interestingly, the gene expression results in this study correlate with a recent report that showed that during replication senescence of a normal human cell, p53 preferentially targets genes that induce cell cycle arrest (Jackson and Pereira-Smith, 2006). Since the loss of HdmX or Hdm2 seemed to preferentially induce growth arrest genes also, suggests that HdmX removal leads to a similar phenotype as replication senescence. The hypothesis that HdmX or Hdm2 knockdown leads to cellular senescence was tested by beta-galactosidase staining; however, no differences in the numbers of senescent cells were observed between MCF7 cells with or without HdmX or Hdm2 (data not shown). These experiments were performed following transient siRNA transfection, thus the long term effect of HdmX or Hdm2 knockdown on cellular senescence may produce a different result.

Although the removal of overexpressed HdmX or Hdm2 in tumor cells harboring wild-type p53 appears to be limited to an anti-proliferative effect, the ability to sensitize cells to chemotherapeutic agents by knockdown of HdmX was examined. Recent studies have shown that removal of HdmX will sensitize tumors with overexpressed HdmX to p53 activation by Nutlin (Hu et al., 2006a; Patton et al., 2006), and that cells transfected with MdmX siRNA showed a more robust p53 response to ionizing radiation (Laurie et al., 2006). To examine how the removal of HdmX or Hdm2 would affect the sensitivity of MCF7 cells to various chemotherapy agents, cell viability assays were performed. Removal of HdmX or Hdm2 in MCF7 cells increased the cytotoxicity of DNA damaging agents such as doxorubicin and cisplatin, and of the DNA replication inhibitor, AraC

(Figures 33 and 34). As predicted by the alterations in gene expression, colony formation, and cell proliferation assays, the knockdown of both HdmX and/or Hdm2 led to the greatest cytotoxicity. At high doses of the chemotherapy drugs, the enhanced cell death benefit of HdmX or Hdm2 knockdown was lost. Therefore, removal of HdmX or Hdm2 sensitizes the cells to lower doses of the chemotherapeutic agents, while still achieving the same efficacy as the higher doses. Similar results where reported with other agents, suggesting that tumors with overexpressed HdmX are generally less sensitive to chemotherapy drugs and that knockdown of HdmX increases their chemosensitivity (Gilkes et al., 2006). In contrast, the nongenotoxic activation of p53 with Nutlin demonstrated that the presence of p53 protected human tumor cells from chemotherapy treatments that induce S-phases arrest (Kranz and Dobbelstein, 2006). Unlike the report from Kranz and Dobblestein, the loss of HdmX or Hdm2 in MCF7 cells increased the cytotoxicity of both DNA damaging agents and agents which inhibit DNA replication (Figure 34). These results suggest that HdmX is an important therapeutic target that may improve current chemotherapy treatments for those human tumors harboring wild-type p53 and elevated levels of HdmX.

D. p53 and Hdm2 localization and stabilization following loss of HdmX

Since HdmX directly interacts with both Hdm2 and p53, the cellular localization and stability of Hdm2 and p53 were examined following the loss of HdmX. HdmX is predominantly a cytoplasmic protein, where as Hdm2 can shuttle between the nucleus and cytoplasm due to the presence of nuclear localization and export signals (Shvarts et al., 1996; Roth et al., 1998; Migliorini et al., 2002). One possible function of HdmX may be to retain Hdm2 in the cytoplasm away from p53 to facilitate p53 activation. If this is

true, then the loss of HdmX would shift the nuclear and cytoplasmic distribution of Hdm2. To test this hypothesis, nuclear and cytoplasmic fractionation was performed from MCF7 cells with and without HdmX knockdown. Western blot analysis revealed no significant alterations in Hdm2 or p53 cellular localization following the removal of HdmX (Figure 36). Similarly, the loss of Hdm2 did not appear to alter HdmX or p53 localization. In contrast, others have observed that the knockdown of HdmX led to a more nuclear Hdm2 pool (K. Huang, personal communication), however these studies were conducted in p53-null cell lines suggesting that the removal of p53 may alter the interdependence of Hdm2 and HdmX cellular localization. It would be interesting to knockdown p53 and HdmX, or p53 and Hdm2 simultaneously using siRNA and monitor the nuclear and cytoplasmic distribution to determine if p53 plays a role in the interdependence of Hdm2 and HdmX localization.

The relative abundance of HdmX and Hdm2 appears to be critical to p53 stability (Gu et al., 2002; Stad et al., 2001). Previous reports show that overexpressed MdmX protects p53 from Mdm2-mediated degradation by competing with Mdm2 for direct binding to p53 (Jackson and Berberich, 2000; Mancini et al., 2004). It has also been shown that overexpressed HdmX protects p53 by enhancing the auto-ubiquitination and degradation of Hdm2 (Linares et al., 2003; K. Huang, personal communication). To examine the stability of Hdm2 and p53 following knockdown of HdmX, MCF7 cells were treated with a proteasome inhibitor, MG132. My results show that the loss of HdmX increased *hdm2* gene expression, but not Hdm2 protein level implying that the removal of HdmX leads to a decrease in Hdm2 stability. This finding is in contrast to Linares et al., and K. Huang, however, a previous study has shown that overexpressed

MdmX stabilized Mdm2 (Sharp et al., 1999). Western blot analysis of Hdm2 showed that Hdm2 protein levels were increased following the loss of HdmX when proteasomal degradation was inhibited (Figure 36). This result suggests that although Hdm2 transcription is induced by HdmX knockdown via p53 activation, the Hdm2 protein is being degraded at an accelerated rate thus, no net change in Hdm2 protein level is detectable. Additional experiments to assess HdmX, Hdm2, and p53 half-life following siRNA transfection were performed using cycloheximide to inhibit protein synthesis. As expected, loss of Hdm2 increased the half life of p53 slightly, whereas elimination of HdmX had little effect on p53 stability. This is consistent with the idea that HdmX predominantly regulates p53 transactivation, while Hdm2 controls p53 stability (Figure 37). The removal of HdmX, a binding partner of Hdm2, appears to decrease Hdm2 stability possibly by leaving Hdm2 more accessible to auto-ubiquitination and proteasomal degradation. This result agrees with Sharp et al. who suggested that HdmX is necessary for the stabilization of Hdm2. Interestingly, loss of Hdm2 in MCF7 cells appears to destabilize HdmX also (Figure 37) suggesting that Hdm2 and HdmX heterodimerization is required for the stability of both proteins. Another possible explanation is that some other protein may ubiquitinate HdmX in non-stressed cells while Hdm2 promotes HdmX degradation following damage. It is also hypothesized that HAUSP may not bind HdmX as effectively without Hdm2, thus it is not deubiquitinated at the same rate. Previous reports using siRNA to silence HdmX show that knockdown of HdmX decreases Hdm2 protein stability in one study, while others report an increase in Hdm2 stability (Gu et al, 2002; Linares et al, 2004). Further experiments will be necessary to specifically resolve how and under what conditions Hdm2 and HdmX affect

the stability of each other. It will be necessary to determine if the presence of p53 influences the stability of HdmX or Hdm2 following the knockdown of the other one of these proteins. Also, the stability of HdmX and Hdm2 upon DNA damage will need to be assessed when Hdm2 or HdmX is removed. This may determine if other factors are critical for the regulation of Hdm2 and HdmX stability. Furthermore, immuno-fluorescence assays could be used to evaluate localization of HdmX and Hdm2 which may impact stability.

Finally, the effect of HdmX or Hdm2 knockdown on normal non-tumor IMR90 cells was investigated. The loss of HdmX or Hdm2 induced p21 gene and protein expression as expected, however, to a slightly lower extent than in the MCF7 cells (compare Figure 13A to 38A). Interestingly, p53 protein expression was increased after HdmX or Hdm2 knockdown in IMR90 cells. The activation of p53 protein expression was greater following loss of Hdm2 than after the loss of HdmX (Figure 38B), which correlates with the role of Hdm2 as a regulator of p53 stability. In contrast, no significant increase in p53 protein levels was observed via Western blot following the loss of HdmX or Hdm2 in the MCF7 cells (Figures 13, 26, and 34). The difference in p53 protein levels between the non-tumor IMR90 cells and the breast carcinoma MCF7 cells may be due to the overexpression of both HdmX and Hdm2 in MCF7 cells. Results from this study suggest that both HdmX and Hdm2 must be removed from MCF7 cells to induce even a slight increase in p53 protein levels. Regardless of the lack of induction of p53 protein expression, the biological effect of eliminating either HdmX or Hdm2 in MCF7 cells was sufficient to inhibit cell growth and colony formation. The biological effect of the

increased expression of p53 protein in IMR90 cells following the knockdown of HdmX or Hdm2 still needs to be assessed.

Taken together, the results from these studies in MCF7 cells support a model (Figure 40), whereby the RNAi knockdown of HdmX leads to a nongenotoxic activation of p53, the induction of p53 target genes predominantly associated with cell cycle arrest or growth inhibition, and a possible decrease in Hdm2 stability. Additionally, these results support my hypothesis that loss of HdmX in tumor cells with overexpressed HdmX and wild-type p53 activates p53, is anti-proliferative, and enhances the chemosensitivity of the cells to DNA damaging agents.

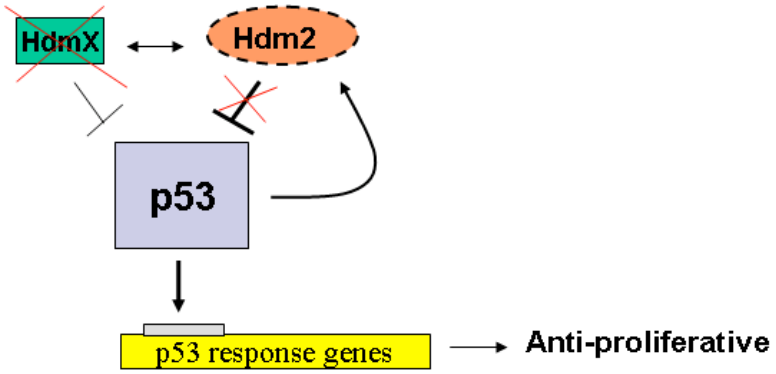

Figure 40. Proposed mechanism of p53 activation following loss of HdmX in MCF7 cells. Loss of HdmX leads to a nongenotoxic activation of p53, induction of p53 target genes predominantly associated with cell cycle arrest, and a possible decrease in Hdm2 stability. Taken together, the loss of HdmX in tumor cells with overexpressed HdmX and wild-type p53 leads to an anti-proliferative effect, and enhances the cytotoxicity of chemotherapeutic agents.

V. CONCLUSION

This dissertation research systematically addresses the effects of loss of HdmX and Hdm2 on gene expression and cell growth in tumors with wild-type p53 and overexpressed HdmX and/or Hdm2. RNAi approaches were utilized to silence HdmX, Hdm2, or p53 either individually or in selected combinations. Using Affymetrix GeneChips and subsequent RT-PCR validations, a subset of p53 target genes induced following HdmX or Hdm2 knockdown were uncovered. These target genes encode proteins predominantly associated with cell cycle arrest and growth inhibition. The induction of these genes resulted in increased p53 transactivation, and occurred in a p53 dependent manner. The increase in p53 transcriptional activity following the loss of HdmX or Hdm2 was not due to p53 phosphorylation, implying a nongenotoxic p53 activation. Results from colony formation and cell proliferation assays were consistent with the induction of genes involved in cell cycle arrest. Flow cytometry analysis of DNA content was used to confirm that the removal of HdmX or Hdm2 led to a significant G1 cell cycle arrest. Furthermore, HdmX or Hdm2 knockdown in MCF7 cells sensitized the cells to several chemotherapeutic agents. Taken together, these results suggest that removal of HdmX may be an important therapeutic strategy that would enhance the efficacy of chemotherapy drugs currently used to treat human tumors possessing wild-type p53 and overexpressed HdmX.

REFERENCES

Appella, E. and Anderson, C.W. (2001) Post-translational modifications and activation of p53 by genotoxic stresses. *Eur J Biochem*, 268, 2764-2772.

Ashcroft, M. and Vousden, K.H. (1999) Regulation of p53 stability. *Oncogene*, 18, 7637-7643.

Baker, S.J., Markowitz, S., Fearon, E.R., Willson, J.K. and Vogelstein, B. (1990) Suppression of human colorectal carcinoma cell growth by wild-type p53. *Science*, 249, 912-915.

Barbieri, E., Mehta, P., Chen, Z., Zhang, L., Slack, A., Berg, S. and Shohet, J.M. (2006) MDM2 inhibition sensitizes neuroblastoma to chemotherapy-induced apoptotic cell death. *Mol Cancer Ther*, 5, 2358-2365.

Birmingham, A., Anderson, E.M., Reynolds, A., Ilsley-Tyree, D., Leake, D., Fedorov, Y., Baskerville, S., Maksimova, E., Robinson, K., Karpilow, J., Marshall, W.S. and Khvorova, A. (2006) 3' UTR seed matches, but not overall identity, are associated with RNAi off-targets. *Nat Methods*, 3, 199-204.

Boesten, L.S., Zadelaar, S.M., De Clercq, S., Francoz, S., van Nieuwkoop, A., Biessen, E.A., Hofmann, F., Feil, S., Feil, R., Jochemsen, A.G., Zurcher, C., Havekes, L.M., van Vlijmen, B.J. and Marine, J.C. (2006) Mdm2, but not Mdm4, protects terminally differentiated smooth muscle cells from p53-mediated caspase-3-independent cell death. *Cell Death Differ*, 13, 2089-2098.

Boiko, A.D., Porteous, S., Razorenova, O.V., Krivokrysenko, V.I., Williams, B.R. and Gudkov, A.V. (2006) A systematic search for downstream mediators of tumor suppressor function of p53 reveals a major role of BTG2 in suppression of Ras-induced transformation. *Genes Dev*, 20, 236-252.

Bond, G.L., Hu, W., Bond, E.E., Robins, H., Lutzker, S.G., Arva, N.C., Bargonetti, J., Bartel, F., Taubert, H., Wuerl, P., Onel, K., Yip, L., Hwang, S.J., Strong, L.C., Lozano, G. and Levine, A.J. (2004) A single nucleotide polymorphism in the MDM2 promoter attenuates the p53 tumor suppressor pathway and accelerates tumor formation in humans. *Cell*, 119, 591-602.

Braasch, D.A., Jensen, S., Liu, Y., Kaur, K., Arar, K., White, M.A. and Corey, D.R. (2003) RNA interference in mammalian cells by chemically-modified RNA. *Biochemistry*, 42, 7967-7975.

Braithwaite, A.W., Royds, J.A. and Jackson, P. (2005) The p53 story: layers of complexity. *Carcinogenesis*, 26, 1161-1169.

Bridge, A.J., Pebernard, S., Ducraux, A., Nicoulaz, A.L. and Iggo, R. (2003) Induction of an interferon response by RNAi vectors in mammalian cells. *Nat Genet*, 34, 263-264.

Brooks, C.L., Li, M. and Gu, W. (2004) Monoubiquitination: the signal for p53 nuclear export? *Cell Cycle*, 3, 436-438.

Buschmann, T., Lerner, D., Lee, C.G. and Ronai, Z. (2001) The Mdm-2 amino terminus is required for Mdm2 binding and SUMO-1 conjugation by the E2 SUMO-1 conjugating enzyme Ubc9. *J Biol Chem*, 276, 40389-40395.

Canman, C.E., Lim, D.S., Cimprich, K.A., Taya, Y., Tamai, K., Sakaguchi, K., Appella, E., Kastan, M.B. and Siliciano, J.D. (1998) Activation of the ATM kinase by ionizing radiation and phosphorylation of p53. *Science*, 281, 1677-1679.

Chavez-Reyes, A., Parant, J.M., Amelse, L.L., de Oca Luna, R.M., Korsmeyer, S.J. and Lozano, G. (2003) Switching mechanisms of cell death in mdm2- and mdm4-null mice by deletion of p53 downstream targets. *Cancer Res*, 63, 8664-8669.

Chen, L., Gilkes, D.M., Pan, Y., Lane, W.S. and Chen, J. (2005a) ATM and Chk2-dependent phosphorylation of MDMX contribute to p53 activation after DNA damage. *Embo J*, 24, 3411-3422.

Chen, L., Li, C., Pan, Y. and Chen, J. (2005b) Regulation of p53-MDMX interaction by casein kinase 1 alpha. *Mol Cell Biol*, 25, 6509-6520.

Chen, P.L., Chen, Y.M., Bookstein, R. and Lee, W.H. (1990) Genetic mechanisms of tumor suppression by the human p53 gene. *Science*, 250, 1576-1580.

Chene, P. (2003) Inhibiting the p53-MDM2 interaction: an important target for cancer therapy. *Nat Rev Cancer*, 3, 102-109.

Comer, K.A., Dennis, P.A., Armstrong, L., Catino, J.J., Kastan, M.B. and Kumar, C.C. (1998) Human smooth muscle alpha-actin gene is a transcriptional target of the p53 tumor suppressor protein. *Oncogene*, 16, 1299-1308.

Crawford, L.V., Pim, D.C., Gurney, E.G., Goodfellow, P. and Taylor-Papadimitriou, J. (1981) Detection of a common feature in several human tumor cell lines--a 53,000-dalton protein. *Proc Natl Acad Sci U S A*, 78, 41-45.

Daniel, R., Kao, G., Taganov, K., Greger, J.G., Favorova, O., Merkel, G., Yen, T.J., Katz, R.A. and Skalka, A.M. (2003) Evidence that the retroviral DNA integration process triggers an ATR-dependent DNA damage response. *Proc Natl Acad Sci U S A*, 100, 4778-4783.

Danovi, D., Meulmeester, E., Pasini, D., Migliorini, D., Capra, M., Frenk, R., de Graaf, P., Francoz, S., Gasparini, P., Gobbi, A., Helin, K., Pelicci, P.G., Jochemsen, A.G. and Marine, J.C. (2004) Amplification of Mdmx (or Mdm4) directly contributes to tumor formation by inhibiting p53 tumor suppressor activity. *Mol Cell Biol*, 24, 5835-5843.

de Graaf, P., Little, N.A., Ramos, Y.F., Meulmeester, E., Letteboer, S.J. and Jochemsen, A.G. (2003) Hdmx protein stability is regulated by the ubiquitin ligase activity of Mdm2. *J Biol Chem*, 278, 38315-38324.

Donehower, L.A., Harvey, M., Slagle, B.L., McArthur, M.J., Montgomery, C.A., Jr., Butel, J.S. and Bradley, A. (1992) Mice deficient for p53 are developmentally normal but susceptible to spontaneous tumours. *Nature*, 356, 215-221.

Dornan, D., Wertz, I., Shimizu, H., Arnott, D., Frantz, G.D., Dowd, P., O'Rourke, K., Koeppen, H. and Dixit, V.M. (2004) The ubiquitin ligase COP1 is a critical negative regulator of p53. *Nature*, 429, 86-92.

Dykxhoorn, D.M. and Lieberman, J. (2006) Running Interference: Prospects and Obstacles to Using Small Interfering RNAs as Small Molecule Drugs. *Annu Rev Biomed Eng*.

Dykxhoorn, D.M., Novina, C.D. and Sharp, P.A. (2003) Killing the messenger: short RNAs that silence gene expression. *Nat Rev Mol Cell Biol*, 4, 457-467.

Elbashir, S.M., Harborth, J., Lendeckel, W., Yalcin, A., Weber, K. and Tuschl, T. (2001a) Duplexes of 21-nucleotide RNAs mediate RNA interference in cultured mammalian cells. *Nature*, 411, 494-498.

Elbashir, S.M., Lendeckel, W. and Tuschl, T. (2001b) RNA interference is mediated by 21- and 22-nucleotide RNAs. *Genes Dev*, 15, 188-200.

el-Deiry, W.S., Kern, S.E., Pietenpol, J.A., Kinzler, K.W. and Vogelstein, B. (1992) Definition of a consensus binding site for p53. *Nat Genet*, 1, 45-49.

el-Deiry, W.S., Tokino, T., Velculescu, V.E., Levy, D.B., Parsons, R., Trent, J.M., Lin, D., Mercer, W.E., Kinzler, K.W. and Vogelstein, B. (1993) WAF1, a potential mediator of p53 tumor suppression. *Cell*, 75, 817-825.

Fang, S., Jensen, J.P., Ludwig, R.L., Vousden, K.H. and Weissman, A.M. (2000) Mdm2 is a RING finger-dependent ubiquitin protein ligase for itself and p53. *J Biol Chem*, 275, 8945-8951.

Fedorov, Y., Anderson, E.M., Birmingham, A., Reynolds, A., Karpilow, J., Robinson, K., Leake, D., Marshall, W.S. and Khvorova, A. (2006) Off-target effects by siRNA can induce toxic phenotype. *Rna*, 12, 1188-1196.

Finch, R.A., Donoviel, D.B., Potter, D., Shi, M., Fan, A., Freed, D.D., Wang, C.Y., Zambrowicz, B.P., Ramirez-Solis, R., Sands, A.T. and Zhang, N. (2002) mdmx is a negative regulator of p53 activity in vivo. *Cancer Res*, 62, 3221-3225.

Finlay, C.A., Hinds, P.W. and Levine, A.J. (1989) The p53 proto-oncogene can act as a suppressor of transformation. *Cell*, 57, 1083-1093.

Fire, A., Xu, S., Montgomery, M.K., Kostas, S.A., Driver, S.E. and Mello, C.C. (1998) Potent and specific genetic interference by double-stranded RNA in Caenorhabditis elegans. *Nature*, 391, 806-811.

Fish, R.J. and Kruithof, E.K. (2004) Short-term cytotoxic effects and long-term instability of RNAi delivered using lentiviral vectors. *BMC Mol Biol*, 5, 9.

Francoz, S., Froment, P., Bogaerts, S., De Clercq, S., Maetens, M., Doumont, G., Bellefroid, E. and Marine, J.C. (2006) Mdm4 and Mdm2 cooperate to inhibit p53 activity in proliferating and quiescent cells in vivo. *Proc Natl Acad Sci U S A*, 103, 3232-3237.

Gentiletti, F., Mancini, F., D'Angelo, M., Sacchi, A., Pontecorvi, A., Jochemsen, A.G. and Moretti, F. (2002) MDMX stability is regulated by p53-induced caspase cleavage in NIH3T3 mouse fibroblasts. *Oncogene*, 21, 867-877.

Ghosh, M., Weghorst, K. and Berberich, S.J. (2005) MdmX inhibits ARF mediated Mdm2 sumoylation. *Cell Cycle*, 4, 604-608.

Giglio, S., Mancini, F., Gentiletti, F., Sparaco, G., Felicioni, L., Barassi, F., Martella, C., Prodosmo, A., Iacovelli, S., Buttitta, F., Farsetti, A., Soddu, S., Marchetti, A., Sacchi, A., Pontecorvi, A. and Moretti, F. (2005) Identification of an aberrantly spliced form of HDMX in human tumors: a new mechanism for HDM2 stabilization. *Cancer Res*, 65, 9687-9694.

Gilkes, D.M., Chen, L. and Chen, J. (2006) MDMX regulation of p53 response to ribosomal stress. *Embo J*, 25, 5614-5625.

Gooch, J.L., Herrera, R.E. and Yee, D. (2000) The role of p21 in interferon gamma-mediated growth inhibition of human breast cancer cells. *Cell Growth Differ*, 11, 335-342.

Gorina, S. and Pavletich, N.P. (1996) Structure of the p53 tumor suppressor bound to the ankyrin and SH3 domains of 53BP2. *Science*, 274, 1001-1005.

Grossman, S.R., Deato, M.E., Brignone, C., Chan, H.M., Kung, A.L., Tagami, H., Nakatani, Y. and Livingston, D.M. (2003) Polyubiquitination of p53 by a ubiquitin ligase activity of p300. *Science*, 300, 342-344.

Gu, J., Kawai, H., Nie, L., Kitao, H., Wiederschain, D., Jochemsen, A.G., Parant, J., Lozano, G. and Yuan, Z.M. (2002) Mutual dependence of MDM2 and MDMX in their functional inactivation of p53. *J Biol Chem*, 277, 19251-19254.

Harms, K.L. and Chen, X. (2006) The functional domains in p53 family proteins exhibit both common and distinct properties. *Cell Death Differ*, 13, 890-897.

Haupt, Y., Maya, R., Kazaz, A. and Oren, M. (1997) Mdm2 promotes the rapid degradation of p53. *Nature*, 387, 296-299.

Hellborg, F., Qian, W., Mendez-Vidal, C., Asker, C., Kost-Alimova, M., Wilhelm, M., Imreh, S. and Wiman, K.G. (2001) Human wig-1, a p53 target gene that encodes a growth inhibitory zinc finger protein. *Oncogene*, 20, 5466-5474.

Hirao, A., Kong, Y.Y., Matsuoka, S., Wakeham, A., Ruland, J., Yoshida, H., Liu, D., Elledge, S.J. and Mak, T.W. (2000) DNA damage-induced activation of p53 by the checkpoint kinase Chk2. *Science*, 287, 1824-1827.

Hollstein, M., Shomer, B., Greenblatt, M., Soussi, T., Hovig, E., Montesano, R. and Harris, C.C. (1996) Somatic point mutations in the p53 gene of human tumors and cell lines: updated compilation. *Nucleic Acids Res*, 24, 141-146.

Honda, R., Tanaka, H. and Yasuda, H. (1997) Oncoprotein MDM2 is a ubiquitin ligase E3 for tumor suppressor p53. *FEBS Lett*, 420, 25-27.

Hu, B., Gilkes, D.M., Farooqi, B., Sebti, S.M. and Chen, J. (2006a) MDMX overexpression prevents p53 activation by the MDM2 inhibitor Nutlin. *J Biol Chem*, 281, 33030-33035.

Hu, M., Gu, L., Li, M., Jeffrey, P.D., Gu, W. and Shi, Y. (2006b) Structural basis of competitive recognition of p53 and MDM2 by HAUSP/USP7: implications for the regulation of the p53-MDM2 pathway. *PLoS Biol*, 4, e27.

Issaeva, N., Bozko, P., Enge, M., Protopopova, M., Verhoef, L.G., Masucci, M., Pramanik, A. and Selivanova, G. (2004) Small molecule RITA binds to p53, blocks p53-HDM-2 interaction and activates p53 function in tumors. *Nat Med*, 10, 1321-1328.

Jackson, A.L., Bartz, S.R., Schelter, J., Kobayashi, S.V., Burchard, J., Mao, M., Li, B., Cavet, G. and Linsley, P.S. (2003) Expression profiling reveals off-target gene regulation by RNAi. *Nat Biotechnol*, 21, 635-637.

Jackson, A.L., Burchard, J., Leake, D., Reynolds, A., Schelter, J., Guo, J., Johnson, J.M., Lim, L., Karpilow, J., Nichols, K., Marshall, W., Khvorova, A. and Linsley, P.S. (2006) Position-specific chemical modification of siRNAs reduces "off-target" transcript silencing. *RNA*, 12, 1197-1205.

Jackson, J.G. and Pereira-Smith, O.M. (2006) p53 Is Preferentially Recruited to the Promoters of Growth Arrest Genes p21 and GADD45 during Replicative Senescence of Normal Human Fibroblasts. *Cancer Res*, 66, 8356-8360.

Jackson, M.W. and Berberich, S.J. (2000) MdmX protects p53 from Mdm2-mediated degradation. *Mol Cell Biol*, 20, 1001-1007.

Jackson, M.W., Lindstrom, M.S. and Berberich, S.J. (2001) MdmX binding to ARF affects Mdm2 protein stability and p53 transactivation. *J Biol Chem*, 276, 25336-25341.

Jones, S.N., Roe, A.E., Donehower, L.A. and Bradley, A. (1995) Rescue of embryonic lethality in Mdm2-deficient mice by absence of p53. *Nature*, 378, 206-208.

Katoh, T., Susa, M., Suzuki, T., Umeda, N. and Watanabe, K. (2003) Simple and rapid synthesis of siRNA derived from in vitro transcribed shRNA. *Nucleic Acids Res Suppl*, 249-250.

Kawai, H., Wiederschain, D., Kitao, H., Stuart, J., Tsai, K.K. and Yuan, Z.M. (2003a) DNA damage-induced MDMX degradation is mediated by MDM2. *J Biol Chem*, 278, 45946-45953.

Kawai, H., Wiederschain, D. and Yuan, Z.M. (2003b) Critical contribution of the MDM2 acidic domain to p53 ubiquitination. *Mol Cell Biol*, 23, 4939-4947.

Khosravi, R., Maya, R., Gottlieb, T., Oren, M., Shiloh, Y. and Shkedy, D. (1999) Rapid ATM-dependent phosphorylation of MDM2 precedes p53 accumulation in response to DNA damage. *Proc Natl Acad Sci U S A*, 96, 14973-14977.

Kim, W.J., Christensen, L.V., Jo, S., Yockman, J.W., Jeong, J.H., Kim, Y.H. and Kim, S.W. (2006) Cholesteryl oligoarginine delivering vascular endothelial growth factor siRNA effectively inhibits tumor growth in colon adenocarcinoma. *Mol Ther*, 14, 343-350.

Ko, L.J. and Prives, C. (1996) p53: puzzle and paradigm. *Genes Dev*, 10, 1054-1072.

Kobet, E., Zeng, X., Zhu, Y., Keller, D. and Lu, H. (2000) MDM2 inhibits p300-mediated p53 acetylation and activation by forming a ternary complex with the two proteins. *Proc Natl Acad Sci U S A*, 97, 12547-12552.

Kohn, K.W. (1999) Molecular interaction map of the mammalian cell cycle control and DNA repair systems. *Mol Biol Cell*, 10, 2703-2734.

Kojima, K., Konopleva, M., Samudio, I.J., Shikami, M., Cabreira-Hansen, M., McQueen, T., Ruvolo, V., Tsao, T., Zeng, Z., Vassilev, L.T. and Andreeff, M. (2005) MDM2 antagonists induce p53-dependent apoptosis in AML: implications for leukemia therapy. *Blood*, 106, 3150-3159.

Kranz, D. and Dobbelstein, M. (2006) Nongenotoxic p53 activation protects cells against S-phase-specific chemotherapy. *Cancer Res*, 66, 10274-10280.

Kubbutat, M.H., Jones, S.N. and Vousden, K.H. (1997) Regulation of p53 stability by Mdm2. *Nature*, 387, 299-303.

Kubbutat, M.H., Ludwig, R.L., Ashcroft, M. and Vousden, K.H. (1998) Regulation of Mdm2-directed degradation by the C terminus of p53. *Mol Cell Biol*, 18, 5690-5698.

Lane, D.P. and Crawford, L.V. (1979) T antigen is bound to a host protein in SV40-transformed cells. *Nature*, 278, 261-263.

Laurie, N.A., Donovan, S.L., Shih, C.S., Zhang, J., Mills, N., Fuller, C., Teunisse, A., Lam, S., Ramos, Y., Mohan, A., Johnson, D., Wilson, M., Rodriguez-Galindo, C., Quarto, M., Francoz, S., Mendrysa, S.M., Guy, R.K., Marine, J.C., Jochemsen, A.G. and Dyer, M.A. (2006) Inactivation of the p53 pathway in retinoblastoma. *Nature*, 444, 61-66.

Lavin, M.F. and Gueven, N. (2006) The complexity of p53 stabilization and activation. *Cell Death Differ*, 13, 941-950.

LeBron, C., Chen, L., Gilkes, D.M. and Chen, J. (2006) Regulation of MDMX nuclear import and degradation by Chk2 and 14-3-3. *Embo J*, 25, 1196-1206.

Leng, R.P., Lin, Y., Ma, W., Wu, H., Lemmers, B., Chung, S., Parant, J.M., Lozano, G., Hakem, R. and Benchimol, S. (2003) Pirh2, a p53-induced ubiquitin-protein ligase, promotes p53 degradation. *Cell*, 112, 779-791.

Levine, A.J., Hu, W. and Feng, Z. (2006) The P53 pathway: what questions remain to be explored? *Cell Death Differ*, 13, 1027-1036.

Li, M., Brooks, C.L., Kon, N. and Gu, W. (2004) A dynamic role of HAUSP in the p53-Mdm2 pathway. *Mol Cell*, 13, 879-886.

Li, M., Brooks, C.L., Wu-Baer, F., Chen, D., Baer, R. and Gu, W. (2003) Mono- versus polyubiquitination: differential control of p53 fate by Mdm2. *Science*, 302, 1972-1975.

Li, M., Chen, D., Shiloh, A., Luo, J., Nikolaev, A.Y., Qin, J. and Gu, W. (2002) Deubiquitination of p53 by HAUSP is an important pathway for p53 stabilization. *Nature*, 416, 648-653.

Li, W.J., Kloetzer, W.S. and Arlinghaus, R.B. (1988) A novel 53 kDa protein complexed with P210bcr-abl in human chronic myelogenous leukemia cells. *Oncogene*, 2, 559-566.

Liang, S.H. and Clarke, M.F. (1999) The nuclear import of p53 is determined by the presence of a basic domain and its relative position to the nuclear localization signal. *Oncogene*, 18, 2163-2166.

Lin, X., Ruan, X., Anderson, M.G., McDowell, J.A., Kroeger, P.E., Fesik, S.W. and Shen, Y. (2005) siRNA-mediated off-target gene silencing triggered by a 7 nt complementation. *Nucleic Acids Res*, 33, 4527-4535.

Linares, L.K., Hengstermann, A., Ciechanover, A., Muller, S. and Scheffner, M. (2003) HdmX stimulates Hdm2-mediated ubiquitination and degradation of p53. *Proc Natl Acad Sci U S A*, 100, 12009-12014.

Linares, L.K. and Scheffner, M. (2003) The ubiquitin-protein ligase activity of Hdm2 is inhibited by nucleic acids. *FEBS Lett*, 554, 73-76.

Linzer, D.I. and Levine, A.J. (1979) Characterization of a 54K dalton cellular SV40 tumor antigen present in SV40-transformed cells and uninfected embryonal carcinoma cells. *Cell*, 17, 43-52.

Liu, C.M., Liu, D.P., Dong, W.J. and Liang, C.C. (2004) Retrovirus vector-mediated stable gene silencing in human cell. *Biochem Biophys Res Commun*, 313, 716-720.

Lowe, S.W. and Sherr, C.J. (2003) Tumor suppression by Ink4a-Arf: progress and puzzles. *Curr Opin Genet Dev*, 13, 77-83.

Lu, H., Taya, Y., Ikeda, M. and Levine, A.J. (1998) Ultraviolet radiation, but not gamma radiation or etoposide-induced DNA damage, results in the phosphorylation of the murine p53 protein at serine-389. *Proc Natl Acad Sci U S A*, 95, 6399-6402.

Maetens, M., Doumont, G., De Clercq, S., Francoz, S., Froment, P., Bellefroid, E., Klingmuller, U., Lozano, G. and Marine, J.C. (2006) Distinct Roles of Mdm2 and Mdm4 in Red Cell Production. *Blood*.

Maki, C.G. (1999) Oligomerization is required for p53 to be efficiently ubiquitinated by MDM2. *J Biol Chem*, 274, 16531-16535.

Makinen, P.I., Koponen, J.K., Karkkainen, A.M., Malm, T.M., Pulkkinen, K.H., Koistinaho, J., Turunen, M.P. and Yla-Herttuala, S. (2006) Stable RNA interference: comparison of U6 and H1 promoters in endothelial cells and in mouse brain. *J Gene Med*, 8, 433-441.

Malkin, D., Li, F.P., Strong, L.C., Fraumeni, J.F., Jr., Nelson, C.E., Kim, D.H., Kassel, J., Gryka, M.A., Bischoff, F.Z., Tainsky, M.A. and et al. (1990) Germ line p53 mutations in a familial syndrome of breast cancer, sarcomas, and other neoplasms. *Science*, 250, 1233-1238.

Mancini, F., Gentiletti, F., D'Angelo, M., Giglio, S., Nanni, S., D'Angelo, C., Farsetti, A., Citro, G., Sacchi, A., Pontecorvi, A. and Moretti, F. (2004) MDM4 (MDMX) overexpression enhances stabilization of stress-induced p53 and promotes apoptosis. *J Biol Chem*, 279, 8169-8180.

Marine, J.C., Francoz, S., Maetens, M., Wahl, G., Toledo, F. and Lozano, G. (2006) Keeping p53 in check: essential and synergistic functions of Mdm2 and Mdm4. *Cell Death Differ*, 13, 927-934.

Marine, J.C. and Jochemsen, A.G. (2004) Mdmx and Mdm2: brothers in arms? *Cell Cycle*, 3, 900-904.

Maya, R., Balass, M., Kim, S.T., Shkedy, D., Leal, J.F., Shifman, O., Moas, M., Buschmann, T., Ronai, Z., Shiloh, Y., Kastan, M.B., Katzir, E. and Oren, M. (2001) ATM-dependent phosphorylation of Mdm2 on serine 395: role in p53 activation by DNA damage. *Genes Dev*, 15, 1067-1077.

Mayo, L.D., Seo, Y.R., Jackson, M.W., Smith, M.L., Rivera Guzman, J., Korgaonkar, C.K. and Donner, D.B. (2005) Phosphorylation of human p53 at serine 46 determines promoter selection and whether apoptosis is attenuated or amplified. *J Biol Chem*, 280, 25953-25959.

McLure, K.G. and Lee, P.W. (1998) How p53 binds DNA as a tetramer. *Embo J*, 17, 3342-3350.

Meek, D.W. (2002) p53 Induction: phosphorylation sites cooperate in regulating. *Cancer Biol Ther*, 1, 284-286.

Meister, G. and Tuschl, T. (2004) Mechanisms of gene silencing by double-stranded RNA. *Nature*, 431, 343-349.

Mercer, W.E., Amin, M., Sauve, G.J., Appella, E., Ullrich, S.J. and Romano, J.W. (1990) Wild type human p53 is antiproliferative in SV40-transformed hamster cells. *Oncogene*, 5, 973-980.

Meulmeester, E., Frenk, R., Stad, R., de Graaf, P., Marine, J.C., Vousden, K.H. and Jochemsen, A.G. (2003) Critical role for a central part of Mdm2 in the ubiquitylation of p53. *Mol Cell Biol*, 23, 4929-4938.

Meulmeester, E., Pereg, Y., Shiloh, Y. and Jochemsen, A.G. (2005) ATM-mediated phosphorylations inhibit Mdmx/Mdm2 stabilization by HAUSP in favor of p53 activation. *Cell Cycle*, 4, 1166-1170.

Michael, D. and Oren, M. (2003) The p53-Mdm2 module and the ubiquitin system. *Semin Cancer Biol*, 13, 49-58.

Migliorini, D., Danovi, D., Colombo, E., Carbone, R., Pelicci, P.G. and Marine, J.C. (2002) Hdmx recruitment into the nucleus by Hdm2 is essential for its ability to regulate p53 stability and transactivation. *J Biol Chem*, 277, 7318-7323.

Moll, U.M. and Petrenko, O. (2003) The MDM2-p53 interaction. *Mol Cancer Res*, 1, 1001-1008.

Momand, J., Zambetti, G.P., Olson, D.C., George, D. and Levine, A.J. (1992) The mdm-2 oncogene product forms a complex with the p53 protein and inhibits p53-mediated transactivation. *Cell*, 69, 1237-1245.

Montes de Oca Luna, R., Wagner, D.S. and Lozano, G. (1995) Rescue of early embryonic lethality in mdm2-deficient mice by deletion of p53. *Nature*, 378, 203-206.

Nakano, K. and Vousden, K.H. (2001) PUMA, a novel proapoptotic gene, is induced by p53. *Mol Cell*, 7, 683-694.

Oda, E., Ohki, R., Murasawa, H., Nemoto, J., Shibue, T., Yamashita, T., Tokino, T., Taniguchi, T. and Tanaka, N. (2000a) Noxa, a BH3-only member of the Bcl-2 family and candidate mediator of p53-induced apoptosis. *Science*, 288, 1053-1058.

Oda, K., Arakawa, H., Tanaka, T., Matsuda, K., Tanikawa, C., Mori, T., Nishimori, H., Tamai, K., Tokino, T., Nakamura, Y. and Taya, Y. (2000b) p53AIP1, a potential mediator of p53-dependent apoptosis, and its regulation by Ser-46-phosphorylated p53. *Cell*, 102, 849-862.

Okamoto, K., Kashima, K., Pereg, Y., Ishida, M., Yamazaki, S., Nota, A., Teunisse, A., Migliorini, D., Kitabayashi, I., Marine, J.C., Prives, C., Shiloh, Y., Jochemsen, A.G. and Taya, Y. (2005) DNA damage-induced phosphorylation of MdmX at serine 367 activates p53 by targeting MdmX for Mdm2-dependent degradation. *Mol Cell Biol*, 25, 9608-9620.

Oliner, J.D., Kinzler, K.W., Meltzer, P.S., George, D.L. and Vogelstein, B. (1992) Amplification of a gene encoding a p53-associated protein in human sarcomas. *Nature*, 358, 80-83.

Oliner, J.D., Pietenpol, J.A., Thiagalingam, S., Gyuris, J., Kinzler, K.W. and Vogelstein, B. (1993) Oncoprotein MDM2 conceals the activation domain of tumour suppressor p53. *Nature*, 362, 857-860.

Oren, M. (2003) Decision making by p53: life, death and cancer. *Cell Death Differ*, 10, 431-442.

Paddison, P.J., Caudy, A.A., Bernstein, E., Hannon, G.J. and Conklin, D.S. (2002) Short hairpin RNAs (shRNAs) induce sequence-specific silencing in mammalian cells. *Genes Dev*, 16, 948-958.

Pan, Y. and Chen, J. (2003) MDM2 promotes ubiquitination and degradation of MDMX. *Mol Cell Biol*, 23, 5113-5121.

Parant, J., Chavez-Reyes, A., Little, N.A., Yan, W., Reinke, V., Jochemsen, A.G. and Lozano, G. (2001) Rescue of embryonic lethality in Mdm4-null mice by loss of Trp53 suggests a nonoverlapping pathway with MDM2 to regulate p53. *Nat Genet*, 29, 92-95.

Patton, J.T., Mayo, L.D., Singhi, A.D., Gudkov, A.V., Stark, G.R. and Jackson, M.W. (2006) Levels of HdmX expression dictate the sensitivity of normal and transformed cells to Nutlin-3. *Cancer Res*, 66, 3169-3176.

Pereg, Y., Shkedy, D., de Graaf, P., Meulmeester, E., Edelson-Averbukh, M., Salek, M., Biton, S., Teunisse, A.F., Lehmann, W.D., Jochemsen, A.G. and Shiloh, Y. (2005) Phosphorylation of Hdmx mediates its Hdm2- and ATM-dependent degradation in response to DNA damage. *Proc Natl Acad Sci U S A*, 102, 5056-5061.

Prives, C. and Hall, P.A. (1999) The p53 pathway. *J Pathol*, 187, 112-126.

Qian, H., Wang, T., Naumovski, L., Lopez, C.D. and Brachmann, R.K. (2002) Groups of p53 target genes involved in specific p53 downstream effects cluster into different classes of DNA binding sites. *Oncogene*, 21, 7901-7911.

Rallapalli, R., Strachan, G., Cho, B., Mercer, W.E. and Hall, D.J. (1999) A novel MDMX transcript expressed in a variety of transformed cell lines encodes a truncated protein with potent p53 repressive activity. *J Biol Chem*, 274, 8299-8308.

Rallapalli, R., Strachan, G., Tuan, R.S. and Hall, D.J. (2003) Identification of a domain within MDMX-S that is responsible for its high affinity interaction with p53 and high-level expression in mammalian cells. *J Cell Biochem*, 89, 563-575.

Ramos, Y.F., Stad, R., Attema, J., Peltenburg, L.T., van der Eb, A.J. and Jochemsen, A.G. (2001) Aberrant expression of HDMX proteins in tumor cells correlates with wild-type p53. *Cancer Res*, 61, 1839-1842.

Riemenschneider, M.J., Buschges, R., Wolter, M., Reifenberger, J., Bostrom, J., Kraus, J.A., Schlegel, U. and Reifenberger, G. (1999) Amplification and overexpression of the MDM4 (MDMX) gene from 1q32 in a subset of malignant gliomas without TP53 mutation or MDM2 amplification. *Cancer Res*, 59, 6091-6096.

Rodriguez, M.S., Desterro, J.M., Lain, S., Lane, D.P. and Hay, R.T. (2000) Multiple C-terminal lysine residues target p53 for ubiquitin-proteasome-mediated degradation. *Mol Cell Biol*, 20, 8458-8467.

Roth, J., Dobbelstein, M., Freedman, D.A., Shenk, T. and Levine, A.J. (1998) Nucleo-cytoplasmic shuttling of the hdm2 oncoprotein regulates the levels of the p53 protein via a pathway used by the human immunodeficiency virus rev protein. *Embo J*, 17, 554-564.

Sabbatini, P. and McCormick, F. (2002) MDMX inhibits the p300/CBP-mediated acetylation of p53. *DNA Cell Biol*, 21, 519-525.

Saito, S., Goodarzi, A.A., Higashimoto, Y., Noda, Y., Lees-Miller, S.P., Appella, E. and Anderson, C.W. (2002) ATM mediates phosphorylation at multiple p53 sites, including Ser(46), in response to ionizing radiation. *J Biol Chem*, 277, 12491-12494.

Sandy, P., Ventura, A. and Jacks, T. (2005) Mammalian RNAi: a practical guide. *Biotechniques*, 39, 215-224.

Scacheri, P.C., Rozenblatt-Rosen, O., Caplen, N.J., Wolfsberg, T.G., Umayam, L., Lee, J.C., Hughes, C.M., Shanmugam, K.S., Bhattacharjee, A., Meyerson, M. and Collins, F.S. (2004) Short interfering RNAs can induce unexpected and divergent changes in the levels of untargeted proteins in mammalian cells. *Proc Natl Acad Sci U S A*, 101, 1892-1897.

Sharp, D.A., Kratowicz, S.A., Sank, M.J. and George, D.L. (1999) Stabilization of the MDM2 oncoprotein by interaction with the structurally related MDMX protein. *J Biol Chem*, 274, 38189-38196.

Shibue, T., Suzuki, S., Okamoto, H., Yoshida, H., Ohba, Y., Takaoka, A. and Taniguchi, T. (2006) Differential contribution of Puma and Noxa in dual regulation of p53-mediated apoptotic pathways. *Embo J*, 25, 4952-4962.

Shvarts, A., Bazuine, M., Dekker, P., Ramos, Y.F., Steegenga, W.T., Merckx, G., van Ham, R.C., van der Houven van Oordt, W., van der Eb, A.J. and Jochemsen, A.G. (1997) Isolation and identification of the human homolog of a new p53-binding protein, Mdmx. *Genomics*, 43, 34-42.

Shvarts, A., Steegenga, W.T., Riteco, N., van Laar, T., Dekker, P., Bazuine, M., van Ham, R.C., van der Houven van Oordt, W., Hateboer, G., van der Eb, A.J. and Jochemsen, A.G. (1996) MDMX: a novel p53-binding protein with some functional properties of MDM2. *Embo J*, 15, 5349-5357.

Sledz, C.A., Holko, M., de Veer, M.J., Silverman, R.H. and Williams, B.R. (2003) Activation of the interferon system by short-interfering RNAs. *Nat Cell Biol*, 5, 834-839.

Stad, R., Little, N.A., Xirodimas, D.P., Frenk, R., van der Eb, A.J., Lane, D.P., Saville, M.K. and Jochemsen, A.G. (2001) Mdmx stabilizes p53 and Mdm2 via two distinct mechanisms. *EMBO Rep*, 2, 1029-1034.

Stark, G.R., Kerr, I.M., Williams, B.R., Silverman, R.H. and Schreiber, R.D. (1998) How cells respond to interferons. *Annu Rev Biochem*, 67, 227-264.

Stojdl, D.F., Lichty, B., Knowles, S., Marius, R., Atkins, H., Sonenberg, N. and Bell, J.C. (2000) Exploiting tumor-specific defects in the interferon pathway with a previously unknown oncolytic virus. *Nat Med*, 6, 821-825.

Szulc, J., Wiznerowicz, M., Sauvain, M.O., Trono, D. and Aebischer, P. (2006) A versatile tool for conditional gene expression and knockdown. *Nat Methods*, 3, 109-116.

Takei, Y., Kadomatsu, K., Yuzawa, Y., Matsuo, S. and Muramatsu, T. (2004) A small interfering RNA targeting vascular endothelial growth factor as cancer therapeutics. *Cancer Res*, 64, 3365-3370.

Tanimura, S., Ohtsuka, S., Mitsui, K., Shirouzu, K., Yoshimura, A. and Ohtsubo, M. (1999) MDM2 interacts with MDMX through their RING finger domains. *FEBS Lett*, 447, 5-9.

Tao, W. and Levine, A.J. (1999) P19(ARF) stabilizes p53 by blocking nucleo-cytoplasmic shuttling of Mdm2. *Proc Natl Acad Sci U S A*, 96, 6937-6941.

Thompson, T., Tovar, C., Yang, H., Carvajal, D., Vu, B.T., Xu, Q., Wahl, G.M., Heimbrook, D.C. and Vassilev, L.T. (2004) Phosphorylation of p53 on key serines is dispensable for transcriptional activation and apoptosis. *J Biol Chem*, 279, 53015-53022.

Toledo, F., Krummel, K.A., Lee, C.J., Liu, C.W., Rodewald, L.W., Tang, M. and Wahl, G.M. (2006) A mouse p53 mutant lacking the proline-rich domain rescues Mdm4 deficiency and provides insight into the Mdm2-Mdm4-p53 regulatory network. *Cancer Cell*, 9, 273-285.

Toledo, F. and Wahl, G.M. (2006) Regulating the p53 pathway: in vitro hypotheses, in vivo veritas. *Nat Rev Cancer*, 6, 909-923.

Unger, T., Juven-Gershon, T., Moallem, E., Berger, M., Vogt Sionov, R., Lozano, G., Oren, M. and Haupt, Y. (1999) Critical role for Ser20 of human p53 in the negative regulation of p53 by Mdm2. *Embo J*, 18, 1805-1814.

Vassilev, L.T. (2004) Small-molecule antagonists of p53-MDM2 binding: research tools and potential therapeutics. *Cell Cycle*, 3, 419-421.

Vassilev, L.T., Vu, B.T., Graves, B., Carvajal, D., Podlaski, F., Filipovic, Z., Kong, N., Kammlott, U., Lukacs, C., Klein, C., Fotouhi, N. and Liu, E.A. (2004) In vivo activation of the p53 pathway by small-molecule antagonists of MDM2. *Science*, 303, 844-848.

Vogelstein, B., Fearon, E.R., Kern, S.E., Hamilton, S.R., Preisinger, A.C., Nakamura, Y. and White, R. (1989) Allelotype of colorectal carcinomas. *Science*, 244, 207-211.

Vousden, K.H. and Lu, X. (2002) Live or let die: the cell's response to p53. *Nat Rev Cancer*, **2,** 594-604.

Weber, J.D., Kuo, M.L., Bothner, B., DiGiammarino, E.L., Kriwacki, R.W., Roussel, M.F. and Sherr, C.J. (2000) Cooperative signals governing ARF-mdm2 interaction and nucleolar localization of the complex. *Mol Cell Biol*, 20, 2517-2528.

Weber, J.D., Taylor, L.J., Roussel, M.F., Sherr, C.J. and Bar-Sagi, D. (1999) Nucleolar Arf sequesters Mdm2 and activates p53. *Nat Cell Biol*, 1, 20-26.

Wiznerowicz, M., Szulc, J. and Trono, D. (2006) Tuning silence: conditional systems for RNA interference. *Nat Methods*, 3, 682-688.

Wiznerowicz, M. and Trono, D. (2003) Conditional suppression of cellular genes: lentivirus vector-mediated drug-inducible RNA interference. *J Virol*, 77, 8957-8961.

Wu, X., Bayle, J.H., Olson, D. and Levine, A.J. (1993) The p53-mdm-2 autoregulatory feedback loop. *Genes Dev*, 7, 1126-1132.

Xiong, S., Van Pelt, C.S., Elizondo-Fraire, A.C., Liu, G. and Lozano, G. (2006) Synergistic roles of Mdm2 and Mdm4 for p53 inhibition in central nervous system development. *Proc Natl Acad Sci U S A*, 103, 3226-3231.

Yakovleva, T., Pramanik, A., Kawasaki, T., Tan-No, K., Gileva, I., Lindegren, H., Langel, U., Ekstrom, T.J., Rigler, R., Terenius, L. and Bakalkin, G. (2001) p53 Latency. C-terminal domain prevents binding of p53 core to target but not to nonspecific DNA sequences. *J Biol Chem*, 276, 15650-15658.

Yang, Y., Li, C.C. and Weissman, A.M. (2004) Regulating the p53 system through ubiquitination. *Oncogene*, 23, 2096-2106.

Yang, Y., Ludwig, R.L., Jensen, J.P., Pierre, S.A., Medaglia, M.V., Davydov, I.V., Safiran, Y.J., Oberoi, P., Kenten, J.H., Phillips, A.C., Weissman, A.M. and Vousden, K.H. (2005) Small molecule inhibitors of HDM2 ubiquitin ligase activity stabilize and activate p53 in cells. *Cancer Cell*, 7, 547-559.

Yu, J., Zhang, L., Hwang, P.M., Kinzler, K.W. and Vogelstein, B. (2001) PUMA induces the rapid apoptosis of colorectal cancer cells. *Mol Cell*, 7, 673-682.

Yu, Y., Sun, P., Sun, L.C., Liu, G.Y., Chen, G.H., Shang, L.H., Wu, H.B., Hu, J., Li, Y., Mao, Y.L., Sui, G.J. and Sun, X.W. (2006) Downregulation of MDM2 expression by RNAi inhibits LoVo human colorectal adenocarcinoma cells growth and the treatment of LoVo cells with mdm2siRNA3 enhances the sensitivity to cisplatin. *Biochem Biophys Res Commun*, 339, 71-78.

Zhang, R., Wang, H. and Agrawal, S. (2005) Novel antisense anti-MDM2 mixed-backbone oligonucleotides: proof of principle, in vitro and in vivo activities, and mechanisms. *Curr Cancer Drug Targets*, 5, 43-49.